# CRAY CHANNELS

VOLUME 16, NUMBER 1 • A CRAY RESEARCH, INC. PUBLICATION

# Chemistry and Chemical Engineering

# The future isn't what it used to be.

## The Cray Research Fortran 90 Environment for SPARC

For years, Cray Research has developed the most advanced compiler technologies in the industry. Now users of workstations and servers can take advantage of that technology with the CraySoft Fortran 90 Environment for SPARC. An automatically parallelizing complete ANSI/ISO standard compiler combined with powerful development tools creates a sophisticated Fortran development environment. And, for a limited time, you can take advantage of this powerful environment for only $995*. For more information about CraySoft, email us at craysoft@cray.com or call us at 1-800-BUY-CRAY or, outside the United States, at +1 612 683-3030.


CRAYSOFT

Because no workstation is an island™

*Promotional price for US customers only.

# CONTENTS

## IN THIS ISSUE

Since DuPont became Cray Research's first chemical industry customer in 1986, Cray Research's contributions to the chemistry and chemical engineering fields have grown tremendously. This issue of CRAY CHANNELS reflects that growth, both in the breadth of science and engineering being done and in the increasing numbers of chemical and pharmaceutical companies applying Cray Research supercomputers to their R&D problems.

In one article, Bayer AG engineers write that it is now possible to dynamically simulate an entire chemical production facility. DuPont scientists are designing—with the help of Cray Research systems—alternatives to chlorofluorocarbon (CFC) compounds. Computational fluid dynamics, associated primarily with the aerospace and automotive industries, has become an effective decision-making tool in process engineering as well, a development made possible by the computational power and expertise provided by Cray Research. Researchers at Bristol-Myers Squibb are now able to study the transport of drugs across biomembranes. Continually expanding the capabilities of traditional computational chemistry methods on Cray Research systems, scientists can study increasingly larger molecules with higher accuracy—as discussed in an article from Gaussian, Inc. about fullerenes. Computational methods in materials science are adding to our understanding of the properties of surfaces and solids.

As always, we invite your comments and queries regarding the content of CRAY CHANNELS; please use the address below or our new email address, channels@cray.com.

## CRAY CHANNELS



CRAY CHANNELS is a publication of the Cray Research, Inc. Marketing Communications Department. Published three times per year, it is intended for users of Cray Research computer systems and others interested in the company and its products. Subscription inquiries and address changes should be sent to Department D, CRAY CHANNELS, Cray Research, Inc., 655D Lone Oak Drive, Eagan, Minnesota 55121. Other comments and queries may be emailed to channels@cray.com.

Volume 16, Number 1

**Editorial Staff**
Chris Kruell, editor
Molly Sachse, associate editor
Heidi Hagen, Ken Jopp, and Jeff Paulson, contributing editors

**Design and production**
Barbara Cahlander, electronic production artist
Eric Hanson, graphic design
Jim Morgan, art director

## FEATURES

2 **Bayer AG and Cray Research collaborate on plantwide dynamic process simulations**
*Ludger Brüll and Lothar Lang, Bayer AG, Leverkusen, Germany*
*Robert Zeller and Stephen Zitney, Cray Research, Inc.*

7 **Computational chemical design for CFC alternatives at DuPont**
*David A. Dixon, Kerwin D. Dobbs, and Scott C. Walker, DuPont, Wilmington, Delaware*

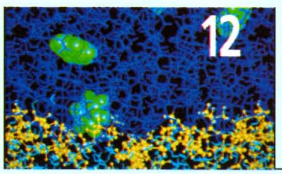


**Studies of biomembranes by supercomputer**
*Terry R. Stouch, Donna Bassolino, and Howard E. Alper, Bristol-Myers Squibb Pharmaceutical Research Institute, Princeton, New Jersey*

18 **Cray Research supercomputers advance stirred tank simulation**
*Richard D. LaRoche, Cray Research, Inc.*


**Materials science from first-principles: $CoSi_2$ surfaces**
*D. Vogtenhuber and R. Podloucky, Institute for Physical Chemistry of the University of Vienna, Vienna, Austria*
*S.G. Steinemann, Institute for Experimental Physics of the University of Lausanne, Dorigny-Lausanne, Switzerland*

26 **Investigating fullerene species with electronic structure theory**
*Douglas J. Fox, Gaussian, Inc., Pittsburgh, Pennsylvania*

31 **Pharmaceutical process modeling and simulation development**
*Willis Bell, Eli Lilly and Company, Lafayette, Indiana*
*Dale Eckart, Cray Research, Inc.*

## DEPARTMENTS

34 **Corporate Register**

36 **Applications Update**


**User News**

40 **Gallery**

# Bayer AG and Cray Research collaborate on plantwide dynamic process simulations

*Ludger Brüll and Lothar Lang, Bayer AG, Leverkusen, Germany*
*Robert Zeller and Stephen Zitney, Cray Research, Inc.*

Faced with an increasingly competitive global chemical market, challenging production requirements, and stringent environmental regulations, companies in the chemical process industry use process simulation to optimize plant operations and control. The future success of the chemical process industry, and its ability to meet these challenges, depends on its being able to design complex, highly interconnected plants that are as profitable and as environmentally compatible as possible. Process simulation, the computational modeling of chemical processes in a chemical plant, is a technology that helps engineers improve plant performance in terms of resource usage, safety, environmental impact, and economics. To make process simulation a reality for large-scale industrial processes, however, requires adequate computational resources.

In a demonstration of just how much computational power is needed, Bayer AG, a major German chemical company in Leverkusen, recently teamed up with Cray Research to perform plantwide simulations of an entire Bayer production facility. The collaboration clearly demonstrated that dynamic process simulation on a Cray Research supercomputer provides a powerful and valuable extension to traditional process engineering activities, and most importantly, delivers tangible financial benefits to Bayer's bottom line. This article discusses Bayer's interest in dynamic process simulation, describes the collaborative project and the software (SPEEDUP from Aspen Technology) used in the process, and analyzes some of the results gained from the simulations as well as their significance for Bayer's chemical production facilities.

## Chemical plant simulation at Bayer

Bayer's long and successful history of developing process simulation software began in the early 1970s. VTPLAN, Bayer's current generation of inhouse software, is considered one of the most advanced inhouse process flowsheeting systems in the chemical industry. Flowsheeting is an analysis procedure used by engineers to model any type of steady-state and dynamic process involving a continuous flow of materials and energy from one process unit to the next. Typical process units include reactors, distillation columns for separating products, heat exchangers, pumps, and compressors. Strong interactions between process units make many of today's complex, highly integrated plants difficult to operate.

To meet the challenges of running its plants profitably while pursuing its commitment to environmentally sound uses of resources and energy, Bayer centers its process engineering efforts around the development and use of plantwide dynamic process simulation technology. Unlike steady-state methods, dynamic simulation provides a continuous view of a chemical plant in action by calculating the transient behavior of a process over time.

## The project

To demonstrate the advantages of supercomputer simulations for process design and operations, Bayer and Cray Research recently collaborated to develop a plantwide dynamic model for a complex, heat-integrated distillation system, one of the largest within Bayer. With the SPEEDUP package the dynamic process model of more than five coupled distillation columns required the repeated solution of a differential-algebraic system containing over 75,000 equations, making it the world's largest known industrial SPEEDUP application.

Software optimization and algorithm developments, including a new sparse matrix solver, provided more than a thirtyfold increase in SPEEDUP performance. Coupling these software enhancements with the fast performance of a CRAY C90 supercomputer, the Bayer engineers were able to perform plantwide optimization and dynamic simulations that are not possible on modern workstations or mainframe computers.

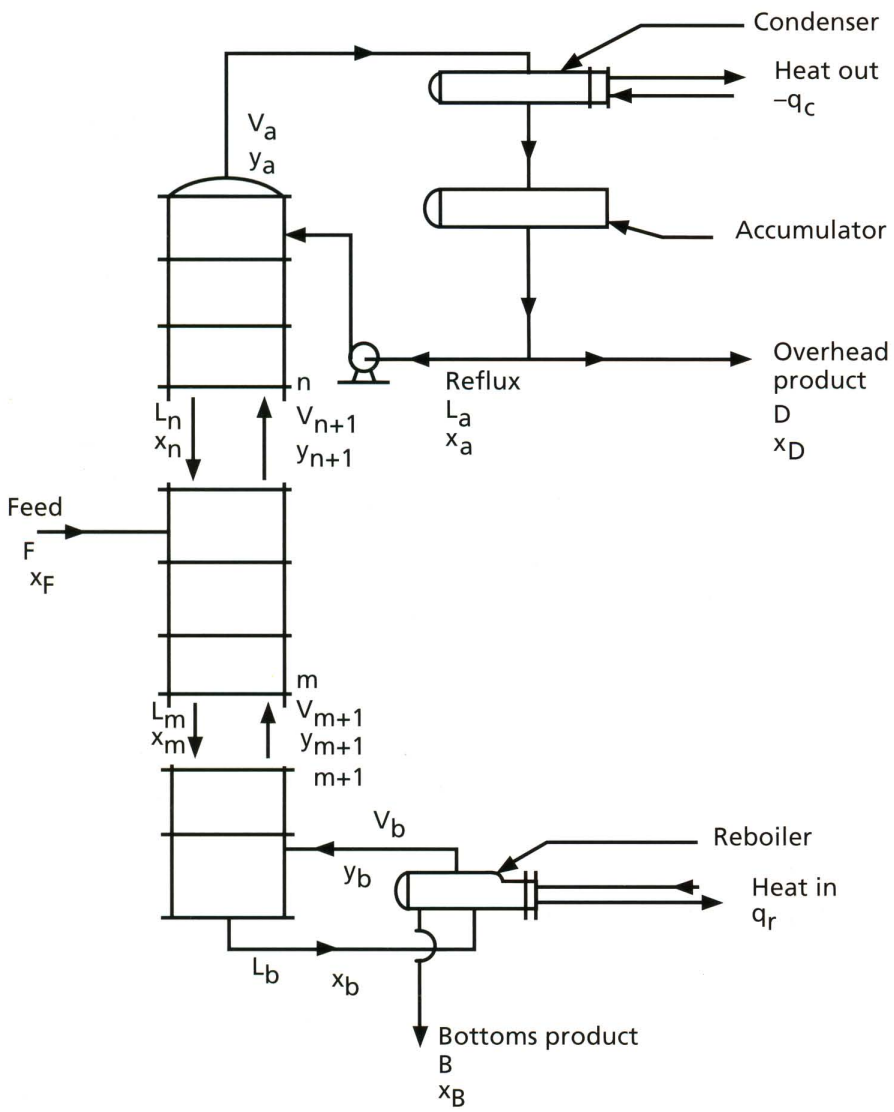


Figure 1. Basic components of a distillation column.

## Modeling the Bayer distillation plant

With distillation columns towering to a height of nearly 80 meters (see front cover), the Bayer plant considered here takes several chemical components from an upstream plant, separates them into pure valuable products, and recycles the others back to the upstream plant.

This plant is characterized by very large liquid holdups and time-varying feed conditions. Depending on the yield in the upstream reaction, the composition of the feed changes by a considerable amount (changes of up to 100 percent in some components). Moreover, the plant has nearly no buffering between the single distillation columns, which actually leads to an unsteady continuous process. This is quite unusual since most continuous processes are thought of as steady-state processes. The incentives for Bayer to look at this specific plant were process control problems and plans for a capacity increase that would result in a major revamp of the production facility.

Each distillation column (Figure 1) physically separates a chemical mixture into two or more fractions with different boiling points. The higher boiling components are withdrawn from the reboiler at the bottom of the column. The vapor from the reboiler is enriched with the lower boiling components along its path up the column. Upon leaving the top plate, the overhead vapor enters the condenser, where it is either partially or totally condensed. The lower boiling components are withdrawn from the top product stream, often called the distillate. A chain of such distillation towers can therefore separate a complex chemical mixture into its pure chemical components. Heat integration within the plant is possible by using the latent heat of condensation of the vapor at the top of one column to reboil another column, which results in an important savings in the energy consumption of the plant.

## SPEEDUP simulations

A detailed mathematical model of the entire distillation plant was developed with SPEEDUP using process flowsheet information and actual plant data. This model describes the steady-state and dynamic behavior of the individual distillation columns and the whole plant.

Performing dynamic simulations for a large-scale industrial distillation process requires significant amounts of computational resources, even on high-performance supercomputers. The solution time not only depends on the plant operation time being simulated, but it is also strongly correlated to the number of external perturbations affecting the chemical process during the simulation. To illustrate the computational requirements, two dynamic simulations representing eight hours

| | RUN1 | RUN2 |
|---|---|---|
| Number of equations | 75,724 | 75,724 |
| Number of time steps | 172 | 270 |
| Number of residual evaluations | 172 | 792 |
| Number of Jacobian evaluations | 17 | 39 |
| Maximum memory used (Mbytes) | 548 | 548 |
| Data transfer to disk (Gbytes) | 13 | 42 |
| CPU time (seconds) | 1082 | 3343 |
| Elapsed wall-clock time (seconds) | 1126 | 3415 |

Table 1. Dynamic process simulation of eight hours plant operation time.

of plant operation were run on a single-processor CRAY C90 supercomputer using SPEEDUP. The Cray Frontal Solver (FAMP) was used in both simulations (see sidebar). In RUN1 no perturbations occurred, whereas one external perturbation was applied in RUN2. The problem characteristics, resource allocations, and solution times are given in Table 1.

These examples clearly demonstrate that the introduction of a single process disturbance can significantly increase the computational requirements—CPU time and I/O capacity. Since the relaxation times of several components are relatively long, plant operation times of several days with many external perturbations must be simulated to obtain a realistic picture. When it comes to designing and optimizing the control strategy of a plant of this complexity, a CRAY C90-class system with optimized software is indispensable.

## Analysis of results

We carried out a combination of steady-state and dynamic simulations using SPEEDUP on the model (Figure 2). Steady-state simulations were done to optimize on the basis of different feed concentrations and loads. The result of these optimizations is the plant characteristic, which

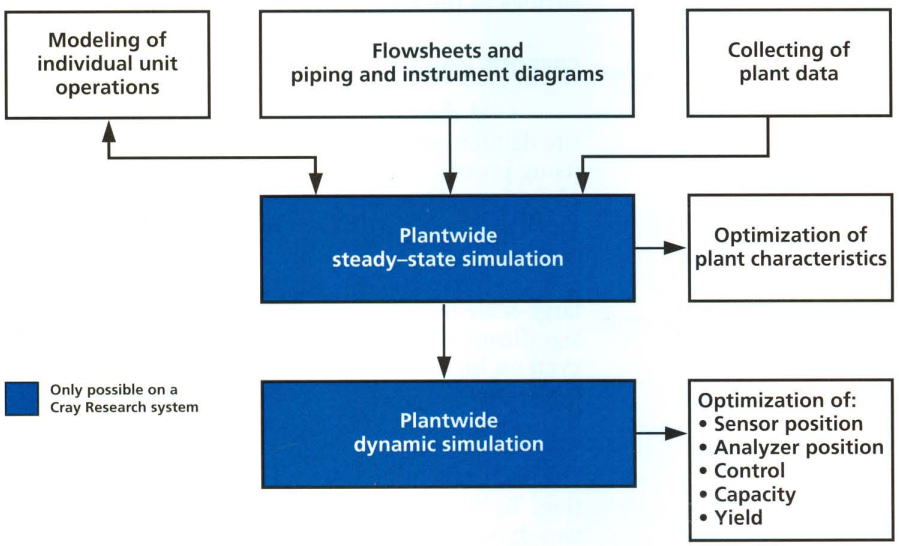


Figure 2 (below left). Debottlenecking and process control of chemical plants with the help of simulation.

# Sparse matrix methods

The fundamental mathematical problem for dynamic simulation is the solution of large, sparse differential-algebraic equation (DAE) systems. These systems arise from the algebraic equations and ordinary differential equations that describe the various process units, unit interconnections, and design specifications. The SPEEDUP program transforms the resulting DAE system into a set of nonlinear equations which is solved at various time steps using a Newton-type method. By simultaneously linearizing this set of equations, the key computational step, representing as much as 90 percent of the computation time on industrial problems, becomes the solution of large sparse linear systems.

The conventional sparse matrix methods in SPEEDUP use indirect addressing, which can degrade vector performance. By relying on vectorized dense matrix kernels, the frontal method provides much better performance on supercomputers. The basic idea is to factor a sparse matrix with a series of dense frontal matrices, each of which corresponds to one or more steps of the overall LU factorization. The Cray Research version of SPEEDUP uses the frontal code FAMP, which originated at the University of Illinois (Zitney and Stadtherr, 1993). It was later extended at Cray Research to include the use of BLAS2 and BLAS3 kernels and an out-of-core memory option for solving very large-scale problems. The extension also included separate analysis-factor, factor-only, and solve options for use in dynamic simulation.

Comparisons on a single processor of a CRAY C90 system using SPEEDUP show that FAMP is 267 times faster than Harwell's MA28 routine when solving a single linear system from the dynamic simulation of the Bayer distillation process (Table 2). Since slightly over 90 percent of the total solution time is spent in MA28, a tenfold improvement in overall SPEEDUP performance is gained by using FAMP.

| | | | Linear time (CPU seconds) | |
|---|---|---|---|---|
| Order | Nonzeros | % Sparsity | MA28 | FAMP |
| 75,724 | 349,716 | 99.994 | 854.8 | 3.2 |

Table 2. Comparison of sparse matrix methods on Bayer distillation problem.

reveals how much of the plant needs to be revamped to achieve a given increase in plant capacity. The plant characteristic found with the simulations indicated that to double capacity requires revamping only half of the plant. This translates into potential savings of several million dollars. But plant characteristics only provide optimal operating points. A method must be developed to run the plant at these optimal operating conditions regardless of load changes and varying feed conditions. Such a process control strategy requires dynamic simulation of the plant. Our dynamic simulations had the following objectives:

- ☐ Perform sensitivity studies to define the necessary process measurements (temperature, pressure, analyzers) for control purposes.
- ☐ Perform sensitivity analyses to define the control structure, i.e., which variable should be controlled by which manipulated variable. Determine if a conventional PID (proportional integral derivative) control can be used or if a more advanced control is required.
- ☐ Test the designed process control by simulation of load and setpoint changes of the complete plant, including controllers.

Figure 3 shows part of the sensitivity analysis for a heat-integrated distillation column. We are looking at an increase of the reboiler duty in the column. Figures 3a and 3b show temperature profiles along the column and concentration profiles of the main component in this column. The profiles are moving from the operating point (red line) upward. The time difference for the profiles is four hours, which provides excellent insight into the dynamics within this unit. From these sensitivity studies for all the manipulated variables

Figure 3. Sensitivity analysis and measurement selection.

3a

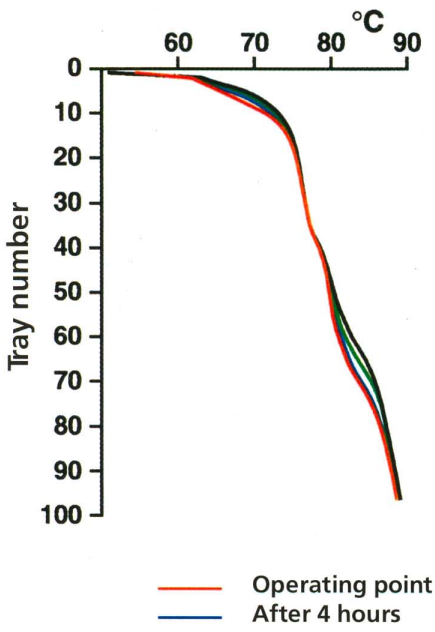


3b

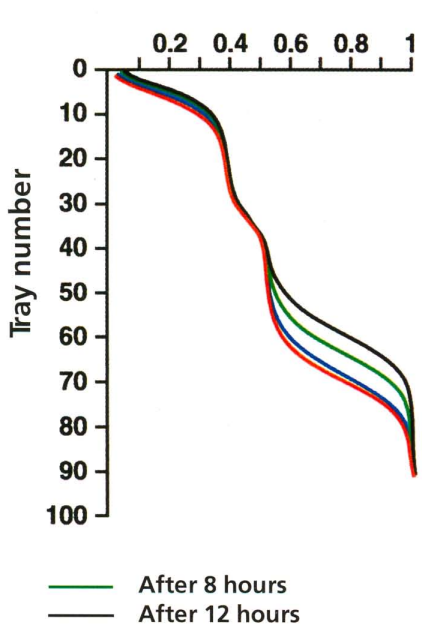


3c

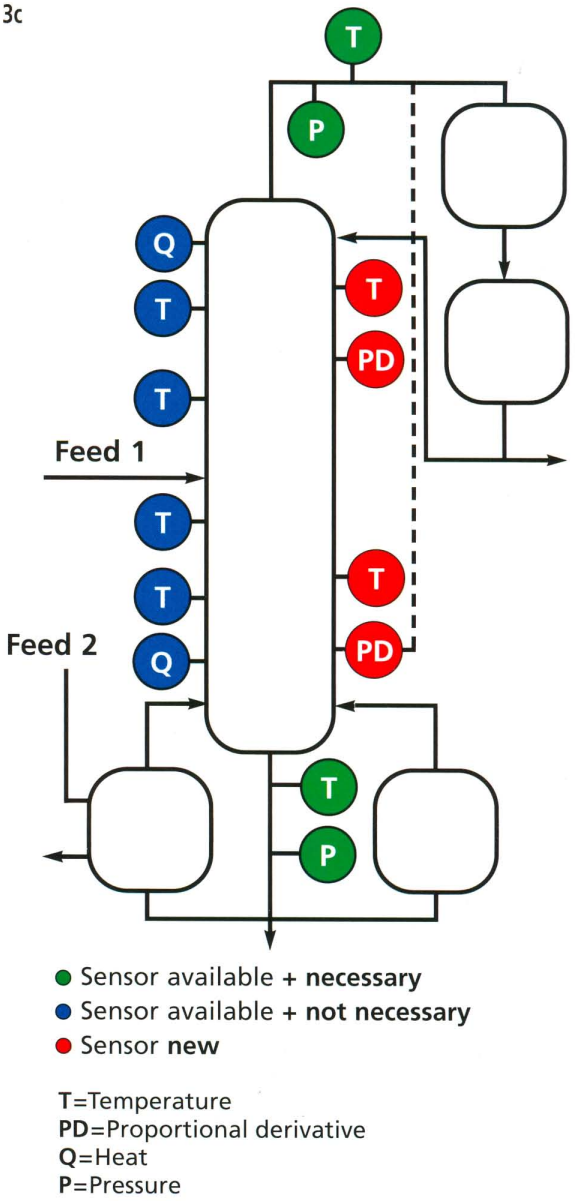


(approximately 30) in the plant, we can define the necessary process control measurements (Figure 3c). The chief result was that one-third of the existing analyzers on the plant were no longer necessary.

Based on the newly defined process control measurements, we developed a completely new control strategy for the plant, which will eventually lead to a fully automated operation. To test the new controllers in simulation, we first had to design all the controllers by evaluating the necessary controller parameters. Then controllers and plant models are simulated together to check the controllers' performance. The major points of interest in this case are disturbance rejection, for example the ability to handle changing feed conditions and decoupling. By decoupling we mean that we want as few influences as possible by one control loop on another one.

Being able to test all the controllers before actually implementing them on the plant saves a lot of troubleshooting and leads to a faster and more successful startup of the new controllers. Moreover,

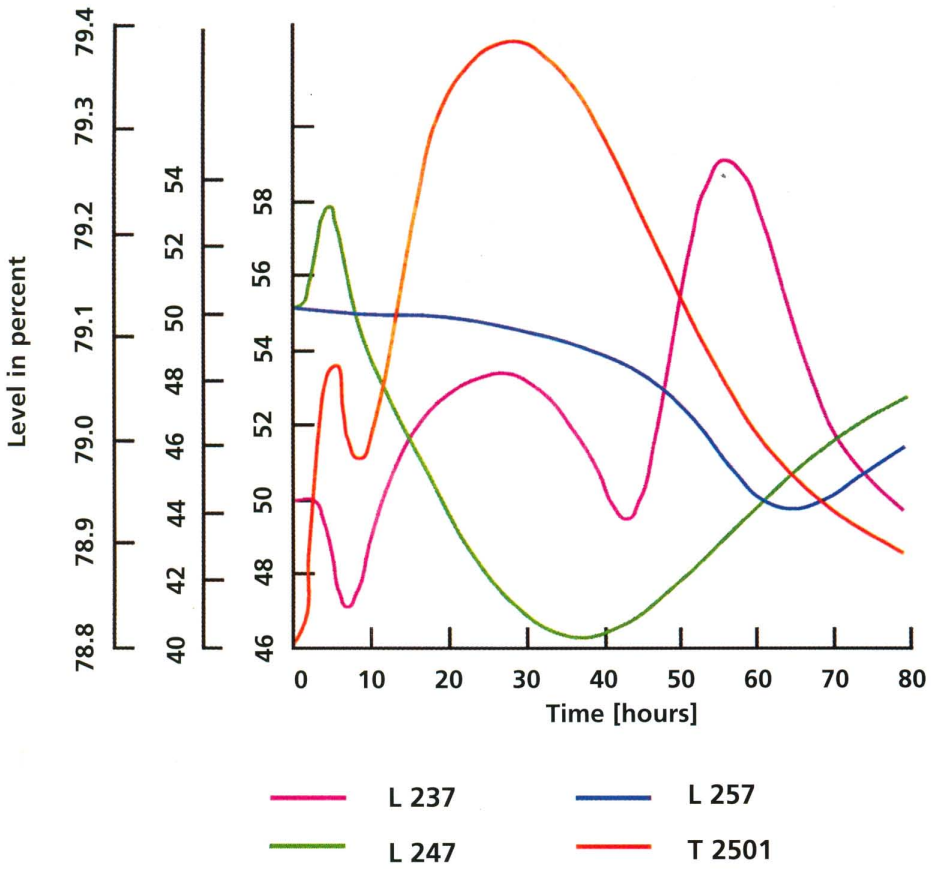


Figure 4. Dynamic plant behavior for a change in feed concentration.

the well-defined experiments, which we can do in simulation but which are virtually impossible in the real plant, lead to a much better understanding of the process and may also yield decisive directions for further optimization and, ultimately, a competitive advantage.

The enormous time constants within the plant are another interesting outcome of the simulation experiments with the complete plant model. Figure 4 shows the response of some level controllers for a simulation of 80 hours plant operating time for a change of feed concentration. Looking at these extremely long transients and keeping in mind that plant operators usually make some setpoint changes and perform some manual operations during their shifts, it became apparent that these operators never see the result of their manipulations, but a later shift does.

We concluded that plant operators should leave their process in automatic operation for as long as possible. This will require the operators to change their basic approach to work. Again, simulation can be helpful here by showing possible reactions of the plant controllers to disturbances, thereby leading to a faster acceptance of the process controller as a member of the team.

The results described above confirm that total plant simulation offers great potential for reducing operating and capital costs, leading to the optimization of chemical plant processes, such as Bayer's, and ultimately to a competitive advantage in quality, flexibility, and costs. The results of the joint project demonstrated to Bayer AG the effectiveness of dynamic simulation made possible by the high performance of the Cray Research supercomputer. To continue these efforts, Bayer AG has installed a CRAY C92 system at its Leverkusen facility. Bayer AG, Cray Research, and Aspen Technology plan to carry out further improvements in the capabilities and the performance of process simulation software. ▬


### *Acknowledgments*

*The authors wish to thank James Goom, Phil Mahoney, and Peter Ward of Aspen Technology, Inc. for their responsiveness and support in using SPEEDUP. We also wish to thank the Corporate Computing and Networking group at Cray Research for providing generous amounts of computer time on CRAY M90 and CRAY C90 systems in Eagan, Minnesota and Chippewa Falls, Wisconsin, and express our appreciation to Lori Gilbertson, Cindy Nuss, and Brian Kuznia of the Benchmarking Group at Cray Research for setting up the systems.*


### *About the authors*


*Ludger Brüll is a mathematician in the R&D Department at Bayer AG, Leverkusen. He is responsible for applied numerical methods and supercomputing in process engineering at Bayer. He received a Ph.D. degree in applied mathematics at the University of Cologne in 1983. He joined Bayer in 1986 and became professor of applied mathematics in Cologne in 1993.*

*Lothar Lang, process engineer in the R&D Department at Bayer AG, Leverkusen, is responsible for dynamic simulation and optimization of chemical plants at Bayer. He received a B.S. degree in chemical engineering from the University of Minnesota in 1983, graduated from the University of Karlsruhe in 1985, and received a Ph.D. degree from the University of Stuttgart in 1991. Lang joined Bayer in 1990.*

*Robert Zeller, sales support analyst with Cray Research GmbH, received a Ph.D. degree in theoretical solid-state physics from the Technical University of Braunschweig in 1973. Before joining Cray Research in 1987, he worked as a group leader in the German nuclear fuel industry for 11 years, managing the design and dynamic simulation of centrifuge cascades in the German uranium enrichment plant.*

*Stephen Zitney is group leader for the chemical process simulation project in the Applications Department at Cray Research, Inc. He received a B.S. degree in chemical engineering/engineering and public policy from Carnegie Mellon University, and M.S. and Ph.D. degrees in chemical engineering from the University of Illinois at Urbana-Champaign.*


### *References*


1. Fouhy, K., "Process Simulation Gains a New Dimension," *Chemical Engineering*, pp. 47-53, October 1991.
2. Sawyer, P., "Simulation on the Move," *The Chemical Engineer*, pp. 31-34, July 1991.
3. SPEEDUP User Manual, Vols. I and II, Version 5.4, Aspen Technology, Inc., Cambridge, Massachusetts, 1993.
4. Zitney, S. E. and M. A. Stadtherr, "Frontal Algorithms for Equation-Based Chemical Process Flowsheeting on Vector and Parallel Computers," *Computers & Chemical Engineering*, Vol. 17, No. 4, pp. 319-338, 1993.
5. Zitney, S. E., "Sparse Matrix Methods for Chemical Process Separation Calculations on Supercomputers," Supercomputing '92 Proceedings, (Minneapolis, Minnesota, November 16-20, 1992), IEEE Press Los Alamitos, California, pp. 414-423, 1992.

# Computational chemical design for CFC alternatives at DuPont

*David A. Dixon, Kerwin D. Dobbs, and Scott C. Walker, DuPont Central Science and Engineering, Experimental Station, Wilmington, Delaware*

Industry has become very conscious of the need to develop new materials and processes that have minimal impact on the environment. This is due, in large part, to the growth of our understanding about how manmade materials affect the environment. Because of the time and distance scales involved in environmental processes, numerical simulation has been shown to be a critical technology for assessing environmental impact. For example, experiments cannot be done many years into the future to assess the long-term impact of a chemical released into the atmosphere. There are a large number of elegant models of the environment, including local and global atmospheric models, groundwater models, and even global ocean models. One thing that all models have in common is the need for good input data. The better the data and the more extensive the model, the more accurately the model will predict physical reality.

Just as supercomputers are the primary tools for solving these large environmental models, they are also important tools for predicting the input data needed for the models. We need to know how various molecules will behave in the environment, and thus we need a good set of molecular

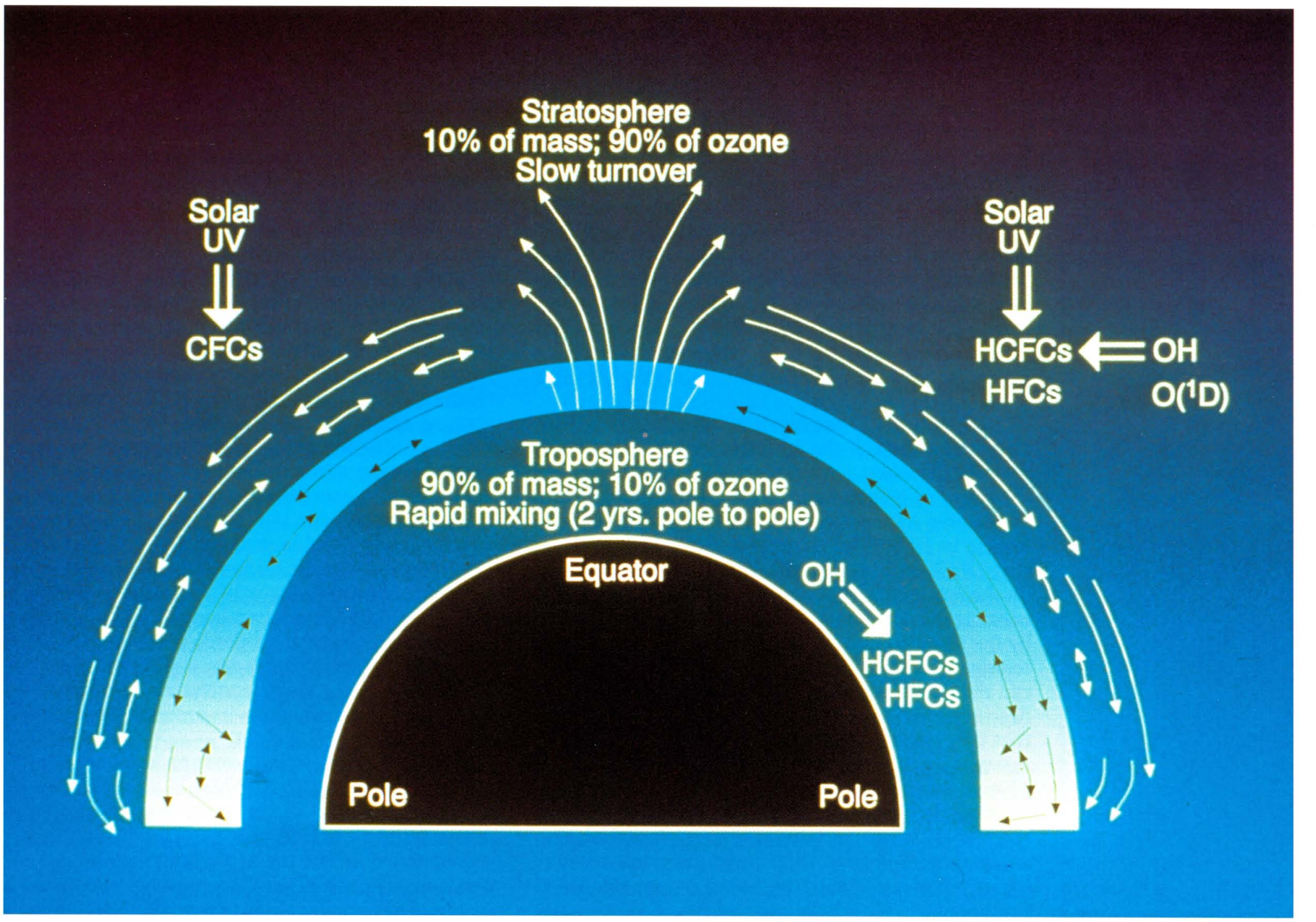


Figure 1. Simple schematic of the Earth's atmosphere showing circulation between the troposphere and stratosphere and the regions where the important chemistry occurs that leads to the decomposition of CFCs, hydrofluorocarbons (HFCs), and hydrochlorofluorocarbons (HCFCs).

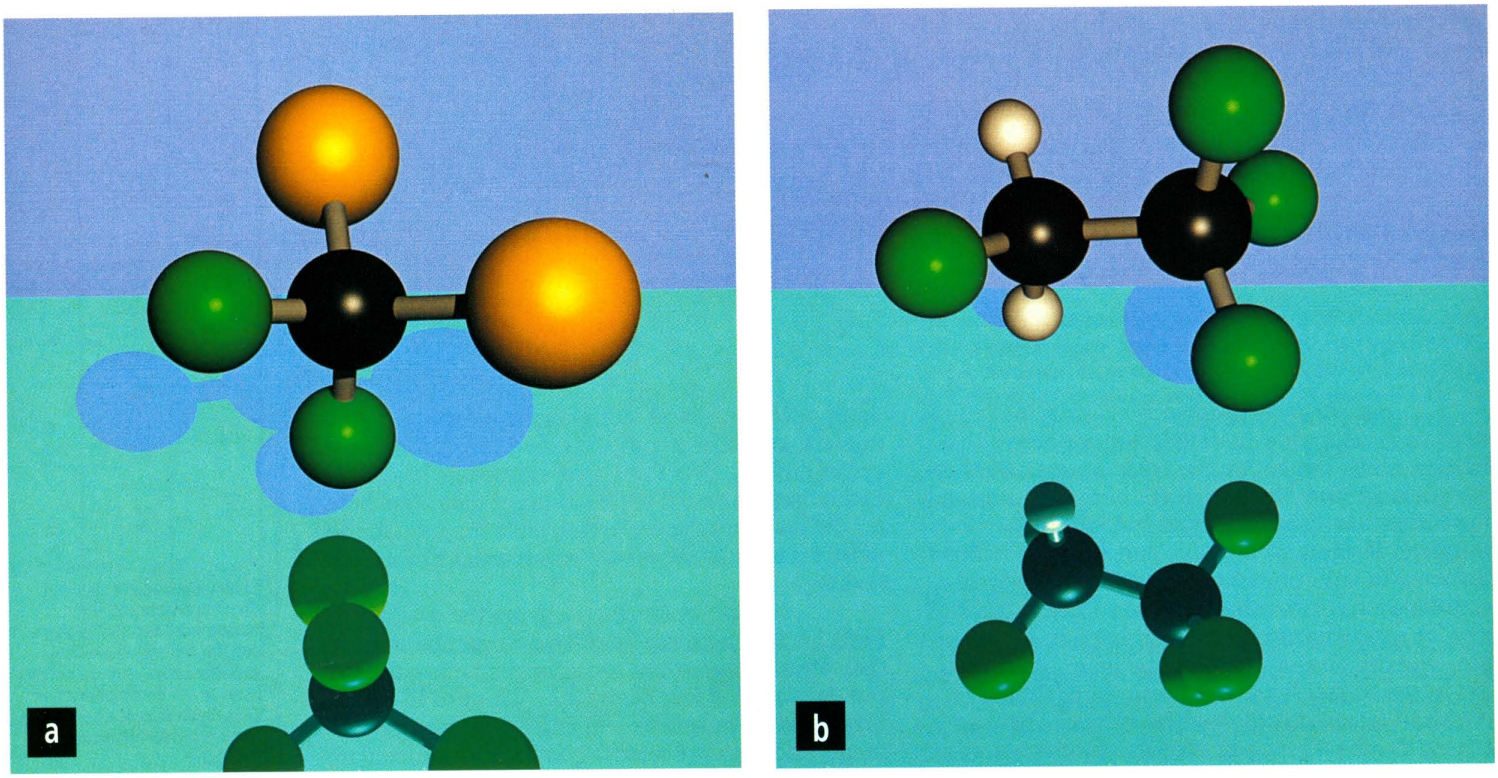


Figure 2. (a) Difluorodichloromethane ($CF_2Cl_2$), or CFC-12, is a common refrigerant being replaced by (b) 1,1,1,2-tetrafluoroethane ($CF_3CH_2F$), or HFC-134a. Figures were generated with the program OASIS on a CRAY Y-MP supercomputer from the ab initio molecular orbital predicted structures. Carbon is shown in black, fluorine in green, chlorine in yellow, and hydrogen in white.

properties. These properties can also be used as aids for scouting proposed synthetic pathways as well as for the development of manufacturing processes that are safe and inexpensive and have minimal environmental impact.

Chemical process design is another example of the use of high-performance computing on Cray Research supercomputers at DuPont to expedite the production of chlorofluorocarbon (CFC) alternatives. In one case, process simulations of a complex flowsheet led to the elimination of three unit operations in a chemical plant, resulting in capital savings of tens of millions of dollars.

## Replacements for the CFCs

Interest in the effect of trace gases on the chemical nature of the atmosphere began in the early 1970s when scientists raised concerns about the effect of $NO_x$ emissions from the proposed supersonic transport aircraft on stratospheric ozone levels.[1] In 1974, Molina and Rowland suggested that CFCs could have a similar deleterious effect on the amount of stratospheric ozone.[2] This occurs because the carbon-chlorine bond can be broken by the absorption of ultraviolet radiation, leading to release of chlorine atoms. The chlorine atoms can then participate in a catalytic cycle, leading to destruction of ozone. Although models suggested that CFCs could lead to ozone depletion, there was no strong evidence for such effects in the atmosphere. This situation changed with the observation of the ozone hole over Antarctica during springtime in the mid-1980s. A number of experimental measurements implicated chlorine as the prime reason for loss of ozone (Figure 1). This led to the Montreal Protocol in 1987, which would freeze CFC production to 1986 levels and lead to a cutback by 50 percent over the next decade. In early 1988, DuPont announced its decision to stop selling CFCs in developed industrial nations by the end of 1996. DuPont voluntarily committed to phasing out this production by the end of 1994. Subsequently, the U.S. Environmental Protection Agency (EPA) requested that DuPont make CFCs through the end of 1995 to meet current national needs.

CFCs have a wide range of applications, including coolants for refrigerators and air conditioners, blowing agents, electronic cleaning agents, and industrial solvents. These simple compounds have dramatically improved the quality of life. For example, 75 percent of the U.S. food supply requires refrigeration somewhere in the production and distribution chain. CFCs have a wide range of desirable properties, including being nonflammable, noncorrosive, nonexplosive, and very low in toxicity. They also have excellent physical characteristics, including appropriate boiling points, heat capacities, solubilities, and high stabilities, which make them compatible with many materials. Any alternatives need to have as many of the same properties as possible. The alternatives had to be chosen (or designed), synthesized, undergo property testing (Would they work as a drop-in replacement?), and tested for toxicity. Viable commercial production processes with minimal environmental impact also had to be developed.

CFCs can harm the ozone layer because of their chemical stability, which is also why they have been so safe to use in so many applications. This stability allows the CFCs to pass through the troposphere and into the stratosphere without decomposing. Knowledge of atmospheric chemistry suggested that compounds that could react rapidly

with hydroxyl radical would decompose in the lower atmosphere (upper troposphere) and thus have much shorter atmospheric lifetimes. Furthermore, if they do not contain Cl, then they should have zero ozone depletion potential (ODP). As concern was raised about ozone depletion, a similar concern arose about the greenhouse effect or global warming. As a result, not only does one have to design for minimizing the ODP of a compound, one also has to be concerned about its global warming potential (GWP).

## Molecular properties

To calculate molecular properties, we solve the Schrödinger equation for the motion of the electrons in a molecule. This solution for a many-electron wavefunction is not exact, and we have to use various approximations to solve it. One way to solve the equation is to use ab initio molecular orbital (MO) methods. Here we use the best possible description of the 1-particle space (the basis set) and of the *n*-particle space (the correlation energy treatment), given the computational resources and desired accuracy. Another technique for solving the electronic motion problem is to employ density functional theory (DFT). In this method, an approximation is made to the energy expression, and this expression is solved as exactly as possible in the limit of the 1-particle space that is used. Improvement of the approximations to the energy expression expressed as a function of the electron density should lead to an exact solution of the Schrödinger equation. In both cases, the solution as described so far yields only the energy and a wavefunction (or density) at a fixed nuclear geometry. One also needs to calculate the first derivatives of the energy with respect to the nuclear coordinates to find the optimum geometry and then to calculate various second derivatives (with respect to nuclear coordinates, applied electric field, etc.) to characterize whether the structure is a minimum and to calculate vibrational spectra. There has been much research over the past few years on how best to solve the MO and DFT expressions on high-performance computers to obtain the highest quality results with the least amount of computer time. There is considerable effort in a number of laboratories aimed at developing new methods, basis sets, algorithms, and interfaces and implementing them into usable code. The availability of such software has had a large impact on the field by making very sophisticated computational methods widely available and easily accessible. For example, the work described herein was done with the programs Gaussian 92 from Gaussian, Inc.,[3] GRADSCF from Polyatomics Research, and Cray Research's UniChem suite of programs. The calculations were carried out on DuPont's Cray Research supercomputers, beginning with a CRAY-1 system, then on CRAY X-MP and CRAY Y-MP systems. The success of this work together with the success of a number of engineering applications led to DuPont's decision to acquire a CRAY C94/364 system, which was installed in the first quarter of 1994.

The types of molecular properties needed to design the CFC replacements are defined, in part, by the data required for process and environmental models. An important technical problem that must be solved is the development of new catalysts for the economic production of CFC alternatives. The development of suitable catalysts is complicated by the increased reactivity of the desired products. Thus it is important to have thermodynamic data available for a wide range of molecules to design the best thermodynamic routes to the CFC alternatives. However, thermodynamic data has not yet been measured for many of the desired compounds. For example, experimental thermodynamic data is available for about 30 percent of the C1 and C2 compounds that contain F, Cl, and H as substituents. The unknown data such as heats of formation can be calculated from the electronic energies and the appropriate thermodynamic equations.[4] The molecular geometries and vibrational frequencies are needed to calculate the heats of formation. With this information, statistical thermodynamic expressions can be used to calculate the heat capacity and entropy of a system. With this data, a wide range of temperatures can be covered, the only issue being the validity of the statistical mechanical models. Other molecular properties such as dipole moments and charge distributions, which are useful in investigating materials compatibility, can also be calculated from the wavefunction.

The Cray Research supercomputers at DuPont were used to calculate the above properties for a large number of prospective CFC alternatives (or their precursors). We were able to provide essential data in a timely and cost-effective manner. A typical set of calculations of the thermodynamic properties of an alternative can be done in less than a week, including setup and analysis time, at a computational cost of less than $5000. Experimental measurements typically would cost $50,000, not including the time required to synthesize and purify reasonable amounts of the compound. The calculations clearly provide both an economic and time advantage and have given DuPont the most complete (and proprietary) library of thermochemical data for the CFC alternatives, which gives us an advantage in a very competitive global market.

One can extend the above calculations from stable, closed-shell species, with all of the electrons paired, to radicals, which have unpaired electrons and are very reactive. Because these molecules are difficult to characterize experimentally, predictions of their properties are very useful to experimentalists. Furthermore, if one can accurately predict the heat of formation of radicals, one can calculate important properties such as bond strengths, which are important in determining stability. Given such information, one can work out the thermodynamics for various reaction schemes as described below.

The pathway for atmospheric destruction of alternatives to the CFCs has been developed based on known species in the atmosphere and on hydrocarbon combustion chemistry. Although there is a significant amount of kinetic work on the initial reaction leading to the decomposition of a CFC alternative, very little is known about the actual thermodynamics governing the decomposition pathways, other than what has been obtained from

| Reaction | ΔH(kcal/mol) |
|---|---|
| $CF_3CH_2F + OH\cdot \rightarrow CF_3CHF\cdot + H_2O$ | −14.7 |
| $CF_3CHF\cdot + O_2 \rightarrow CF_3CHFOO\cdot$ | −37.7 |
| $CF_3CHFOO\cdot + H_2O \rightarrow CF_3CHFOOH + OH\cdot$ | 28.1 |
| $CF_3CHFOO\cdot + OOH\cdot \rightarrow CF_3CHFOOH + O_2$ | −39.5 |
| $CF_3CHFOOH + h\upsilon \rightarrow CF_3CHFO\cdot + OH\cdot$ | 45.2 |
| $CF_3CHFO\cdot \rightarrow HC(O)F + CF_3\cdot$ | −6.2 |
| $\rightarrow CF_3C(O)F + H\cdot$ | 9.0 |
| $\rightarrow CF_3C(O)H + F\cdot$ | 39.2 |
| $CF_3CHFO\cdot + O_2 \rightarrow CF_3C(O)F + OOH\cdot$ | −42.6 |
| $CF_3CHFO\cdot + H_2O \rightarrow CF_3CHFOH + OH\cdot$ | 9.8 |

Table 1 (above left). Atmospheric decomposition reactions for HFC-134a.

| | I (calculated) | I (experimental) |
|---|---|---|
| | **$H_2O$** | |
| $\nu_1$ | 2.24 | 2.24 |
| $\nu_2$ | 64.5 | 53.6 |
| $\nu_3$ | 44.7 | 44.6 |
| | **$CH_4$** | |
| $\nu_3$ | 72.9 | 65.7±4.2 |
| $\nu_4$ | 35.7 | 35.4±0.8 |

Table 2 (above right). Absolute infrared intensities (km/mol) for $H_2O$ and $CH_4$.

simple models. Because of this lack of information, we have calculated as much of the thermochemistry as possible based on ab initio MO methods and the few pieces of known experimental data. A summary of the results for important steps for HFC-134a ($CF_3CH_2F$), an important refrigerant replacement (Figure 2), is shown in Table 1.

Up to this point, only properties at the endpoints of chemical reactions have been discussed. These properties can tell us whether a reaction will proceed or not, but they tell us nothing about how fast the reaction could occur; this requires rate constants. Knowledge of rate constants is extremely important if one wants to understand environmental effects from a microscopic viewpoint. For example, a simple expression for the relative global warming potential is given by Equation (1) relative to a standard compound denoted by subscript:

$$\text{Relative GWP(per lb.)} \sim I(IR)/I_o(IR) \cdot \tau/\tau_o \cdot M_o/M \quad (1)$$

with $I(IR)$ the infrared absorption of a compound, $\tau$ the atmospheric lifetime of a compound, and $M$ its molecular weight. Thus, the atmospheric lifetime is required for the prediction of the GWP of a compound. The atmospheric lifetime is also critical for determining the potential for ozone depletion.

As shown in Equation (1), the intensity of the infrared transitions in the appropriate region is required. The important absorption region in the atmosphere is the window between 500 and 1250 $cm^{-1}$ where $H_2O$ does not absorb. $CO_2$ is the largest absorber due to the amount of it in the atmosphere, and it absorbs between 600 and 800 $cm^{-1}$. Absorptions in the region of 800 to 1250 $cm^{-1}$ could lead to an increased GWP. Experimental measurements can be made, but significant care is required, and the systematic errors can be large. It is possible to calculate such transitions quite accurately for two simple compounds that are important in the atmosphere, $H_2O$ and $CH_4$ (Table 2). Density functional theory was used to predict these intensities. The agreement between the calculated and experimental intensities is excellent.

CFC replacements must not only have properties compatible with those of CFCs, but also react rapidly and decompose in the troposphere. Based on the known radicals in the troposphere, it was suggested that alternatives should contain a hydrogen atom so that the following reaction with the relatively abundant hydroxyl radical would occur:

$$R\text{-}H + OH\cdot \rightarrow R\cdot + H_2O \quad (2)$$

Rate constants for Reaction (2) are known for some R-H but not all are available. We thus developed a method to calculate the rate constants for Reaction (2) by using ab initio molecular orbital theory in combination with transition state theory. To obtain a benchmark calculation,[5] we studied the reaction of the simplest R, R=$CH_3$, as shown in Reaction (3).

$$CH_4 + OH\cdot \rightarrow [H_3C\text{—}H\text{—}OH]^{\ddagger} \rightarrow CH_3\cdot + H_2O \quad (3)$$

This reaction is important in its own right in terms of global warming due to natural releases of $CH_4$ and in combustion chemistry. A very large

Figure 3. Rate constant k($cm^3$ $molecule^{-1}$ $sec^{-1}$) for Reaction (3) as a function of temperature T (K).

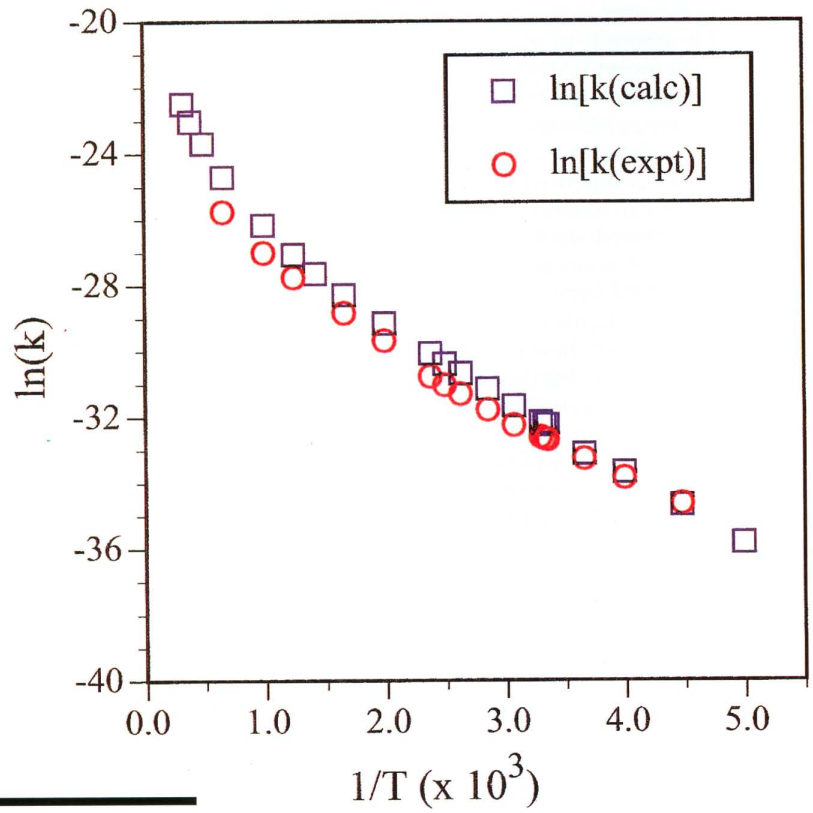

basis set was used with a high level treatment (QCISD(T)) of the correlation problem. Figure 3 shows a comparison of calculated and experimental rate constants. Over the temperature range of 200 to 1500 K the calculated rate constants are within a factor of 2 of the experimental values. Thus, we can predict such rate constants quite accurately if the calculations carefully treat both the 1-particle and *n*-particle spaces.

Of course, the reaction with OH· is just the first step in the atmospheric decomposition cycle. Although the compound can be destroyed before it damages any ozone or leads to significant global warming, one must consider the ultimate fate of anything released into the environment. As shown in Table 1, a number of processes lead to the formation of the alkoxy radical $CF_3CHFO\cdot$. The lifetime of this very reactive and unstable species is critical to the determination of the ultimate degradation products. The lifetime of this species is short, on the order of microseconds. The important question is whether reaction with oxygen to form $CF_3C(O)F$ will occur before decomposition to form HC(O)F. These two carbonyl compounds have quite different environmental loss mechanisms. There are no direct experimental measurements of the lifetime of the alkoxy radical. Although we would like to calculate the rates of both the unimolecular decomposition reaction and the reaction with $O_2$, the latter is still beyond our capability if we desire high accuracy due to the different spin interactions. However, we can study the decomposition process by both MO and DFT methods, which can be used to bracket the lifetime and provide information about the activation energy and the pre-exponential factor for the rate constant when combined with unimolecular decomposition theory. The calculations show that the radical's lifetime is on the order of 0.3 to 10 microseconds and suggest that the decomposition process should be significantly faster than the reaction with $O_2$. The calculations also allow us to study the nature of the electron distribution in the transition state which cannot be done experimentally. This is shown in Figure 4 for the electron density at the transition state, which was calculated with the DGauss program in the UniChem software package.

## Summary

Predicting molecular properties as accurately as possible by using the techniques of electronic structure theory is very valuable. The calculated properties provide qualitative insight and good numerical values that can be used to design new processes and provide input data for environmental models. This helps reduce the cost to manufacture and produce environmentally safe materials by shortening development time and by allowing one to scout a broader range of materials. Furthermore, the calculations can provide us with information about properties, such as the electron density at a transition state, which cannot yet be measured experimentally. The simulations are needed to understand the entire product life cycle from conception and discovery to a product's final fate in the environment. ▬

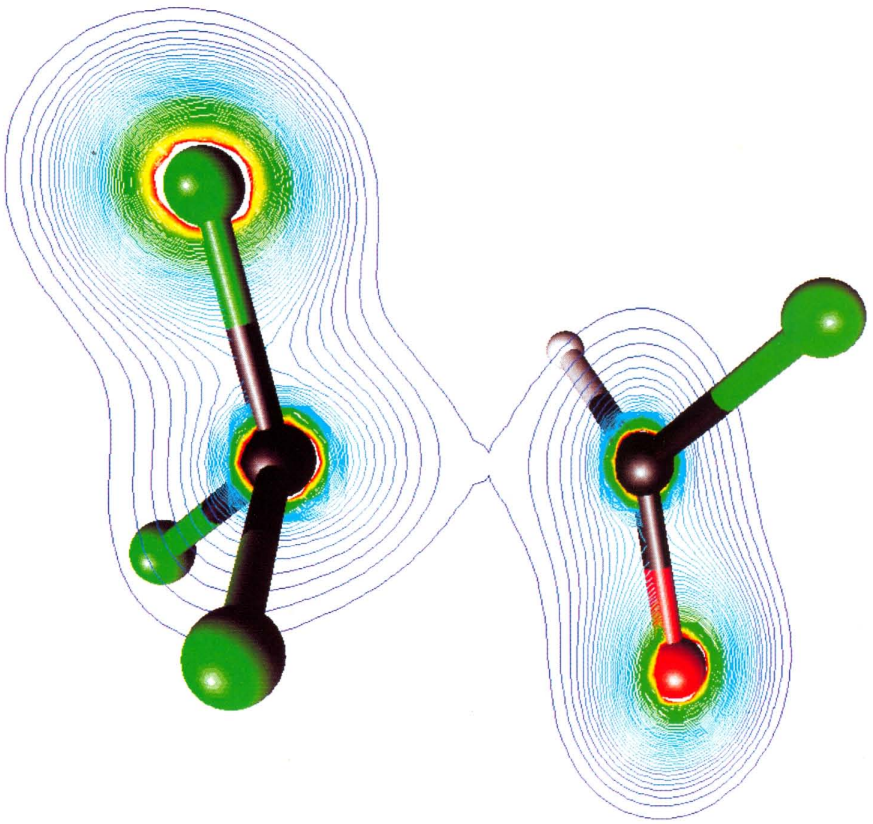

Figure 4. Electron density at the transition state for the unimolecular decomposition of $CF_3CHFO\cdot$ into $CF_3\cdot$ and HC(O)F. Transition state optimized at the nonlocal DFT level with the program DGauss from the UniChem package. Contours displayed from 0.26 to 15.0 e/Å$^3$ with an interval of 0.2 e/Å$^3$ by using the UniChem interface on a Silicon Graphics workstation.


### *About the authors*

*The authors are members of the research staff at DuPont's Science and Engineering Laboratories at the Experimental Station in Wilmington, Delaware. David Dixon is a research fellow and research leader. He received a B.S. degree from the California Institute of Technology and a Ph.D. degree in physical chemistry from Harvard University. Kerwin Dobbs is a research chemist. He received a B.S. degree from William and Mary College and a Ph.D. degree in physical chemistry from the University of California-Irvine. Scott Walker is a research technician. He received his education at Carnegie-Mellon University and Newman College. The authors' primary research interest is the computational solution of problems in the chemical industry, with a focus on molecular electronic structures.*


### *References*


1. Johnston, H. S., *Annual Reviews of Physical Chemistry*, 1992, Vol. 43, p. 1.
2. Molina, M. J. and F. S. Rowland, *Nature*, 1974, Vol. 249, p. 810; Rowland, F. S., *Annual Reviews of Physical Chemistry*, 1991, Vol. 42, p. 731.
3. *Gaussian 92*, Frisch, M. J., G. W. Trucks, M. Head-Gordon, P. M. W. Gill, M. W. Wong, J. B. Foresman, B. G. Johnson, H. B. Schlegel, M. A. Robb, E. S. Replogle, R. Gomperts, J. L. Andres, K. Raghavachari, J. S. Binkley, C. Gonzalez, R. L. Martin, D. J. Fox, D. J. DeFrees, J. Baker, J. J. P. Stewart, J. A. Pople, Gaussian Inc., Pittsburgh, Pennsylvania,1992.
4. Dixon, D. A. and B. E. Smart, *Chemical Engineering Communications*, 1990, Vol. 98, p. 173; Dixon, D. A., *Journal of Physical Chemistry*, 1988, Vol. 92, p. 86.
5. Dobbs, K. D., D. A. Dixon, and A. J. Komornicki, *Journal of Chemical Physics*, 1993, Vol. 98, p. 8852.

# Studies of biomembranes by supercomputer

*Terry R. Stouch, Donna Bassolino, and Howard E. Alper,*
*Bristol-Myers Squibb Pharmaceutical Research Institute, Princeton, New Jersey*

*Biological membranes (biomembranes) play crucial roles in physiology and biochemistry. As the outer covering of cells, organelles, and viruses, biomembranes compartmentalize biology and regulate the passage of nutrients, ions, and messenger molecules, such as hormones, into and out of cells and organelles. This regulatory function allows the propagation of nerve impulses, the transport of glucose, and the growth and differentiation of cells.*

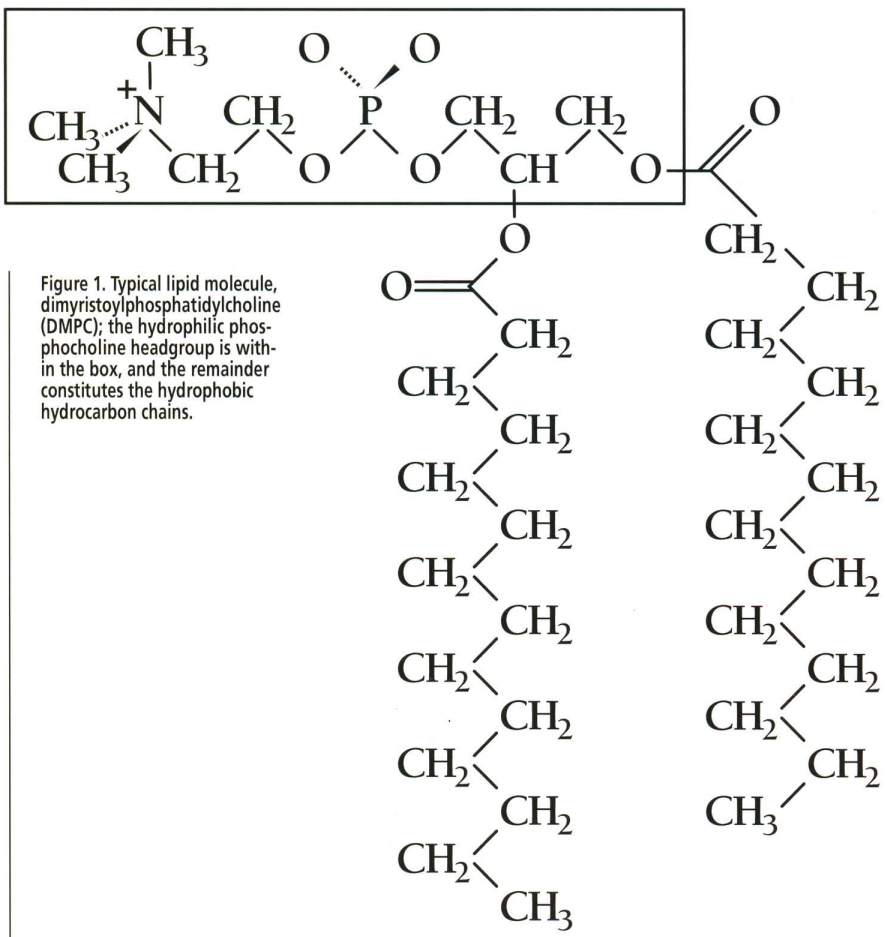

Figure 1. Typical lipid molecule, dimyristoylphosphatidylcholine (DMPC); the hydrophilic phosphocholine headgroup is within the box, and the remainder constitutes the hydrophobic hydrocarbon chains.

Implicit in these functions is the membranes' other important role—to contain the many proteins that regulate biochemical mechanisms. For example, the ion channels that propagate nerve signals are quite large proteins with many membrane domains. The messages transmitted by many messenger molecules are perceived by and transducted into the cellular interior by other large proteins, the seven transmembrane domain G-protein linked receptors. A proper understanding of membrane structure and function is central to an understanding of much of biochemistry.

Biomembrane structures are composed of lipid molecules and proteins. Lipids are amphiphilic molecules: they have both a polar, hydrophilic (water loving) portion that interacts favorably with water and a nonpolar, hydrophobic (water avoiding) portion that, with other hydrophobic molecules, sequesters away from water as demonstrated in Figure 1. In water, the joint hydrophilic and hydrophobic nature of lipids allows them to form many supermolecular assemblies, such as micelles, vesicles, and bilayers. The bilayer, a planar structure, is the most important of these assemblies to the membrane. In the bilayer, the lipids form two layers in which their polar regions interact with water and each other. The hydrophobic regions sequester away from water by interacting with hydrophobic regions of other lipids. The lipid molecules form close relationships with integral membrane proteins that penetrate and protrude on both sides of the bilayer plane. Peripheral membrane proteins that stud the bilayer surface are less closely associated with the bilayer surface and penetrate only partially into the membrane, as shown in Figure 2.

At physiological temperatures and conditions of solvation, lipid molecules experience a great deal of motion, within both the whole bilayer struc-

ture and the bilayer's constituent lipid molecules. This makes lipid bilayers and membranes very fluid, which is important to their proper functioning. In fact, one important role for cholesterol and unsaturated fatty acids is to serve as mediators through which cells control the fluidity of membranes as external conditions, such as temperature, change. Unfortunately, this motion, so important to proper function, also makes experimental study of biological membranes difficult. Experimental methods are just beginning to uncover details of their structure, motion, and function. A view at the atomic level has been particularly elusive, yet an atomic level view is essential to a detailed understanding of many biochemical phenomena and for rational drug design to progress.

To gain an atomistic understanding of biomembrane structure and motion, we use atomic-level molecular dynamics simulations[1-4] to study details that are difficult or impossible to obtain experimentally. Our goals are to

- Reproduce, explain, and coordinate available experimental data on membrane structure and dynamics
- Understand the permeation of membranes by small molecules, such as drugs, and
- Understand the relationships between membranes and membrane proteins.

At the heart of these classical molecular dynamics simulations is a set of potential energy functions that provide the energies and forces of the interactions between pairs of atoms. These interactions include covalent, or intramolecular, interactions such as atom-atom bond stretching, bending of the angle formed by three consecutive atoms, and dihedral angle rotation about an atom-atom bond. Interaction between atom pairs also includes van der Waals and electrostatic intermolecular interactions. We can calculate the trajectories of individual atoms by applying Newton's equations of motion to the positions and velocities of the atoms and the forces acting on them. These trajectories can be averaged to calculate bulk properties of the system or used directly to study dynamical properties of the molecules. The key role of the potential energy functions in every aspect of the simulations has led us to closely examine them, verify their ability to duplicate known properties, and develop a new generation of force fields.[5-9]

Such simulations can be very computationally intensive and would be impossible without the current generation of supercomputers. The molecular models we simulated typically required many thousands of interaction sites. Many of the important biochemical system interactions are quite long-range and require many site-site interaction calculations for their evaluation. Furthermore, many of the motions of interest must be simulated over a period of nanoseconds, instead of over a period of hundreds of picoseconds, which is a more convenient simulation timescale.

So that calculated properties could converge, each simulation was conducted for at least 1 nanosecond, which is 1,000,000 molecular timesteps of 1 femtosecond. Simulations of this magnitude could only be conducted on a supercomputer such as our CRAY Y-MP system. As it turned out, each timestep required from 1.5 to 5 seconds of CRAY Y-MP processor time; consequently, to run a 1-nanosecond simulation, we used from 17 to 58 CPU-days of the CRAY Y-MP system. Substantial code development and modification were also required to conduct and study these simulations—the Cray Research programming environment, productivity tools, and scientific staff accelerated this work.

## Reproduction of experimental data

In pursuit of our first goal, the reproduction of experimental data, we performed simulations on pure bilayers of lipids (dimyristoylphosphatidylcholine) in water.[1-4] We based our starting models as closely as possible on experimental data. Although little atomic-level data on membrane structures was available, we used the known molecular structures of lipid molecules to build a bilayer structure whose general shape and size (thickness, surface area per lipid, amount of water) were determinable from experiment. This resulted in models of 7,000 to 10,000 atoms, equal to the number of sites of interaction. We used simulations of many nanoseconds in duration (of reasonably long length for biomolecular simulations) to evaluate the models, the potential energy functions, and the simulations themselves. The simulation lengths were based on the timescales of the motions within the bilayer.

Some of the more important events, such as torsional isomerization (internal movement within a molecule due to rotation about atom-atom bonds) of various parts of the molecules, are known to take from tens to hundreds of picoseconds, depending on the part of the molecule in question and its position within the bilayer. Lengthy simulations are often required to reliably calculate properties that are influenced by the longer-scale motions.

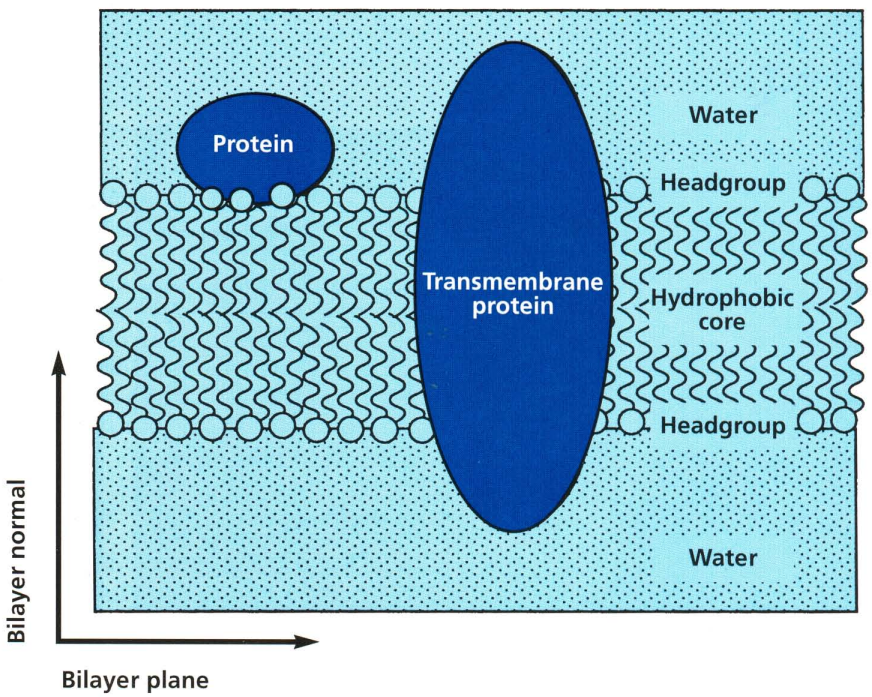


Figure 2. Schematic of a biological membrane showing the bilayer structure, an integral membrane protein traversing the bilayer, and a peripheral membrane protein associating with one face of the bilayer.

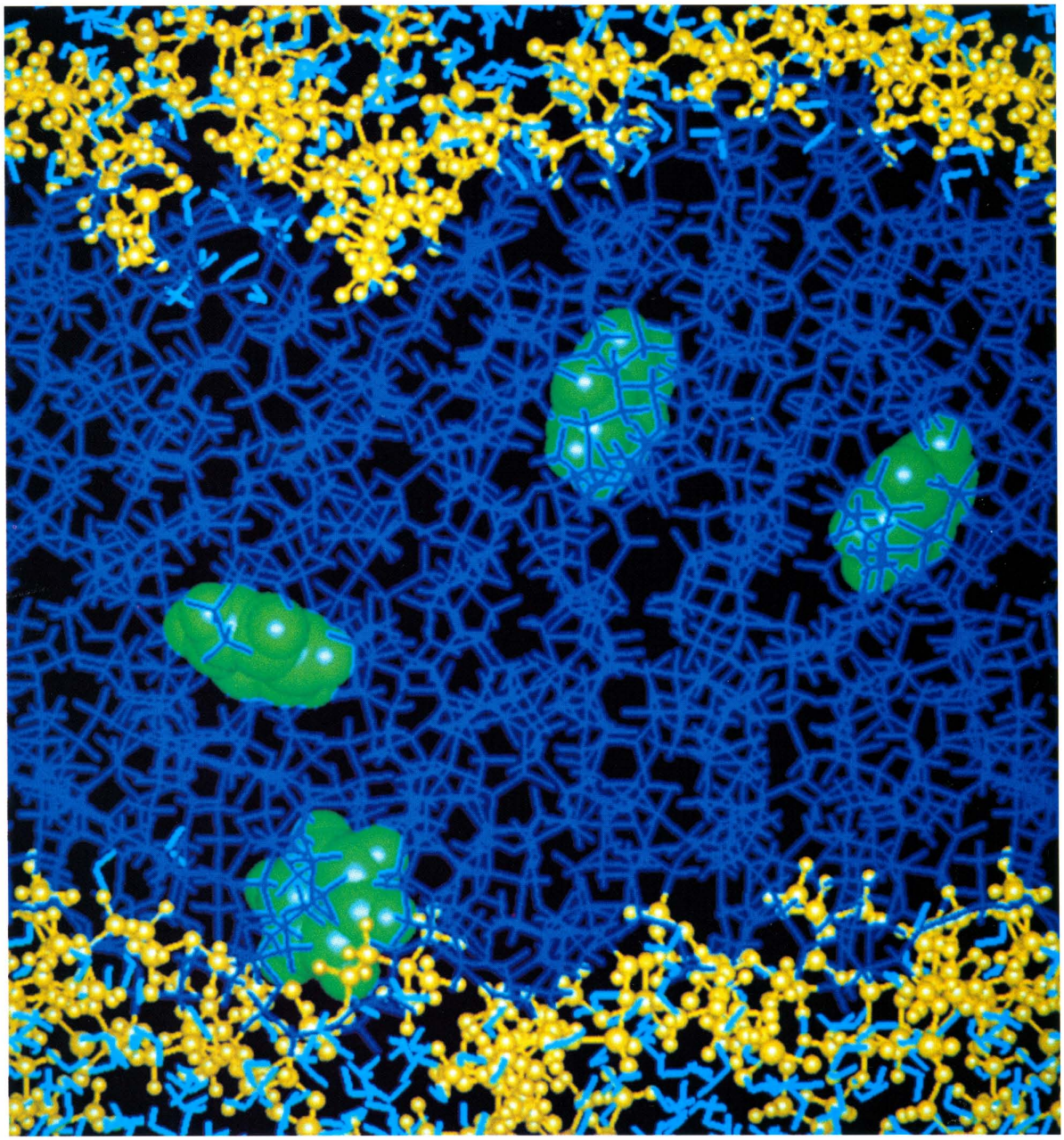

Figure 3. Snapshot from a simulation of four benzene molecules (green) in a fully-hydrated DMPC bilayer after several hundred picoseconds of simulation. Cyan, water molecules; yellow, polar headgroup atoms; dark blue, hydrophobic core (hydrocarbon chains).

Although the bilayers were responsive and fluctuated as expected during the simulations, they were also quite stable. More importantly, structural and dynamical properties of the bilayers (such as thickness, order of the hydrocarbon region, and orientation of the polar groups) that were calculated from the simulations agreed well with those determined from experiment. These results gave us confidence that we could obtain physically and biochemically significant results from the simulations.

## Bioavailability simulations

Bioavailability, the ability of a drug to travel from its site of administration to its site of action, is an important problem in the pharmaceutical industry. The development of many promising drugs has been abandoned because, although the drugs perform well in the test tube, in more complex systems (such as in animals) they fail to arrive at their site of action in sufficient quantity to elicit the desired response. In many cases, bioavailability is determined by a drug's ability to penetrate membranes. A substantial amount of time, effort, and money could be saved if a drug's ability to permeate membranes could be predicted by computer early in the drug design and development process.

To address this issue, we have been using computer simulation to study the diffusion of small, drug-sized molecules through lipid bilayers as shown in Figure 3.[10] These simulations have been very effective at explaining experimental data and bridging the gap between experiment and abstract theory. Diffusion coefficients and rotational correlation times calculated from the molecular dynamics trajectories are quite close to those determined from experiment for similar molecules. In addition to duplicating known properties, the simulations can

provide information that is difficult to determine from experiment. It has long been assumed that membranes could be modeled as a simple two-state system, a water (hydrophilic) region and an organic (hydrophobic) region. However, our studies of tens of nanoseconds of the process of diffusion show us that this process is quite complex, partly because the membrane is more complex than the two-state model. Amid the complexity, the simulations have clarified several important features of the diffusion of small particles within the membrane and of the structure of the membranes. We find that diffusion is fastest in the nonpolar center of the bilayer and slows as it approaches the water-lipid interface. This suggests a gradient of structural and dynamical properties within the membrane which is substantially different from the two-state, water/organic model. This finding also indicates that the step of crossing the lipid/water interface is the rate-determining step in the penetration of the membrane by a drug, as previously suggested by both experiment and theory. Such knowledge will help concentrate our studies on those stages of transport most crucial to rapid membrane permeation. It is rewarding to see that these results agree with experiment and theory.

Bioavailability simulations provide more than just the numerical estimates of diffusion rates. The atomic-level detail allows us to probe the diffusion mechanism, and the reasons for the differential rates of diffusion in the different membrane regions become clear. We find that in the membrane center, small molecules diffuse partially by large, rapid jumps between spontaneously arising voids between the hydrocarbon chains of the hydrophobic regions of the lipid molecules. Both experiment and simulation have shown this region to be of low density, and the presence of voids is expected. Movement between the voids is partly controlled by rotation within the hydrocarbon chains about the carbon-carbon covalent bonds. Rotation about such bonds allows the molecules' atoms on either side of these

Figure 4. Two snapshots of the trajectory of the diffusion of benzene from one region of the bilayer to another showing the "gating" of the "hop" by the lipid hydrocarbon chain. (Colors as in Figure 3 with the exception of the gating lipid, shown with cyan (hydrocarbon chains) and yellow (headgroup) spheres representing the molecule's atoms.) Below left, prehop, the lipid molecule's hydrocarbon chain prevents the passage of the benzene molecule between voids. Below right, posthop, after the lipid's hydrocarbon chain has moved aside (due to torsional interconversion of one dihedral) to allow the benzene molecule to move to the current void.

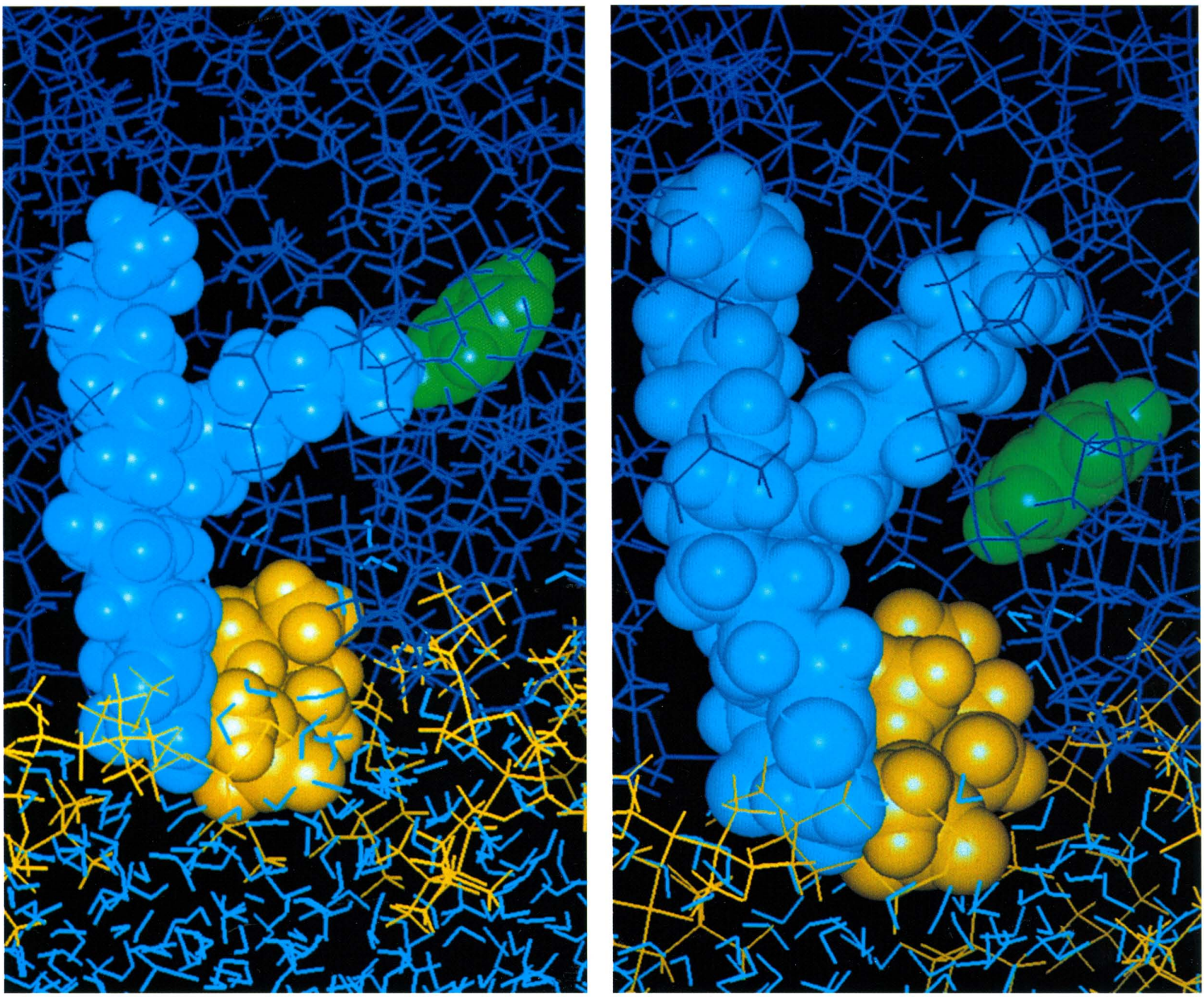

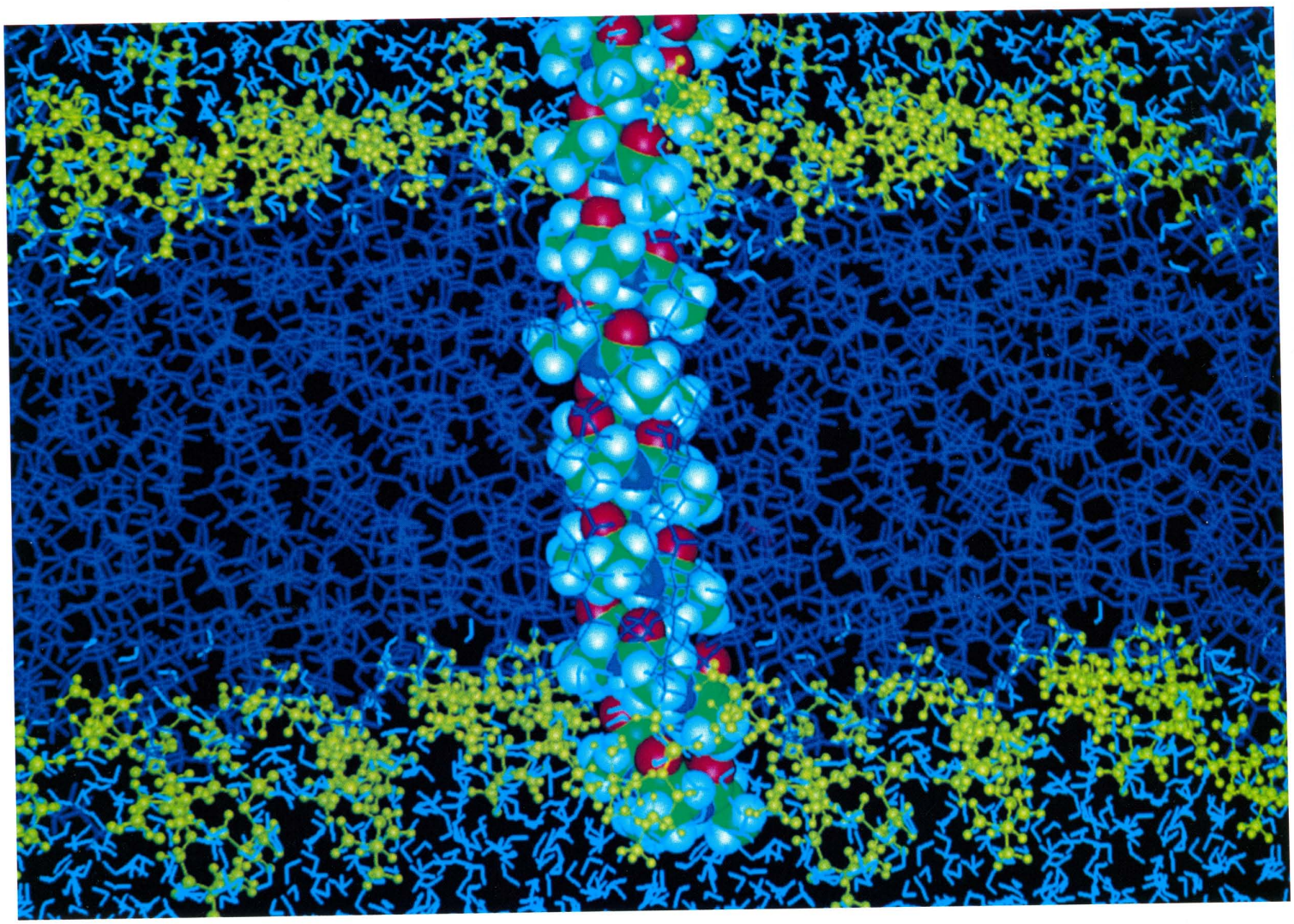

Figure 5. A snapshot from the simulation of a transmembrane protein alpha-helix in a lipid bilayer.

bonds to move in relation to each other. Although the polar regions of the lipid molecules are held in place by interactions with neighboring polar groups and with water, the hydrocarbon chains are fairly free to move. Rotations about the carbon-carbon bonds allow portions of the hydrocarbon chains to swing about in the hydrocarbon region. As the chains swing, they act alternately as walls of voids to constrain the diffusing molecules in place, and when they swing aside, as open doors between voids through which the molecules move as shown in Figure 4.

The membrane center differs from the water interface in that the latter, due to strong electrostatic interactions between the polar groups and water, is dense and tightly packed. Voids, such as those seen in the center, are essentially non-existent. In addition, rotation about the carbon-carbon bonds is known, both from experiment and simulation, to be slower closer to the interface. The simulations show that the two key factors to rapid diffusion in the membrane center—the presence of voids and the ability to move between them—are both less abundant and less frequent toward the water interface, making diffusion slower.

These studies teach us about the process of diffusion and give us insight into biomembrane structure by making clear the gradient in structure from the membrane center toward the water interface. To date we have studied several aspects of the mechanism of diffusion and find that in addition to membrane structure, other factors including diffusant size, polarity, and hydrogen bonding capacity influence a molecule's progression through biological membranes.

## Membrane proteins' relationship to lipid components

Another of our goals is to understand the structure and function of membrane proteins and their relationship to the lipid components of the membrane. These proteins are very complex, and many facets of their structure and function are not well understood. For example, although it is widely accepted that the alpha helix is a principal building block of membrane proteins, it is not obvious how these helices orient within the membrane or how they interact with other helices or other proteins at the atomic level. It is also not known just how the lipid molecules interact and pack with the proteins. To explore these different facets, we are performing molecular dynamics simulations of simple models of membrane

proteins. These models are designed to isolate particular aspects of their function.

A large amount of data suggests that a common structural motif of membrane proteins is the alpha helix, so we have begun studies of one of the simplest of alpha helices, one made exclusively of the simple amino acid alanine, as shown in Figure 5. We find that when inserted into the membrane, the polyalanine helix displays a wide range of motion, including diffusion within the plane of the membrane, "bobbing" perpendicular to the membrane, and tilting on its axis. An alpha helix's structure is defined by the pattern of hydrogen bonds (primarily electrostatic interactions involving hydrogen atoms) between the individual amino acids within the polymer. Within the hydrophobic core of the membrane, where the protein can hydrogen bond to only itself, the network of hydrogen bonds is quite stable. Although the helix fluctuates, it is maintained at close to the ideal geometry for such a structure. However, at the water interface, where the protein encounters water and the lipid polar region, both of which can form hydrogen bonds with the protein, the network is almost immediately broken, and the helix denatured. The simulations show that this water interface is quite rough and can range over several turns of the helix. Coupled with the bobbing motion, the length of the helix that must be considered to be exposed to the membrane/water interface is larger than what was previously expected. It also appears that the helix in this region can break and reform within this region as the protein itself moves and as the lipid molecules themselves fluctuate, changing the profile of the membrane/water interface.

The polyalanine helix is far simpler than an actual membrane protein, but it serves as a useful benchmark for studies of more complex proteins. Through relatively minor changes to the helix—for example, substituting a few of the alanine monomers with other amino acids—we can study in detail how other amino acids that are commonly found in transmembrane proteins alter the properties.

Although much needs to be done, these supercomputer simulations allowed us to make significant progress toward our goals of understanding membrane protein structure and drug diffusion. We have also learned some important lessons about the biochemistry of membranes. The ability to study these biochemical systems in atomic detail is a valuable tool that augments the understanding of these systems gained from experiment. ▬


### *Acknowledgments*

*We are indebted to Richard Shaginaw (Bristol-Myers Squibb), John Stringer (Cray Research, Inc.), Stewart Samuels, (BMS), Richard Gopstein (BMS), and Gregory Burnham (BMS) for building, orchestrating, and maintaining our Cray Research/Silicon Graphics high-performance computing and graphics network. John Mertz (CRI) was responsible for optimizing the version of the Discover (Biosym Technologies, Inc.) program used for these studies. We thank J. Villafranca (BMS) and J. Novotny (BMS) for encouraging these studies.*



### *About the authors*

*Terry Stouch is a senior research investigator in the Exploratory Research Division of the Bristol-Myers Squibb Pharmaceutical Research Institute in Princeton, New Jersey. Before this, he was a research scientist in the x-ray protein crystallography laboratory at the Naval Research Laboratory (NRL) in Washington D.C. and an independent consultant. He earned a Ph.D. degree in chemistry and a B.S. degree in biochemistry at the Pennsylvania State University.*

*Howard Alper is currently a postdoctoral fellow under the direction of Terry Stouch at the Bristol-Myers Squibb Pharmaceutical Research Institute. Before this, he was a postdoctoral fellow at Rutgers University under Ronald Levy. He received a Ph.D. degree in chemical physics from Columbia University in 1987 with Bruce Berne.*

*Donna Bassolino-Klimas is currently a research investigator at the Bristol-Myers Squibb Pharmaceutical Research Institute. She obtained a Ph.D. degree in biophysical chemistry in 1989 with Ronald Levy. After a postdoctoral fellowship at BMS, she joined the Macromolecular Structure group.*


### *References*


1. Stouch, Terry R., "Lipid Membrane Structure and Dynamics Studied by All-Atom Molecular Dynamics Simulations of Hydrated Phospholipid Bilayers," *Molecular Simulations,* Vol. 10, No. 2-3, pp. 317-345, 1993.
2. Stouch, Terry R., Howard E. Alper, and Donna Bassolino, "Supercomputing Studies of Biomembranes," *International Journal of Supercomputer Applications,* 1993.
3. Alper, Howard E., Donna Bassolino, and Terry R. Stouch, "Computer Simulation of a Phospholipid Monolayer-Water System: The Influence of Long Range Forces on Water Structure and Dynamics," *Journal of Chemical Physics,* Vol. 98, No. 12, pp. 9798-9807, 1993.
4. Alper, Howard E., Donna Bassolino, and Terry R. Stouch, "The Limiting Behavior of Water Hydrating a Phospholipid Monolayer: A Computer Simulation Study," *Journal of Chemical Physics,* Vol. 99, No. 7, pp. 5547-5559, 1993.
5. Stouch, Terry R., Keith B. Ward, Amanda Altieri, Arnold T. Hagler, "Simulations of Lipid Crystals: Characterization of Potential Energy Functions and Parameters for Lecithin Molecules," *Journal of Computational Chemistry,* Vol. 12, No. 8, pp. 1033-1046, 1991.
6. Stouch, Terry R. and Donald E. Williams, "On the Conformational Dependence of Electrostatic Potential Derived Charges: Studies of the Fitting Procedure," *Journal of Computational Chemistry*, Vol. 14, No. 7, pp. 858-866, 1993.
7. Liang, Congxin, Carl S. Ewig, Terry R. Stouch, and Arnold T. Hagler, "Ab Initio Studies of Lipid Model Species. 1. Dimethylphosphate and Methylpropylphosphate Anions," *Journal of the American Chemical Society*, Vol. 115 No. 4, pp. 1537-1545, 1993.
8. Stouch, Terry R. and Donald E. Williams, "Conformation Dependence of Electrostatic Potential Derived Charges of a Lipid Headgroup: Glycerylphosporylcholine," *Journal of Computational Chemistry*, Vol. 13, No. 5, pp. 622-632, 1992.
9. Williams, Donald E. and Terry R. Stouch, "Characterization of Force Fields for Lipid Molecules: Applications to Crystal Structures," *Journal of Computational Chemistry*, Vol. 14, No. 8, 1993.
10. Bassolino, Donna, Howard E. Alper, and Terry R. Stouch, "Solute Diffusion in Lipid Bilayer Membranes: An Atomic Level Study by Molecular Dynamics Simulation," *Biochemistry,* Nov. 30, 1993.

# Finding the right mix

## Cray Research supercomputers advance stirred tank simulation

*Richard D. LaRoche, Cray Research, Inc.*

Almost all manufacturing in chemical process industries revolves around the mixing of fluids—industrial chemicals, pharmaceuticals, food, consumer products, and plastics, to name a few. Time to market, product quality, and profitability depend largely on finding the most efficient and cost-effective way to mix these and other fluids during the conversion of raw materials into desired products. This search involves simulating and analyzing the extremely complex fluid dynamics that are part of most manufacturing processes and then making appropriate predictions about and adjustments in mixing equipment designs and operations. Cray Research supercomputers, with an unrivaled track record in computational fluid dynamics (CFD) applications, have become a critical tool for this simulation and analysis.

The stirred tank (Figure 1) is a standard piece of equipment in the process industries, used mostly for operations such as chemical reaction, blending, crystallization, and heating and cooling. The smallest stirred tank is the chemist's beaker, where new products are first created on a laboratory scale. The largest commercial tanks may mix thousands of gallons of process fluids, with feed and product streams continuously moving in and out of these tanks.

A motor-driven shaft extends down the middle of most stirred tanks. One or more impellers mounted on the shaft provide the fluid mixing action. Along the tank walls, plates called baffles enhance mixing by inhibiting solid-body rotation

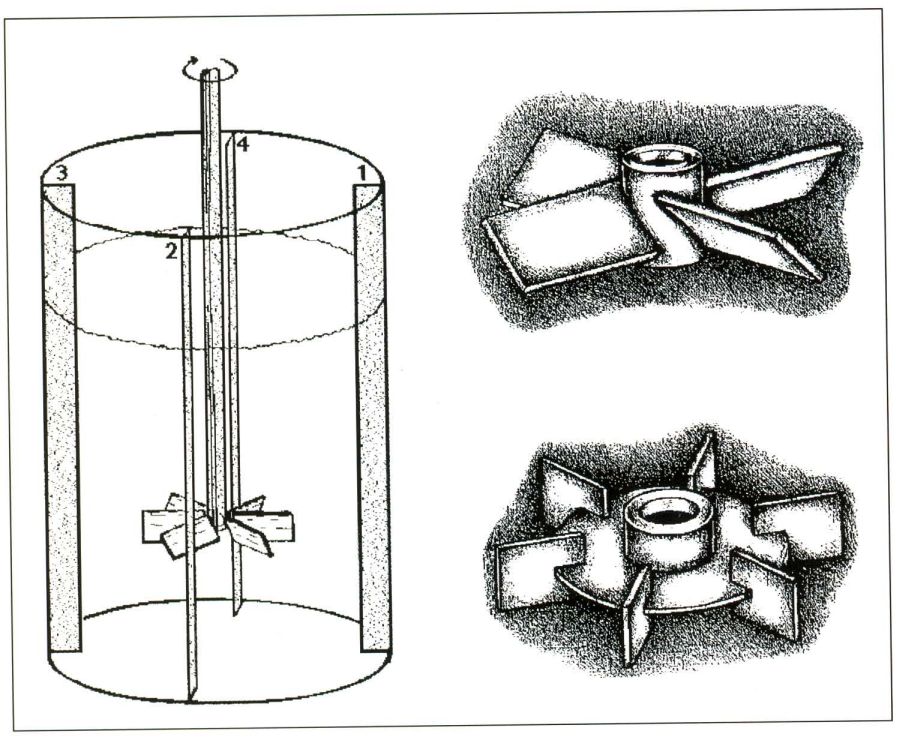


Figure 1 (below). Stirred tank schematic and 45° PBT and DT impellers.

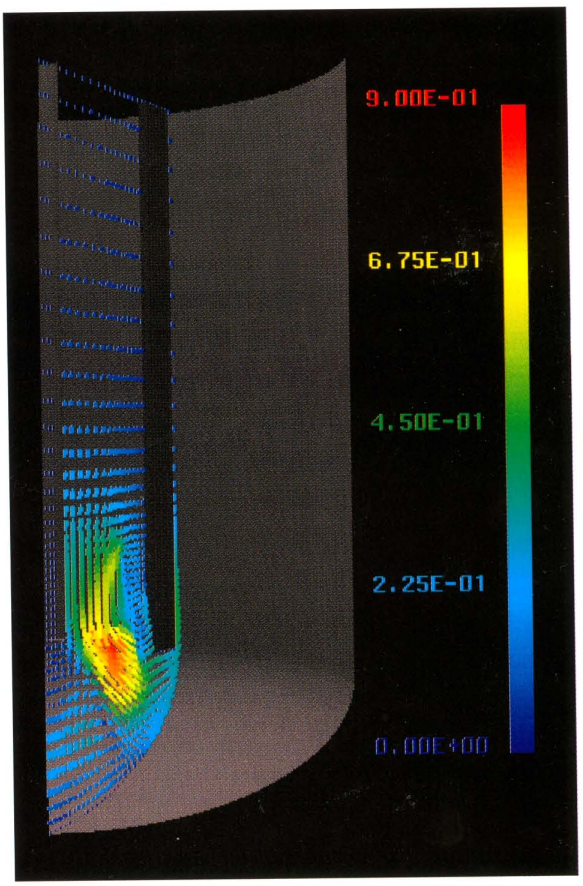


Figure 2 (right). Velocity vectors with a PBT configuration.

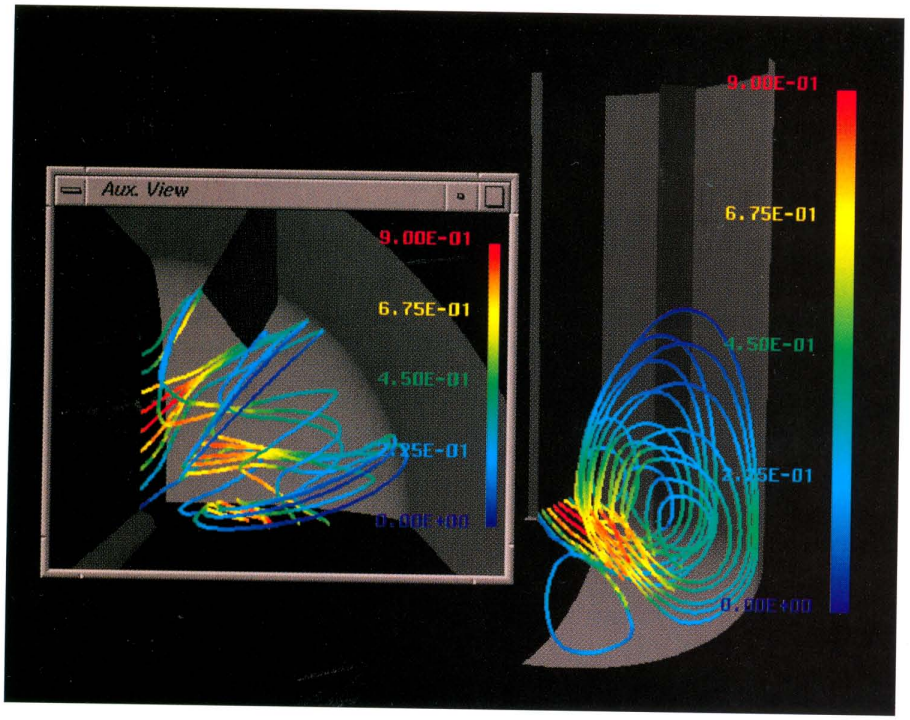


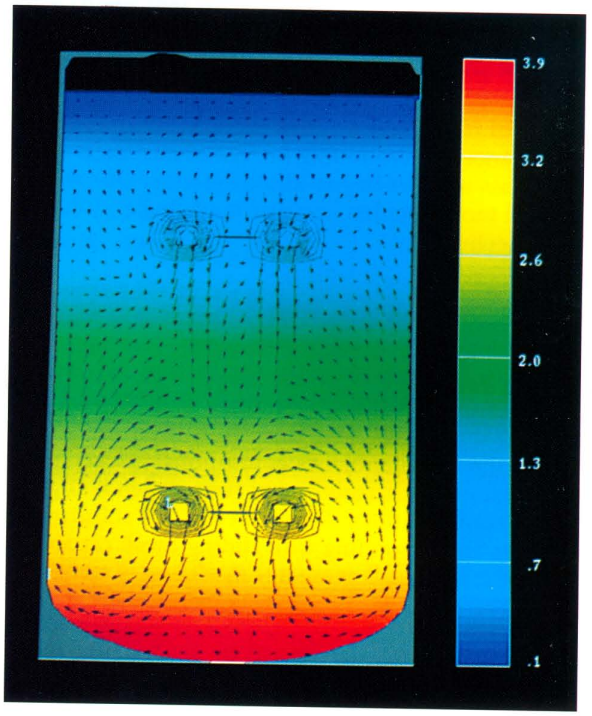


Figure 3 (above left). Particle traces with a PBT configuration.

Figure 4 (above right). Time dependent flow snapshot with a PBT/PBT configuration (Courtesy of Flow Science, Inc.).

of the fluid contents. Figure 1 also shows two basic types of impellers: the 45° pitched blade turbine (PBT) shown in the top right and the disc turbine (DT) shown in the bottom right. The PBT impeller often is called an axial flow impeller since it is designed to pump fluid downward along the shaft's axis. The DT impeller is referred to as a radial flow impeller since it directs fluid outward in the radial direction toward the tank side walls.

## Time-averaged impeller modeling

A top priority with regard to stirred tanks is to identify any regions in which the tank contents are not fully mixed. Poor mixing indicated by relatively low velocity or dead zones within a stirred tank reactor often leads to poor product quality and lower product yields. Often, an appropriate CFD analysis at this stage is to consider single-fluid-phase mixing with no chemical reaction, where the effect of the impellers is modeled as time-average boundary conditions.

Figures 2 and 3 show CFD results in a 90° section of a typical pilot-scale stirred tank (color scale indicates velocity in m/s). This stirred tank employs a single PBT impeller in the lower region which operates at 180 RPM in a fluid with the viscosity and density of water at ambient temperature. The tank diameter is 0.4 m with an impeller diameter of 0.2 m. Velocities were fixed as impeller boundary conditions based on experimental Laser Doppler Anemometer (LDA) data. Note the low velocity region at the top of the tank indicated by the short velocity vectors colored in dark blue in Figure 2. The high velocity region is near the impeller region (pictured in long yellow and red vectors). The particle traces in Figure 3 show a tight circulation region in the immediate vicinity of the PBT impeller, rather than the desired large-scale circulation throughout the entire tank. The inset picture in Figure 3 is a top view showing the mean flow traces around the baffle.

This CFD analysis was performed using 50,000 grid nodes with FLUENT modeling 3-D turbulent flow. Typical run times on a single-CPU CRAY C90 system are approximately two to three hours. An engineer can do several "what if" analyses of this type in a single day, using the Cray Research supercomputer to quickly screen process variables such as impeller types, speed, and placement. Stirred tank simulation may be used as an engineering tool in both the scale-up of new manufacturing processes and the retrofitting of existing manufacturing processes. Additional CFD software used effectively in this way includes CFDS-FLOW3D, FIDAP, Flow Science FLOW-3D, PHOENICS, and STAR-CD.

Another impeller modeling approach is to input a momentum jump boundary condition for the impeller region based on observed LDA data, rather than explicitly fixing fluid velocities. The net effect in the CFD analysis is much the same as fixing velocities, but this strategy may allow the study of some impeller configurations that result in unsteady flow structures. Figure 4 shows a snapshot of the unsteady flow structures predicted in a PBT/PBT 2-impeller configuration using Flow Science FLOW-3D.[1] The color indicates relative pressure in the tank, while the vector arrows indicate the velocity magnitude and direction of the fluid flow.

Time-averaged impeller modeling is now being established as an effective engineering tool used in conjunction with an experimental program to answer large-scale fluid mixing questions. One major limitation of this technique is its heavy reliance on experimental LDA data, which may be very difficult to obtain for many real industrial situations. This technique also simplifies the fluid flow details

in the near-impeller region by imposing time-averaged velocity or momentum boundary conditions.

Effectively modeling the smaller-scale flow structures in the near-impeller region is essential in addressing engineering questions such as enhanced micromixing for chemical reaction and mass transfer in gas-liquid systems. One step toward more detailed impeller modeling is sliding-mesh technology.

## Sliding-mesh impeller modeling

To address near-impeller region fluid mixing issues, it may be necessary to model explicitly the moving blades in a baffled tank to resolve smaller-scale flow structures. In baffled stirred tanks, the impeller blades continuously sweep past stationary baffles, resulting in time-dependent geometry configurations. Commercial CFD software vendors are responding with sliding-mesh capability that enables full geometry modeling of impellers in baffled tanks. Experience reported with the sliding-mesh prototypes for STAR-CD[2] and FLUENT[3] is very encouraging. STAR-CD v2.2, released in the third quarter of 1993, was the first general-purpose CFD package to include sliding-mesh capability. FLUENT v4.25 includes sliding-mesh functionality and is scheduled to be released in 1994. The CFDS-FLOW3D and FIDAP vendors plan to add the capability in the near future.

Figure 5 is an example of the sliding mesh used for STAR-CD stirred tank simulations. Note that portions of the fluid mesh have been removed to show the impeller and baffles clearly. The mesh's inner red portion is body-fitted to the impeller and rotates with it, while the outer blue region is fixed. Figure 6 provides a snapshot of the velocity field in a vertical plane with the radial outflow from the impeller and toroidal vortex structures it drives.

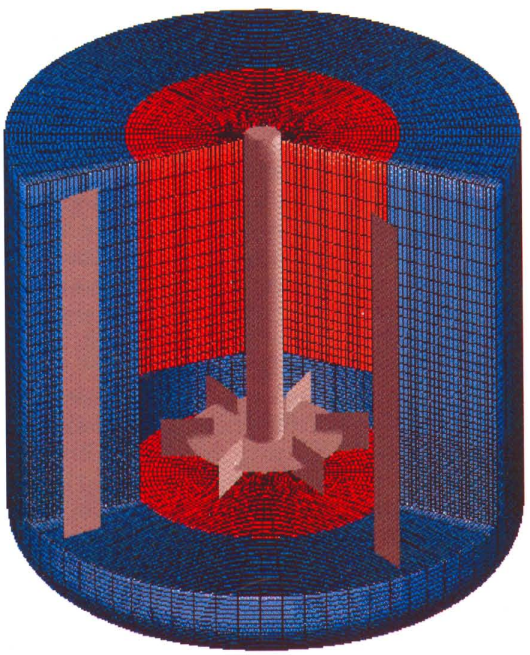

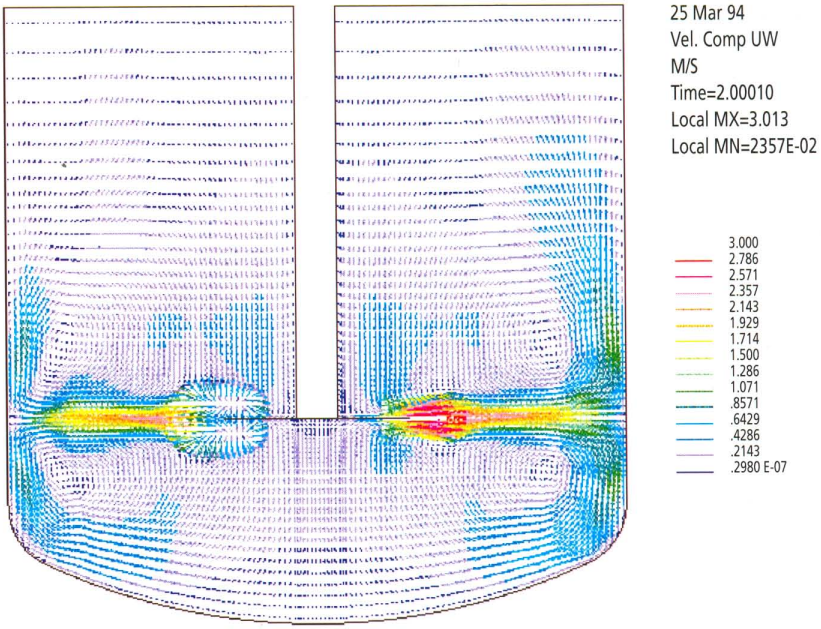


**Figure 5 (below left). STAR-CD sliding mesh for a DT configuration (Courtesy of Computational Dynamics/adapco).**

**Figure 6 (above). Velocity vectors for a DT configuration using STAR-CD sliding mesh (Courtesy of Computational Dynamics/adapco).**

**Figure 7 (below right). Temporal variation of velocity at a fixed point within the impeller jet (Courtesy of Computational Dynamics/adapco using STAR CD).**

The section shown is just ahead of the advancing blade on the left side and just behind on the right side.

To emphasize the periodic nature of stirred tank fluid flows, Figure 7 shows the temporal variation of velocity at a fixed point within the impeller jet.

Figure 8 shows one blade of a PBT impeller used in a FLUENT sliding-mesh simulation. Note that this PBT impeller has a fin which is designed to stabilize the impeller movement while it is rotating in the stirred tank. Figure 9 illustrates the massless particle flow patterns calculated by

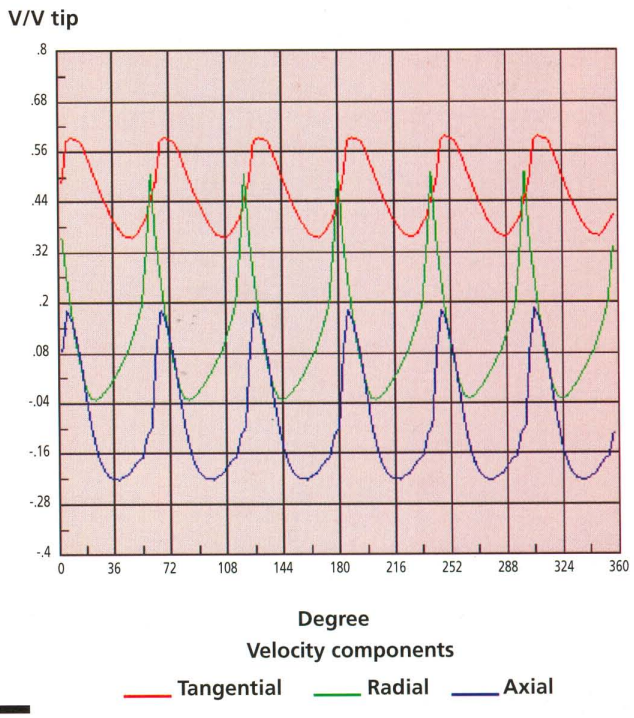

FLUENT using this PBT impeller configuration in a baffled stirred tank.

As promising as preliminary results are, many questions remain about the practical application of sliding-mesh technology to industrial fluid mixing problems. The central issue is how to implement the technology to model fluid flow adequately. What grid density is required, especially in the impeller region? What is the upper limit for time steps? What initial conditions can be used to start these time-dependent calculations? Must quiescent flow conditions always be used with a ramp-up on impeller speed, or can time-averaged results be used to reduce computation time?

All of these questions have a direct impact on computation time, memory, and required disk storage. Current estimates of scaled-down stirred tank simulations with the sliding-mesh prototypes point to computation times of weeks on today's workstations. Given the computational requirements, the CRAY C90 system can be seen as the optimal computer to tackle these complex mixing problems and deliver the required results to the engineer not in weeks but in hours.

Cray Research is coupling its CRAY C90 supercomputer's computational speed and memory with the experience and expert knowledge of process industry engineers to explore the potential of sliding-mesh technology for stirred tank simulation. Cray Research will investigate model implementation issues in a program to validate sliding-mesh results with experimental LDA data. Experience shows that such industry/vendor collaboration accelerates the implementation of new software technology in industry by providing practical guidelines for its use and improving the underlying efficiencies of the software technology. ■

**Figure 8 (below left). PBT impeller blade with stabilizing fin (Courtesy of Fluent Inc.).**

**Figure 9 (below right). Particle traces for a PBT configuration using FLUENT sliding mesh (Courtesy of Fluent Inc.).**

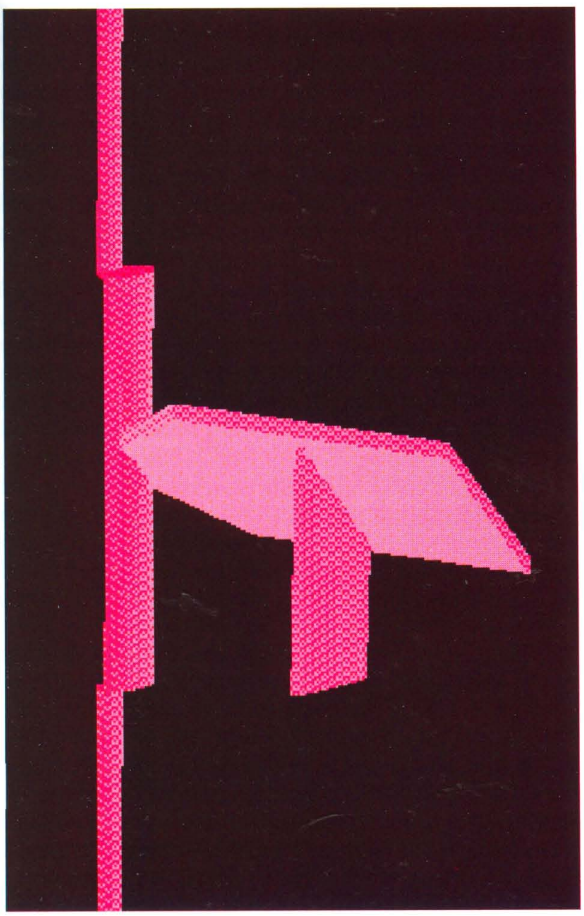

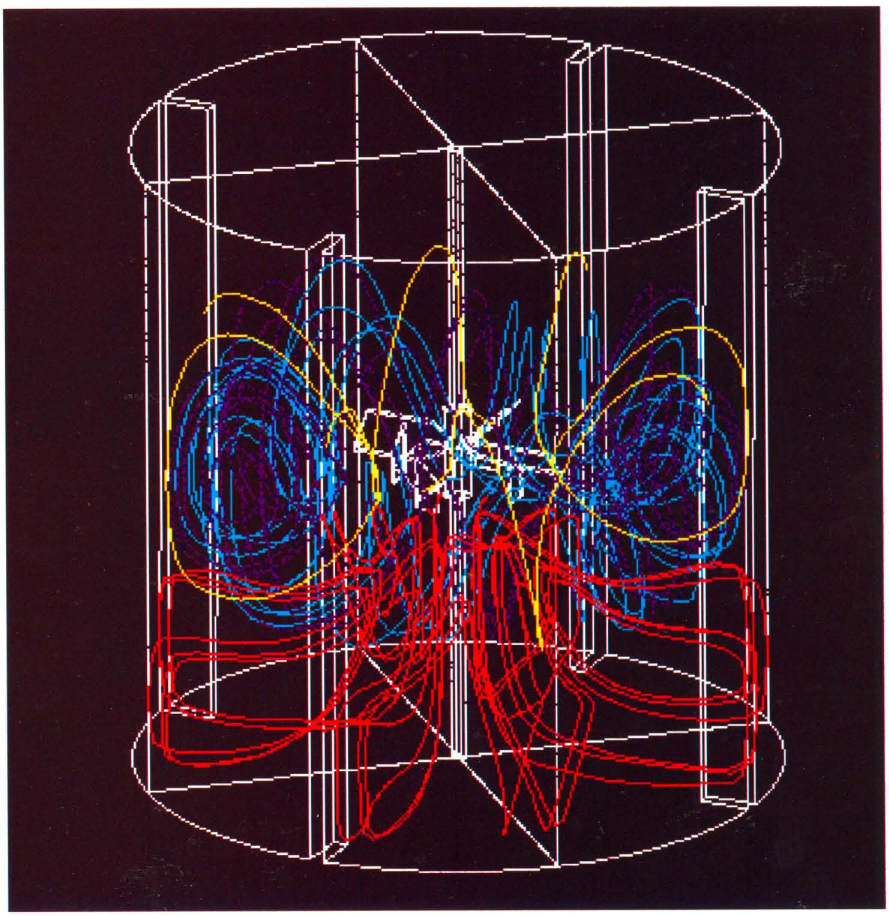

---


***About the author***

*Richard D. LaRoche is a senior chemical engineer in the Engineering Applications Group at Cray Research, Inc., where he focuses on the application of CFD to process industry problems. He received a B.S. degree in chemical engineering from Montana State University and M.S. and Ph.D. degrees in chemical engineering from the University of Illinois at Urbana-Champaign. He previously held positions at Dow Chemical Company and the Pennsylvania State University.*


***References***


1. Ditter, J. L. and C. W. Hirt, "A Scalable Model for Stirred Tanks," 1994 American Society of Mechanical Engineers (ASME) Fluids Engineering Division Summer Meeting, Incline Village, Nevada, June 1994.
2. Luo, J. Y., A. D. Gosman, R. I. Issa, J. C. Middleton, and M. K. Fitzgerald, *Full Flow Field Computation of Mixing in Baffled Stirred Vessels,* Transactions of the Institute of Chemical Engineers, Vol. 71, Part A, pp. 342-344, 1993.
3. Perng, C.-Y. and J. Y. Murthy, "A Sliding-Mesh Technique for Simulation of Flow in Mixing Tanks," presented at the Engineering Foundation Mixing XIV Conference, Santa Barbara, California, June 1993.

# Materials science from first-principles

# $CoSi_2$ surfaces

*Doris Vogtenhuber, Raimund Podloucky, Institute for Physical Chemistry of the University of Vienna, Vienna, Austria*
*Samuel Gotthelf Steinemann, Institute for Experimental Physics of the University of Lausanne, Dorigny-Lausanne, Switzerland*

Transition metal silicides are of growing interest in materials science for several reasons. In particular, $CoSi_2$ (cobalt disilicide) is important because of its applications in special optoelectronic and microelectronic devices such as metal-base and permeable-base transistors.[1] $CoSi_2$ can be grown epitaxially on Si due to the very small mismatch of lattice parameters forming a Schottky barrier at the Si-silicide interface. In that context, surface and interface studies play a growing role because the sizes of electronic devices are so small that the influence of surface- and interface-induced effects can no longer be neglected for such materials.

$CoSi_2$ and other metal silicides are attractive as structural materials because of their medium to high melting points and excellent oxidation resistance.[2] Many of these compounds, however, have poor ductility and fracture toughness at ambient temperatures, which might be connected to their rather complex crystal structure and limited number of equivalent slip systems. $CoSi_2$, however, crystallizes in the cubic fluorite structure which possibly provides a sufficient number of equivalent slip systems. Although its melting point of 1326 °C is not particularly high, it is an interesting material for higher temperature applications because of its low density and remarkable oxidation resistance. $CoSi_2$ is rather brittle, and its mechanical properties must be improved for applications such as watchmaking.[3] Therefore, fundamental insight into the physical properties of the material is necessary. Part of the present study deals with so-called ideal cleavage energy for the ideal brittle fracture, which is inaccessible to experimentation.

Each of the above-mentioned fields of materials science can benefit from investigations of $CoSi_2$ surfaces. Here we focus on the (011) surface, one of the most preferred cleavage planes. Regarding electronic devices, other orientations such as (001) and (111) surfaces are of importance in connection with interfaces formed by pure, epitaxially grown Si. We discuss results for the electronic structure and energetics of the (011) surface which is the easiest to calculate because of its symmetry, but some results about the (001) surface are also included.

The calculations were done by application of the full-potential linearized augmented plane wave (FLAPW) method,[4] which is one of the most precise methods in the field. FLAPW is a first-principles method that does not require any empirical information. Because of its heavy computational demand, we need the most powerful computer systems available. The higher the power of the machines, the more realistic (and more complex) the physical system could be. At present we could reasonably simulate up to 40 atoms on a powerful computer such as the CRAY C90 system. The actual calculations for unit cells of about 20 atoms were done on a CRAY Y-MP M98 system with 1 Gword of memory. Because of its high degree of vectorization, the FLAPW code performs very well on a large vector supercomputer.

## Computational approach

Our approach is based on the concepts of density functional theory in its local density approximation (LDA), which is used by the vast majority of numerical first-principles applications in the solid state field. To precisely solve the corresponding Schrödinger-like equations, we applied the FLAPW method. The FLAPW's fundamental idea is to divide the three-dimensional periodic space (or rather the corresponding unit cell) into natural regions, namely into spherical regions around atomic positions (atomic spheres) and an interstitial region between the spheres. Then one expands all necessary quantities (such as wave functions, densities, and potentials) inside the atomic spheres into spherical harmonics times radial functions, and uses plane waves for the expansions in the interstitial region. The interstitial wave function in terms of plane waves is augmented into the spheres by the solutions inside the atomic spheres. Both types of functions match continuously (also in the first derivative) at the sphere boundaries.

Surface calculations are done for a slab model which consists of a thin film of atomic layers. Now the periodicity in the $z$ direction perpendicular to the surface is destroyed, and a third region, the vacuum region, is defined. In this region, the necessary quantities are expanded into two-dimensional plane waves times $z$-dependent coefficients. The wave functions in the vacuum decay now for $z$ going to infinity. Again, matching of wave functions has to be done, now at the boundary between the interstitial and vacuum region. Due to these subdivisions of space and the possible natural expansions, the potential that we need for the solution of Schrödinger's equation can be of general shape (then it is named "full

potential"). Due to the natural choices of wave functions, any type of atom—for example, transition metal elements as well as free-electron-like cases—can be treated in the same, precise manner.

Like all ab initio and first-principles methods, FLAPW is a self-consistent method. The valence states are treated in a semi-relativistic way without spin-orbit splitting which could, however, be included. All electronic levels are recalculated for each iteration, core states included, which are determined by a fully relativistic procedure. Spin polarization can be easily switched on to study magnetic systems.

## Surface electronic structure

The self-consistent electronic structure was calculated with the film FLAPW method for two surface orientations of $CoSi_2$, namely (110) and (001). This notation means that this particular vector is perpendicular to the surface plane; it refers to specific cuts through the three-dimensional lattice. Due to the fluorite structure of $CoSi_2$, the (110) surface can be described by stacking mixed layers of correct stoichiometric composition. For the (001) orientation, however, the planes parallel to the surface are pure Co and $Si_2$ planes. Because of the slab geometry, we actually have two surfaces which, in the (110) case, are symmetrical mirror images. For the (001) case though, the top and bottom of the slab are different if the overall stoichiometry is maintained. For the (110) case, seven layers were used to construct the slab resulting in a total of 21 atoms per two-dimensional unit cell. For the (001) case, six pure layers of either atomic species were used, which amounts to 18 atoms per unit cell. The (001) results in terms of total energies are discussed later; the (110) electronic structure will now be analyzed in more detail. The bulk lattice constant of 3.79 Å—although it is also possible to calculate it by FLAPW via total energy minimization—was taken from experiment.

Because the atoms at, and near, the surface miss neighbors (in comparison to a perfect bulk case), the atomic positions generally will change; the geometry reconstructs in a more or less complicated atomic arrangement depending on the material. For example, simple face-centered (001) surfaces for metals experience relaxation effects shifting the otherwise unperturbed layers together (at the surface) or apart (deeper down in the material). In other words, the two-dimensional unit cell is preserved. For $CoSi_2$, however, because of the covalent bonding, one expects more complicated geometry effects at the surface. As a first step towards a full reconstruction of atomic positions, we calculated the change in $z$ positions of the top Co and Si atoms by minimizing the total energy as a function of position. At the surface, Si now has only three nearest Co neighbors instead of four. We found that Si moves inside the material by about 0.1 Å, which is about 5 percent of the interlayer distance of 1.90 Å. Co also moves in the same way but only by 0.04 Å. The relaxational effects are rather small—the most important effect is the reduction of one Si-Co bond length by 3 percent.

The change of atomic potentials at the surface and the change of boundary conditions for quantum mechanical states reaching out into the vacuum are consequences of the perturbation that a surface creates in an originally three-dimensional environment. These changes lead to the creation of surface states, which add new energy levels in forbidden regions (or band gaps) of the bulk spectrum. Surface states are localized around the surface atomic positions and decay inside the material. Due to their nature, they are sensitive to surface processes such as reconstruction, adsorption of molecules, and other external interactions.

Figure 1 illustrates the positions of the atoms in the selected box. Co atoms are colored blue and Si atoms purple. In Figures 2 and 3, we show two such surface states for the $CoSi_2$ (110) surface. Because of our finite thin film (instead of a semi-infinite geometry), the definition of surface localization is somewhat arbitrary. In our case, we required that more than 20 percent of the particular state should be localized within the atomic spheres of either Co or Si atoms (or both) in the surface layer. The figures showing electronic charge densities in the two-dimensional unit cell are cuts through the film along the $z$ direction, in the upper half of the seven-layer film. From the figures we can distinguish four different atomic layers, with the

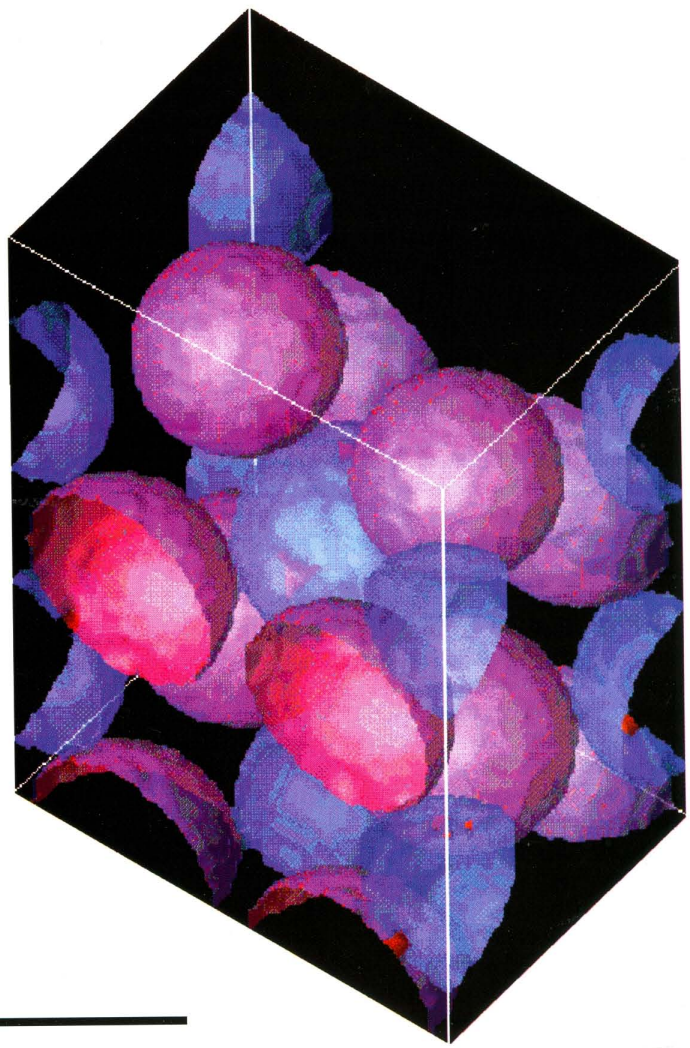

**Figure 1. Positions of Co atoms (blue) and Si atoms (purple) in the selected box.**

top layer, S, as the surface layer. At the corners of the box, atoms in the S and S-2 planes are Co atoms with Si atoms positioned in between. Another Co atom is located at the center of the S-1 plane. Si atoms are also located in this plane, which are not important for our discussion because there is hardly any charge to be found.

Basically, the occupied states consist of s-like Si states as the lowest energy states, and p-like Si and d-like Co states higher in energy. Many of the states are a mixture of these characteristics due to hybridization. Figure 2 shows the charge density of a surface state which is split off the Si s-like energy levels. We see a more or less spherically-shaped cloud around the two Si atoms in the surface layer spreading rather directed bonds towards two Co atoms at the corners and another bond down to Co in layer S-1. This Co atom is characterized by a propeller-like $d_{yz}$ state. These propeller lobes connect the two triangular surface objects. The charge clouds of the two Si atoms avoid each other although both are missing their fourth Co atom which (in the bulk) would be above them. The pictorial expression of removing bonds is beautifully illustrated by the structure above the Si atoms which looks like an opened-up articular capsule.

Figure 3 shows another surface state, one that is of p-like (or more precisely, $p_x$-like) character at the Si-atom. Because the 3p wave function has two radial nodes around Si, we can see a small nodal structure squeezed in between earlobe-shaped structures again reaching down to the central Co in layer S-1. There again we observe a d-like state now of $d_{yz}$ orbital character connecting the two Si-Co structures in the surface layer.

## Cleavage energy

Understanding the behavior of a solid when it is cleaved is important for the study of crack formation because one wants to know how much load a material can sustain before it breaks. First-principles approaches provide useful information not available by experiment, as is the case, for example, for the energy of ideal brittle cleavage. If the material breaks perfectly brittle, all the available energy is consumed by the widening of the crack without any other change of the atomic arrangement in the form of plastic deformations. Then the cleavage energy $Gc$ is given by $Gc = 2\gamma_s$, where $\gamma_s$ denotes the surface energy.[5] The surface energy describes the loss of energy due to breaking of the bonds. In the language of the computational materials scientist, it is related to the difference in total energies between the material containing the surface, $E_{surf}$, and the perfect three-dimensional solid, $E_{bulk}$. Of course, the total energy of the surface is derived from a fully self-consistent calculation that includes all processes of electronic relaxations (change of bonds and potentials) due to the existence of the surface.

In principle, the difference $E_{surf} - E_{bulk}$ can be calculated from first-principles using quantum mechanical methods. The FLAPW code is ideally suited for such a treatment because it treats thin films and bulk systems with the same precision.

One important problem remains: how to properly compare the total energies of the film and bulk cases. The film has to be sufficiently thick for the particular information wanted. Fortunately, properties like surface energies converge rather fast in most cases, as a function of numbers of atomic layers. Usually, the surface energy is obtained by comparing the total energies of several films of different thickness. Such a procedure needs at least two film calculations of sufficient thickness, which could be quite costly. To overcome this problem, we calculated the bulk total energy of $CoSi_2$ for a (011) stacking, so only two bulk layers are necessary. Such a calculation is very fast. The most important point—to get $E_{bulk}$ comparable to $E_{surf}$—is the proper sampling of states in the reciprocal unit cell, for which we found a reliable numerical procedure. Applying this procedure to a film of five layers yields a reasonable surface energy that only deviates by 1 percent from the finally accepted value of 2.20 J/m$^2$ for seven layers. (The surface energies are the discussed total energy differences divided by the area of the two-dimensional unit cell.)

## $CoSi_2$ surface energy

Similarly, the $CoSi_2$ (001) surface energy was calculated. In this case, a film calculation with a larger number of layers is rather costly because of the loss of three-dimensional inversion symmetry which leads to the diagonalization of complex Hermitian matrices instead of symmetric matrices.

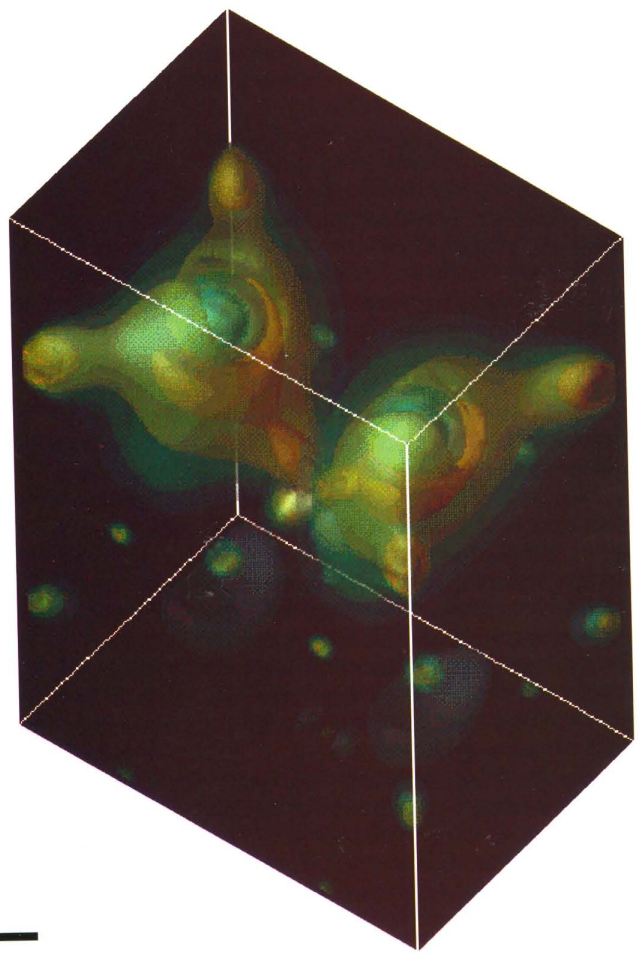

Figure 2. Charge density of s-like Si surface states.

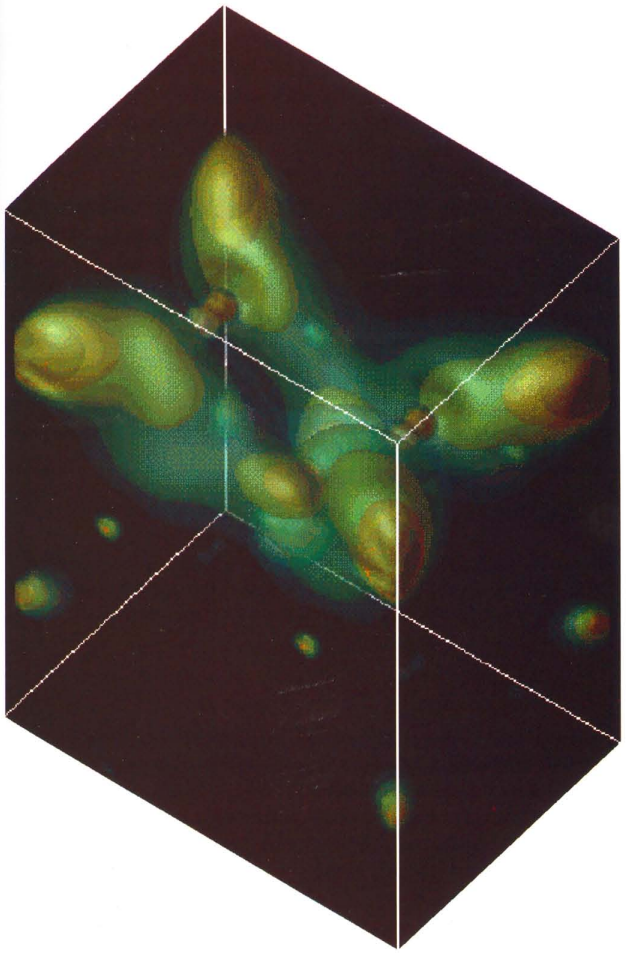

Figure 3. Charge density of $p_x$-like Si surface states.

Again, the bulk calculation with correct stacking of layers can be done rather fast. As described previously, the actual (001) surface calculation was done for six repeat units (or six layers of pure Co and pure $Si_2$). Interestingly, the total energy differences of both cases, (011) as well as (001), are practically the same (the value for (001) is larger by a few percent). The surface energies, however, are substantially different because the area of the two-dimensional (001) unit cell is smaller by a factor of $\sqrt{2}$. This leads to a rather high surface energy of 3.25 J/m$^2$. According to experimental results, $CoSi_2$ does not cleave along (001), and corresponding rupture planes are also hard to find. Compared to some results for aluminides,[6] the (001) cleavage energy is as high as for FeAl (001), which crystallizes in the CsCl structure. Our calculated value for $CoSi_2$ (011) is well in the range of other aluminides such as $Ni_3Al$, NiAl, and TiAl.

The true cleavage energy may be written as $\tilde{G}c = 2\gamma_s + \omega$, where $\omega$ is the energy of plastic deformation. By comparing our calculated result for the ideal brittle cleavage and the experimental data, we find that the calculated $Gc$ is only about 10 percent of $\tilde{G}c$, which means that most of the cleavage energy dissipates. This indicates that there is a reasonable chance for ductilizing the originally very brittle $CoSi_2$ by special treatments such as alloying by third components.

Because cleavage energies are important for fracture models, we used them in studying these quantities. It would be highly desirable to calculate surface energies for geometrically more complicated surfaces that might play a role in cleaving processes and fracture. We hoped that the total energies of monolayers (or rather stoichiometric mono-units), which can be calculated very fast, would give reasonable numbers for the cleavage energies within a few percent. This is the case for the (011) surface, because there the monolayer has a surface energy which is larger only by 5 percent compared to the seven-layer calculation. For the (001) case, however, the difference between mono-unit and thick film is larger than 10 percent and in the opposite direction. Nevertheless we hope that a systematic study of monolayers could lead to useful procedures for the treatment of more complex surfaces. ■


### *Acknowledgments*

*We gratefully acknowledge the support of Cray Research, Inc. and the cooperation of Franz-Karl Schmatzer. Further support was given by the Austrian Science Foundation, project number P8708.*


### *About the authors*


*Doris Vogtenhuber is pursuing postdoctorate research with Raimund Podloucky at the Institute of Physical Chemistry of the University of Vienna. She earned a Ph.D. degree in 1992 from the University of Vienna, working on electronic structure calculations for bulk systems. She is currently involved in several projects in first-principles calculations of energetics and electronic structure of surfaces.*

*Raimund Podloucky is a professor at the Institute of Physical Chemistry at the University of Vienna. He received a Ph.D. degree in 1975 working on positron annihilation. In 1985, he became associate professor. He worked in several computational materials science fields, such as structure maps, first-principles phase diagrams, and magnetic compounds. He uses first-principles methods for the study of metallic and insulating surfaces and is also involved in computational materials science projects on intermetallic alloys.*

*Samuel Gotthelf Steinemann is a full professor at the Institute of Experimental Physics at the University of Lausanne. His Ph.D. thesis research investigated the behavior of ice under pressure. In 1968, he obtained his position at the University of Lausanne. He is active in many experimental and applied fields of materials science, such as intermetallic alloys and developing materials for watchmaking and bone surgery, in close connection with industry.*


### *References*


1. Hensel, J. C., A. F. J. Levi, T. T. Tung, and J. M. Gibson, *Applied Physics Letters*, Vol. 47, p. 151, 1985; J. Zegenhagen, K.-G. Huan, W. M. Gibson, B. D. Hunt, and L. J. Schowalter, *Physical Review B*, Vol. 39, p. 10254, 1989.
2. Anton, D. L. and D. M. Shah, *Materials Research Society Symposia Proceedings*, Vol. 13, p. 361, 1989.
3. Steinemann, S. G., *Europäische Patentschrift*, publication 0284669/B1, 1990.
4. Wimmer, E., H. Krakauer, M. Weinert, and A. J. Freeman, *Physical Review B*, Vol. 24, p. 864, 1981; E. Wimmer, H. Krakauer, and A. J. Freeman, in *Advances in Electronics and Electron Physics*, Vol. 65, p. 357, 1985.
5. Kelly, A. and N. H. Macmillan, *Strong Solids*, Clarendon Press, Oxford, 1986.
6. Yoo, M. H. and C. L. Fu, *Materials Science and Engineering*, Vol. A153, p. 470, 1992.

# Investigating fullerene species with electronic structure theory

*Douglas J. Fox, Gaussian, Inc., Pittsburgh, Pennsylvania*

*Fullerenes are among the most novel and fascinating chemical compounds discovered in several decades.*

Their name alludes to the resemblance of the distinctive molecular structure of $C_{60}$, the first fullerene discovered, to the geodesic domes proposed as dwellings by the philosopher R. Buckminster Fuller. Fullerenes are the subject of intense research scrutiny by many groups on several continents. There has also been a great deal of speculation about potential commercial uses for fullerenes and their derivatives, ranging from electrochemistry and electronics (the latter based in part on the superconducting properties of some of their derivatives) to catalysis to hydrogen storage to antiviral agents, but so far, no actual products have been developed.

Fullerenes have many unusual properties, including low chemical reactivity and high resistance to photodissociation. Substitution reactions are not possible with fullerenes since they contain no atoms or groups for which a substitution can be made. Instead, fullerene reactions are generally addition reactions in which atoms or groups are incorporated into the structure, sometimes within the fullerene cage. In general, fullerene derivatives retain their distinctive general structure as well as the resultant special properties of this class of systems.

At first, the nature of fullerene structures was the subject of intense debate. Richard E. Smalley, Harry F. Kroto, and their coworkers first proposed

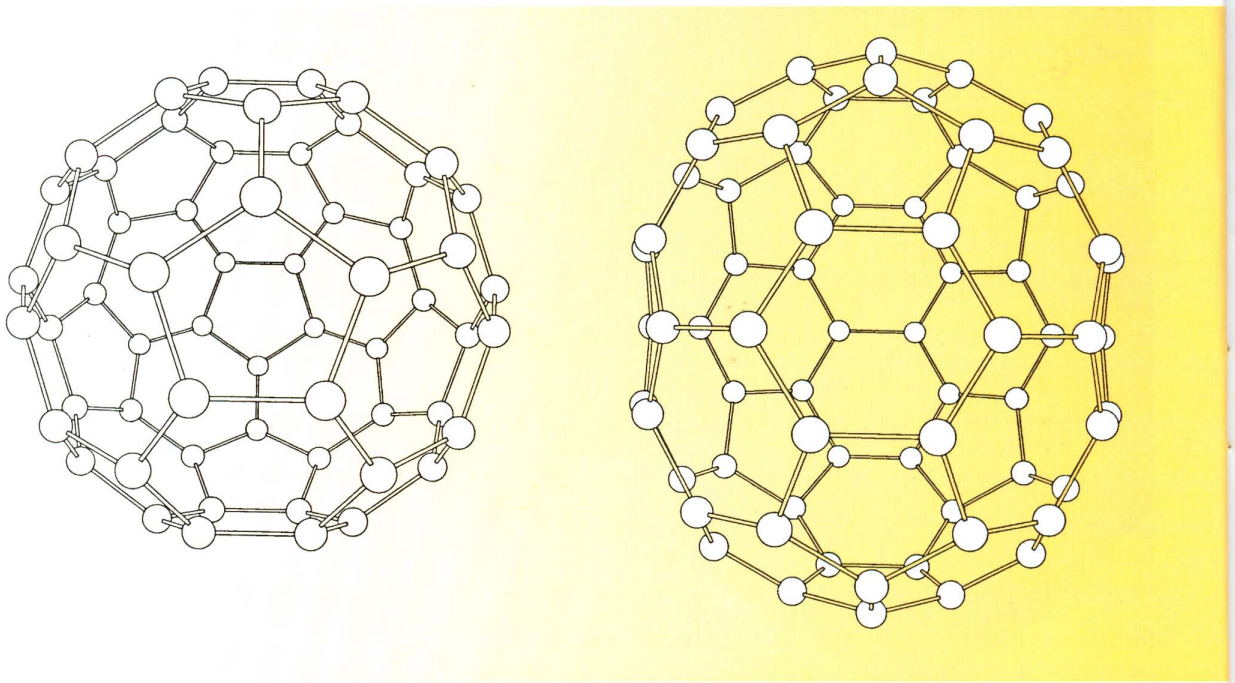

Figure 1. Ground state structures of $C_{60}$ (left) and $C_{70}$ (right).

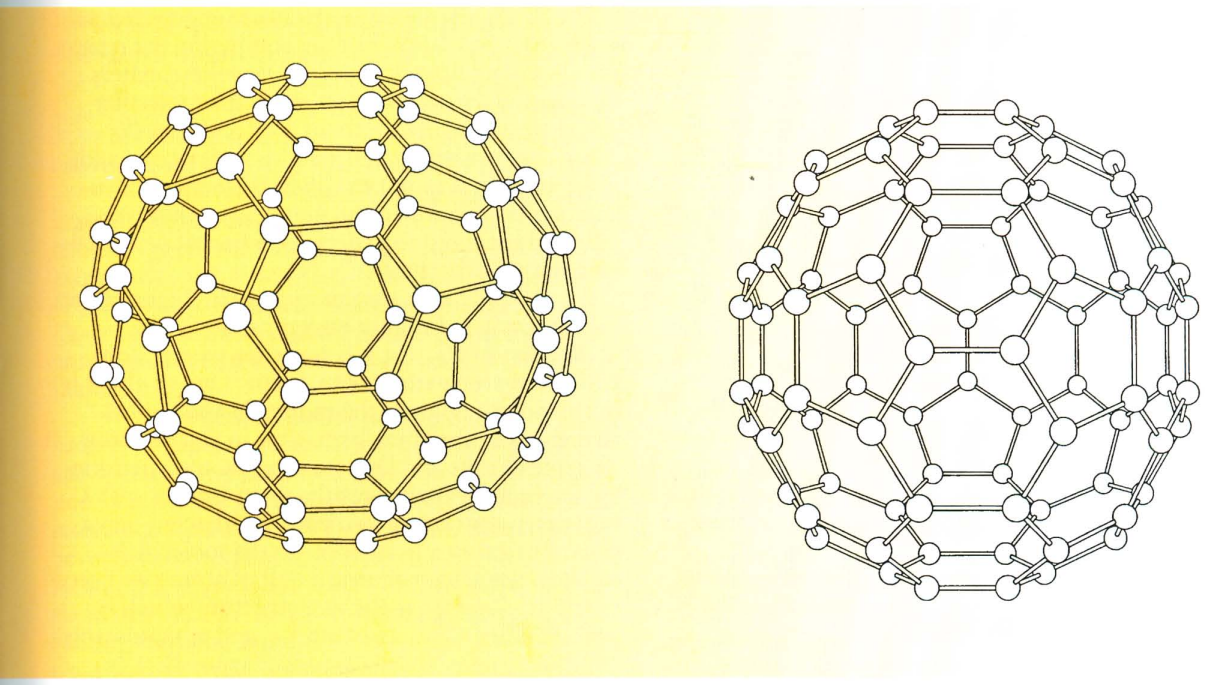

Figure 2. The $D_{2d}$ (left) and $D_2$ (right) forms of $C_{84}$.

the highly symmetric truncated-icosahedral structure for $C_{60}$ in 1985, citing as their initial evidence the very strong peak at 720 atomic mass units in carbon cluster mass spectra. In 1990, Donald R. Huffman and Wolfgang Krätschmer reported the first technique for producing macroscopic amounts of fullerenes. Smalley's structure was universally accepted only when subsequent spectroscopic studies of $C_{60}$ (made possible by the greater availability of fullerenes) confirmed it.

Theoretical studies of fullerenes followed closely upon the initial experimental work. For example, the geometry of $C_{60}$ was first optimized using ab initio techniques by H. P. Lüthi and Jan Almlöf, and their 1987 publication predates Huffman's and Krätschmer's paper. Since then, numerous theoretical investigations of the geometries and vibrational frequencies of many other fullerenes have been performed.

In this article, we focus on the studies of fullerene structures performed by Krishnan Raghavachari of AT&T Bell Laboratories and his collaborators; the majority of these calculations were performed on CRAY Y-MP supercomputers. Due to these structures' size and complexity, accurate calculations on fullerenes tend to be quite computationally intensive, making them ideal candidates for a Cray Research system. For the results we will consider, Raghavachari relied primarily on the ab initio methods in the Gaussian series of programs, as well as employing some semi-empirical and density functional techniques.

## Ground state structure of $C_{84}$

The principal fullerenes isolated thus far are $C_{60}$, $C_{70}$, $C_{76}$, $C_{78}$, $C_{82}$, and $C_{84}$. The structures of $C_{60}$ and $C_{70}$ are unique and well-established. $C_{60}$ exhibits icosahedral symmetry and contains 12 pentagonal rings and 20 hexagonal rings. The geometry of $C_{70}$ ($D_{5h}$ symmetry) is described as a prolate spheroidal structure in which a cylindrical belt of 10 carbon atoms has been added to the "middle" of $C_{60}$, resulting in ellipsoidal distortion of the spherical form as shown in Figure 1.

Apart from $C_{60}$ and $C_{70}$, $C_{84}$ is the most abundant fullerene seen experimentally. There are many possible arrangements for the 84 carbon atoms in its ground state structure. The structures of $C_{60}$ and $C_{70}$ suggest that distributing the strain within a system as uniformly as possible is a way to form stable spheroidal structures. It is well known that 12 pentagonal rings lead to closure; if they were present in $C_{84}$, then the molecule would also contain 32 hexagonal rings.

Raghavachari and his coworker, Celeste McMichael Rohlfing of Sandia National Laboratories, derived potential structures for the ground state of $C_{84}$ by distributing the pentagonal rings uniformly within the molecule, while also requiring that no two pentagons share an edge (a source of strain which inevitably prevents the formation of a stable structure). Raghavachari and Rohlfing initially examined two such high symmetry structures (with $D_{6h}$ and $T_d$ symmetries) as possible candidates. In later work, Raghavachari analyzed the local strains in the 32 hexagonal rings in more detail and predicted that two lower symmetry structures—one with $D_{2d}$ symmetry containing 11distinct kinds of carbon atoms and the other with $D_2$ symmetry containing 21 kinds of carbon atoms—have the most optimal distribution of strain and hence should be candidates for the ground state of $C_{84}$ (Figure 2).

Both $C_{84}$ structures are local minima (verified by vibrational analysis). Both are nearly spherical and almost isoenergetic. Raghavachari predicted that a mixture of the two is likely to be present in experimental studies which should then yield a carbon NMR spectrum with 32 peaks. Subsequent experimental work by Achiba and coworkers obtained an NMR spectrum with 32 lines,

confirming the theoretical predictions. In general, stability increases from $C_{60}$ to $C_{70}$ to $C_{84}$, due to the greater proportion of hexagonal rings in the larger clusters, which progressively approach graphite.

## Isomers of the principal fullerenes

Similar considerations determine the relative stabilities of higher energy isomers of the various fullerenes. Qualitatively, spheroidal structures containing only pentagonal and hexagonal rings are much more stable than ones containing larger rings, and adjacent pentagonal rings increase local strain, thereby lowering the molecule's overall stability. Indeed, the stability of $C_{60}$ and $C_{70}$ with respect to smaller carbon clusters can be explained by noting that $C_{60}$ and $C_{70}$ are the two smallest fullerenes for which it is possible to form a structure containing no adjacent pentagons.

The total number of possible isomers of $C_{60}$ is very large. Raghavachari and Rohlfing narrowed their investigations by focusing first on those connected to the ground state by simple local transformations (first suggested by Stone and Wales) such that the motion of only two atoms is needed to change from one isomer to the other. When starting from the ground state, a Stone-Wales transformation results in a $C_{2v}$ structure containing two pairs of adjacent pentagons. This structure is the only possible isomer containing only two such pairs, and there is no geometrical arrangement which contains only one pair. Their ab initio calculations demonstrated that this structure (see Figure 3) is the lowest energy alternative to the ground state; it is less stable than the icosahedral form by 2.12 eV (HF/3-21G).

Raghavachari and Rohlfing went on to consider other isomers of $C_{60}$ containing three and four pairs of adjacent pentagons. As expected, energies increased with the number of such "defects" (with respect to the lower energy ground state structure). Moreover, by comparing the relative energies of all of these isomers, these researchers determined that each defect made the molecular structure less stable by about 1 eV and that the energy change associated with such defects is additive to within 0.1–0.2 eV. Their theoretical calculations thus quantified the previous qualitative information about the effects of adjacent pentagons within a $C_{60}$ structure.

Applying a similar approach, Raghavachari also investigated higher energy isomers of $C_{70}$. In contrast to $C_{60}$, $C_{70}$ has two sites where Stone-Wales transformations can occur. One of them is in the polar region of the molecule and is thus analogous to the transformation in $C_{60}$ between its ground state and lowest energy isomer; performing the transformation results in an isomer with $C_s$ symmetry containing two pairs of adjacent pentagons. The other site is closer to the molecule's equator, near the cylindrical belt of atoms we noted previously, and it results in a structure which is slightly more elongated than $C_{70}$ and contains only one pair of adjacent pentagons (Figure 3).

As expected, Raghavachari's calculations indicate that the latter is the lowest energy alternative isomer, lying about 1.47 eV above the ground state in energy. This energy difference is larger than in $C_{60}$, and it is probably due to the greater disruption of the dominant resonance configuration. The predicted energies for other isomers indicate that defect effects are not as additive for $C_{70}$ as they are for $C_{60}$.

## Electronic versus steric factors in $C_{78}$

Very recently, Raghavachari and Rohlfing have studied the lowest energy isomers of $C_{78}$. Mixtures of isomers have been observed experimentally, and the ground state structure for this molecule is not known. There are five isolated pentagon struc-

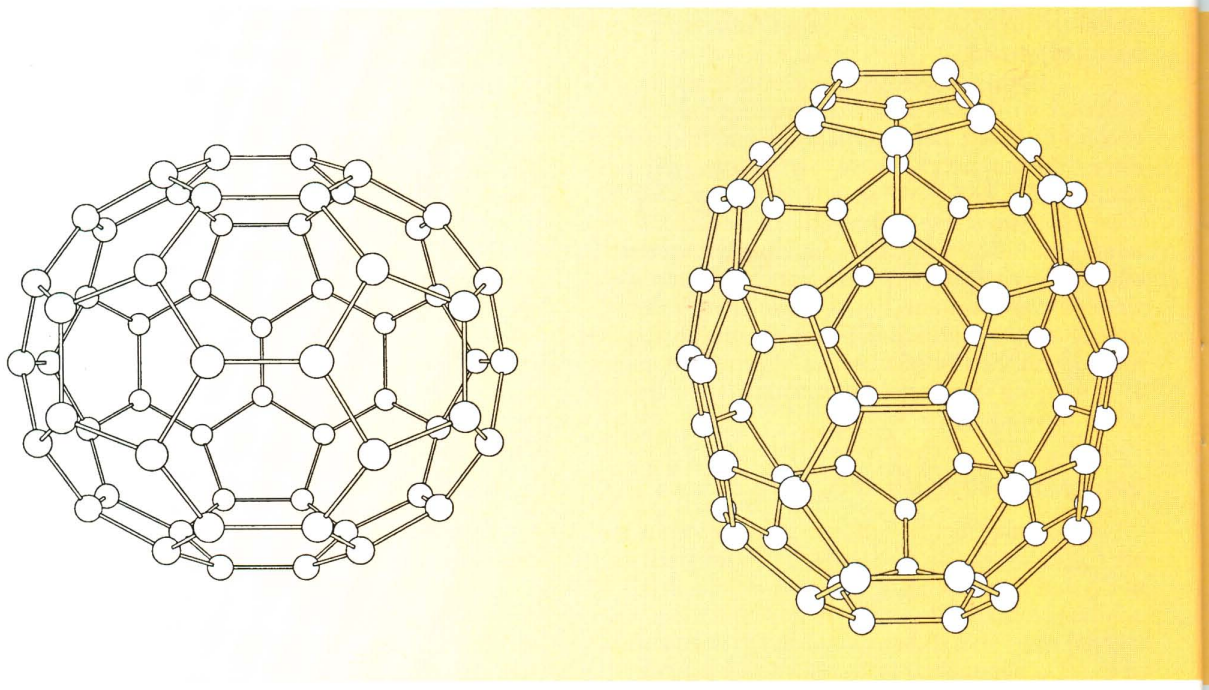

Figure 3. Lowest energy alternative isomer of $C_{60}$ (left) and $C_{70}$ (right).

tures for this system (containing no pairs of adjacent pentagonal rings). Conventionally, these are denoted the $D_{3h}$, $C_{2v}$, $C'_{2v}$, $D'_{3h}$, and $D_3$ forms; of these, the $C_{2v}$, $C'_{2v}$, and $D_3$ forms have been observed thus far. Four of the five structures (all but $D_3$) can be interconverted via a Stone-Wales transformation.

Raghavachari and Rohlfing optimized the structures of all five isomers at the HF/3-21G level and then performed single-point energy calculations using the 6-31G*(5d) basis, which contains one set of spherical harmonic d-functions per carbon atom. Their calculations resulted in this relative energy ordering of the isomers: $C_{2v} < D_3 < C'_{2v} < D_{3h} < D'_{3h}$ (Table 1).

Previously, several factors had been advanced to explain the differing stabilities of fullerene species. One proposed criterion for the prediction of fullerene stability is the maximization of the resonance stabilization effects within the structure. Several variations of this criterion have been put forward; Raghavachari and Rohlfing refer to criteria of this type as the electronic factor. In general, shorter, "double" bonds between adjacent hexagonal rings lead to larger resonance effects and a larger contribution from this factor, while conversely, such bonds in the pentagons lead to antiaromatic structures and a reduction of this factor. Considered alone, the electronic factor favors the $D'_{3h}$ structure, and the overall ordering of the isomers with respect to it is given in Table 1.

Another commonly cited factor influencing molecular stability in fullerenes is the uniform distribution of local strain, which Raghavachari and Rohlfing term the steric factor. They evaluate it by examining the environments of the hexagonal rings within a molecule, noting the number of hexagonal neighbors for each ring, which they refer to as its neighbor index. Considered with respect to this factor alone, the $D_{3h}$ form has the most favorable strain distribution; the ordering of the other isomers is given in Table 1.

| Isomer | Relative energy (kcal/mol) | Ordering based on one factor alone: Steric | Ordering based on one factor alone: Electronic |
|---|---|---|---|
| $C_{2v}$ | 0 | 2nd | 4th |
| $D_3$ | 3 | 4th | 2nd |
| $C'_{2v}$ | 4 | 3rd | 3rd |
| $D_{3h}$ | 7 | 1st | 5th |
| $D'_{3h}$ | 20 | 5th | 1st |

Table 1. Relative energies for $C_{78}$ isomers compared to orderings based on one factor alone.

Interestingly, when considered separately, these two factors lead to opposite orderings of the various isomers. More importantly, they predict that the two highest energy isomers—neither of which has been observed—would be the most stable. Clearly, there is competition between the two factors, and in fact the structure which provides the best compromise between them is the one that is the most stable. This investigation highlights the importance of quantitative predictions—often available only through theoretical calculations—in assessing the relative importance of competing effects on molecular structure.

## Surprising structures for fullerene derivatives

Recent research efforts have been focused on both fullerenes and their functionalized derivatives. One simple class of derivatives is compounds where an atom or group bridges a C–C bond in $C_{60}$. Raghavachari and Carlos Sosa of Cray Research have studied such compounds, including $C_{60}O$, where a single oxygen atom is added to $C_{60}$ in this way.

There are two $C_{60}O$ isomers with such a structure: one in which the oxygen bridges a hexagon-hexagon (6–6) bond, forming an epoxide-like

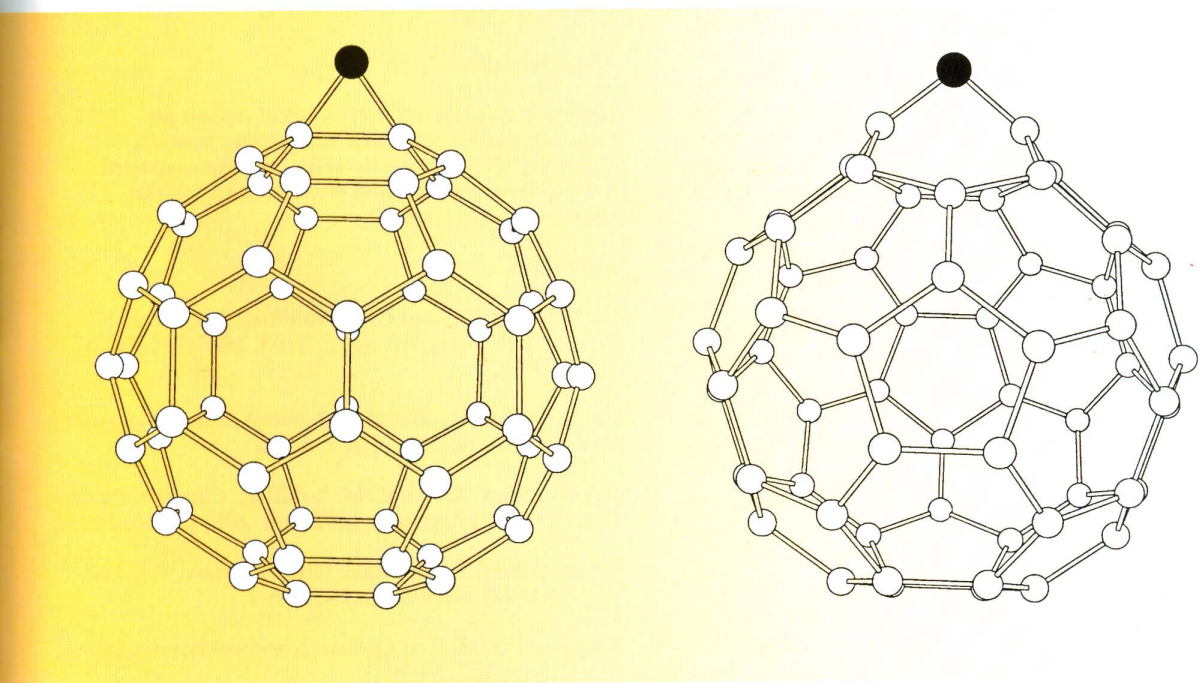

Figure 4. Geometries of the two $C_{60}O$ isomers.

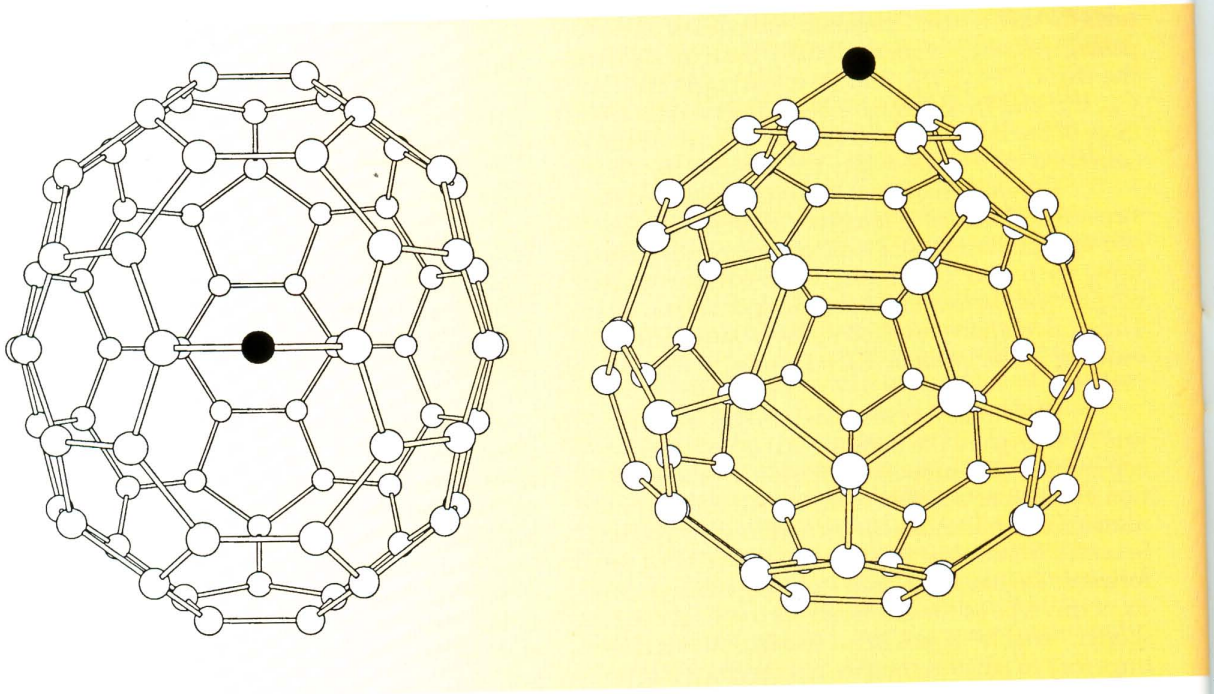

Figure 5. Ground state of $C_{70}O$ viewed perpendicular to (left) and down along (right) the long axis of $C_{70}$.

structure in which the bridging C–C bond is about 1.6 Å in length, and another where the oxygen bridges the hexagon-pentagon (6–5) bond, causing the bridging C–C bond to break and open out to a distance of about 2.2 Å (Figure 4). By performing calculations at a variety of levels of theory, Raghavachari and Sosa concluded that the two isomers are in fact distinct and found that the 6–5 bridged isomer is slightly more stable than the 6–6 form; the HF/6-31G*(5d) level of theory yields an energy difference of about 2 kcal/mol, while density functional results, which include some effects of electron correlation, yield an even smaller value and suggest that the two isomers are essentially isoenergetic.

Raghavachari and Sosa also studied the rearrangement between the two isomers in an effort to understand the energy barrier between them. They found that as the oxygen migrates from one C–C bond to the adjacent one, there is an intermediate where the oxygen is attached to only one carbon atom; vibrational analysis confirms that this structure is also a local minimum. Finding an intermediate means that there are two distinct transition states connecting the two isomers to this intermediate. Energy calculations on these structures indicate that there is a significant overall energy barrier between the two isomers, suggesting that it should be possible to isolate both of them experimentally. Thus far, only the 6–6 isomer has been observed. However, both such isomers have been experimentally characterized recently for the related isoelectronic system, $C_{60}CH_2$.

Raghavachari and Rohlfing also have studied $C_{70}O$. For this system, there are eight distinct C–C bonds and hence eight principal isomers. Raghavachari and Rohlfing determined that the structure that bridges a C–C bond in the equatorial region is the lowest in energy (see Figure 5). While this isomer corresponds to bridging a 6–6 bond, it exhibits an open structure with a long bridging C–C distance of 2.23 Å. This behavior is very different from that observed in the $C_{60}O$ isomers (or, in fact, in $C_{70}O$ isomers bridged away from the equatorial belt). Thus, the ground state structures of $C_{60}O$ and $C_{70}O$ are quite different, repeating a trend we see in their lowest energy alternative isomers.

Taken together, these studies demonstrate the increasingly important role that electronic structure modeling plays in chemical research. It has the potential to predict and illuminate experimental observations and to provide a reliable, quantitative basis for descriptions and explanations of chemical features, trends, and processes. ▬

---


***About the author***

*Douglas J. Fox is director of technical support for Gaussian, Inc. He received a Ph.D. degree from the University of California-Berkeley. He also conducted post-doctoral research with professor John Pople at Carnegie-Mellon University.*


***References***


Raghavachari, K. and C. M. Rohlfing, *Journal of Physical Chemistry,* Vol. 95, p. 5768, 1991; Vol. 96, p. 2463, 1992.

Raghavachari, K., *Materials Research Society Symposia Proceedings,* Vol. 270, p. 287, 1992.

Raghavachari, K. and C. M. Rohlfing, *Chemical Physics Letters,* Vol. 197, p. 495, 1992; Vol. 208, p. 436, 1993.

Raghavachari, K., *Chemical Physics Letters,* Vol. 190, p. 397, 1992; Vol. 195, p. 221, 1992.

Raghavachari, K. and C. Sosa, *Chemical Physics Letters,* Vol. 209, p. 223, 1993.

# Process modeling and simulation development in pharmaceutical processing

*Willis Bell, Eli Lilly and Company, Lafayette, Indiana*
*Dale Eckart, Cray Research, Inc.*

Modeling and simulating chemical processes on a high-end computer—before major decisions are made about expensive equipment and final processes—can yield significant economic benefits for companies, such as Eli Lilly, that develop and manufacture plastics, fertilizer, solvents, pharmaceuticals, and other chemicals. The use of steady-state simulation is now routine in companies that produce these products.[1] Simulation is used to support capacity planning, de-bottlenecking, equipment sizing, optimization, and evaluating the economic impact of alternate process designs. Furthermore, the use of dynamic simulation has been growing since the necessary high-end computational tools became available.[1,2,3] Dynamic simulation can be used for controller and control structure designs, hazard scenario evaluation, evaluating the operability of alternative process designs, and determining the time required to move from one product to another.

Although pharmaceutical processes can realize many of these benefits, additional incentives for computer simulation exist in other areas of product and process development. For example, developing a synthesis route suitable for large-scale production can take years; proposed processing schemes are frequently tested in pilot- and bench-scale equipment before scaling up to full production. Reducing the time required for process development and scale-up can result in an earlier introduction of a product to the marketplace, which can significantly increase market share. Using process modeling and simulation to aid the process development effort can reduce the overall time required to develop a suitable manufacturing process.[4,5]

Because many pharmaceutical processes are batch, or time-varying, processes, dynamic simulation tools are needed to study the various unit operations that comprise such processes. This article describes the early stages of a project using dynamic process simulation to improve manufacturing and process development. The codes used are SPEEDUP and PropertiesPlus, both of which can be licensed from Aspen Technology, Inc., Cambridge, Massachusetts. The dynamic process simulation project plan included

- ☐ Developing a suitably rigorous, generic model for a batch reactor
- ☐ Validating models with a known production-scale process
- ☐ Applying models to development and optimization projects

## SPEEDUP: a powerful tool

Dynamic models were developed for SPEEDUP, an equation-oriented, dynamic process simulation package capable of solving models of several thousand equations. Particularly well-suited to solving batch, time-varying chemical process

models, SPEEDUP allows the user to specify changes in variables as the simulation progresses. The model equations may be either algebraic or ordinary differential equations with a single independent variable, which is usually time. Model equations are constructed from momentum, mass, and energy balances and constitutive relations such as Arrhenius' Law and equations of state. The equations describe the relationships among variables such as density, concentration, enthalpy, pressure, and temperature. These equations, along with physical property data, equipment parameters, and chemical kinetic data, constitute the input to SPEEDUP, which uses state-of-the-art differential-algebraic equation (DAE) solvers. The version of SPEEDUP for the Cray Research platform has been further enhanced through the use of a highly vectorized sparse linear equation solver developed by Cray Research. The PropertiesPlus program, which contains a database that includes physical constants for more than 2000 compounds, provides many of the constitutive relations and physical property data. PropertiesPlus also estimates mixing properties for vapor and liquid mixtures, and, especially important for pharmaceutical applications, it supports the estimation of properties of both mixtures and pure compounds for which no data exist. Based on a description of the molecular structure, PropertiesPlus uses group contribution methods to estimate properties such as heat capacities, viscosities, and densities for complex reactants and products.

## Batch reaction modeling

The basic process unit for which models were built, shown in Figure 1, employs a jacketed stirred tank with ancillary piping for material transfer and temperature control. Both hot and cold heat transfer fluids are supplied to the jacket. Liquid, vapor, and solid reactants are charged to the reactor on a schedule derived from a set of full-scale operating procedures. During the reaction, vapor products may be withdrawn and condensed, and the condensate returns to the reactor as reflux or is diverted to a receiving vessel. The reactor discharges liquid or slurry products for further processing downstream, such as filtering or centrifugation. Some initial assumptions used to formulate the model equations included

- ☐ Reactors and charge tanks are perfectly mixed
- ☐ Initial temperature of tanks and reagents is ambient
- ☐ There is no closed-loop control of temperature and pressure
- ☐ Reactor is initially charged with inert gas and solvent
- ☐ Tank jacket temperature dynamic response is perfect

Except "Reactor is initially charged with inert gas and solvent," these assumptions have been relaxed in subsequent refinements to the models.

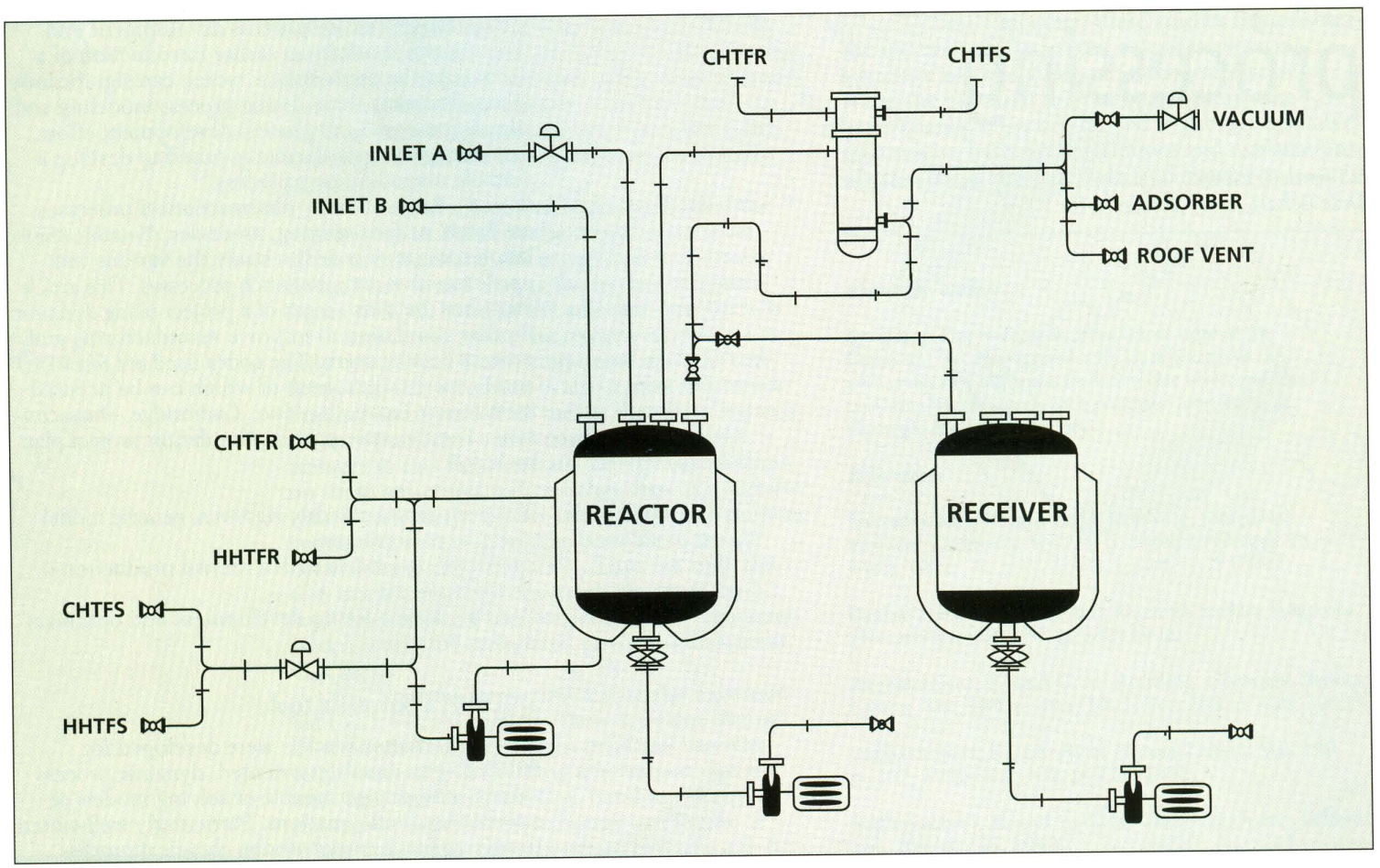


Figure 1. Basic processing unit schematic diagram.

We validated the model using operating data and equipment parameters from an actual chemical synthesis in the manufacture of a pharmaceutical product. The reactions include both series and parallel reactions, as well as formation of undesirable byproducts. Kinetic parameters for the reactions were taken from bench-scale experiments, and heat transfer parameters were taken from pilot- and production-scale test runs. Production data was used to construct an operation protocol used by the SPEEDUP simulation to follow the steps for reactant addition, stir times, and reactor discharge. A typical simulation run for this batch reaction process involved solving 2058 DAEs, which represent the dynamic behavior in two jacketed reactors of over 25 chemical compounds, their associated controls, and the reactant feed and product discharge models. Physical properties for all components were estimated using PropertiesPlus databases and structural information for the novel compounds. A total of 1078 minutes of batch processing time was simulated, with results logged at 1-minute intervals. We solved the model in 3437 CPU seconds on a CRAY-2 supercomputer.

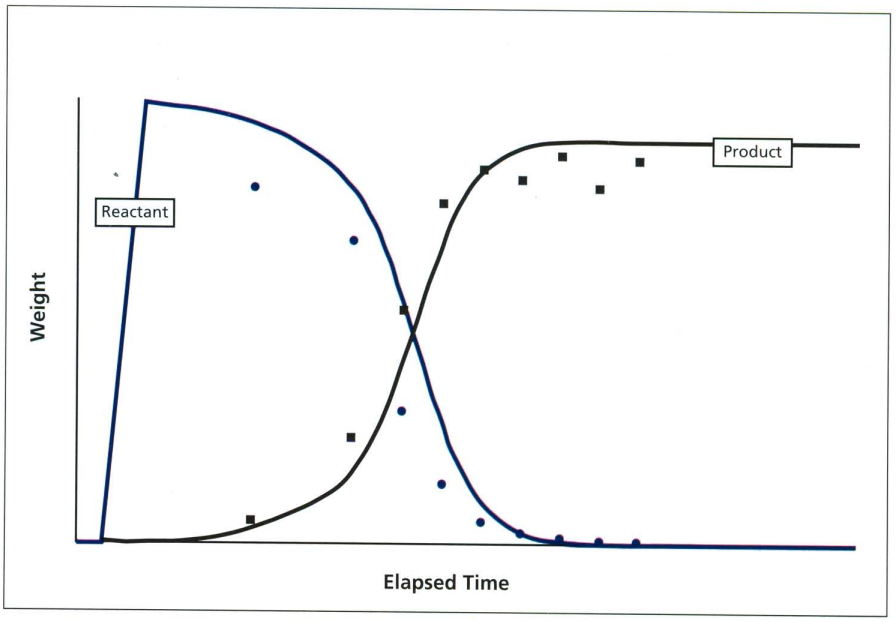


Figure 2. Comparison of model prediction and production data for reactant and product.

## Results

We validated the simulated reactor performance by comparing the final composition with the production assay performed at the conclusion of this synthesis step. The simulation results match the assay results within the experimental error of the assay samples. We created a similar SPEEDUP problem file to follow another lot, for which additional assay samples had been taken during the batch. The simulated composition data matched the samples taken both during and at the end of the batch as shown in Figures 2 and 3. Alternative operating profiles are being run to evaluate the effects of temperature profile and reactor stir times on the product yield and reaction selectivity. Plans are under way to expand the model's complexity to include temperature gradients due to imperfect mixing and a more rigorous model of the heating and cooling utilities to study their dynamics and control. In addition, we are considering other candidate processes, both in development and production, for simulation studies. Dynamic process simulation provides many benefits to the development and improvement of pharmaceutical production processes. Our work with SPEEDUP on the Cray Research supercomputer is helping Eli Lilly realize these benefits.

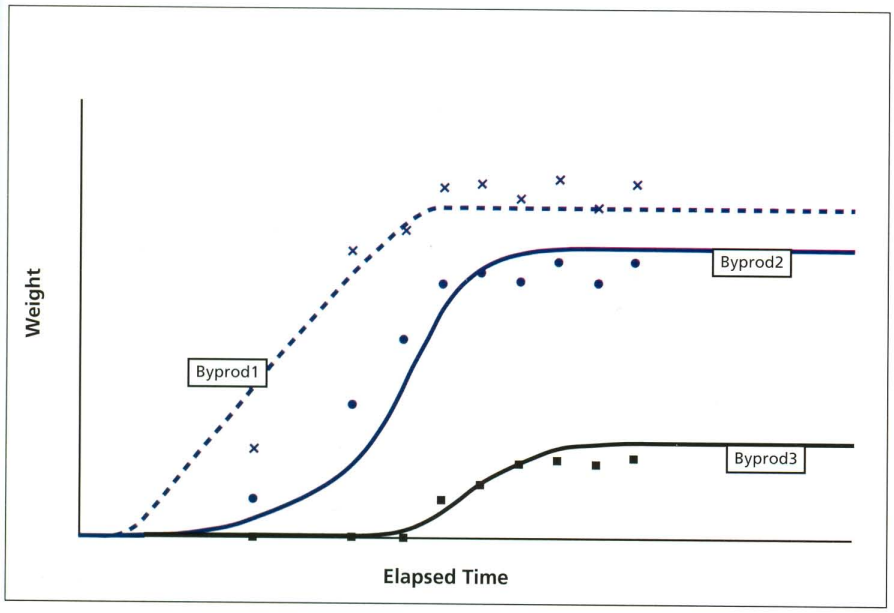


Figure 3. Comparison of model prediction and production data for byproducts.

### *About the authors*

*Willis V. Bell, III is a senior chemical engineer at Eli Lilly and Company. He is currently responsible for the application of process modeling and simulation to the development of new pharmaceutical manufacturing processes at Eli Lilly's production and development facility in Lafayette, Indiana. He received a B.S. degree from the University of Alabama and an M.S. degree from Purdue University, both in chemical engineering, and is a registered engineer in the state of Indiana.*

*Dale E. Eckart is a chemical engineering analyst working in Sales Support for Cray Research. He received B.S. and M.S. degrees in chemical engineering from Purdue University and is pursuing a Ph.D. degree in chemical engineering part-time through Lehigh University. Prior to joining Cray Research, Dale worked in chemical process control for Exxon Chemical in Linden, New Jersey.*

### *References*

1. Stadtherr, M. A. et al., "Hardware: Developing the Meta-Computer," *Chemical Engineering Progress,* pp. 27-37, November 1993.
2. Biegler, T., "Chemical Process Simulation," *Chemical Engineering Progress,* pp. 50-61, October 1989.
3. Boston, J. F. et al., "Software: Tackling Tougher Tasks," *Chemical Engineering Progress,* pp. 38-49, November 1993.
4. Thomas, R. J., "Supercomputing at DuPont," *Cray Channels,* pp. 22-23, Fall 1991.
5. Fouhy, K., "Process simulation Gains a New Dimension," *Chemical Engineering,* pp. 47-53, November 1991.

# CORPORATE REGISTER

## Three of the world's largest chemical companies get CRAY C90 systems

**E.I. du Pont de Nemours & Co. (DuPont)** has ordered a CRAY C94 supercomputer system to be installed at the DuPont Experimental Station in Wilmington, Delaware. DuPont will use the system, which replaces a four-processor CRAY Y-MP supercomputer, in four primary areas: computational chemistry, process (manufacturing) simulation, structural analysis, and environmental modeling. DuPont ran these applications on the CRAY Y-MP system to develop new products, design new chemical plants, and model the environmental impacts of DuPont's products. The CRAY C94 system is the fourth generation of Cray Research systems ordered by DuPont.

**The Dow Chemical Company** has entered into a three-year partnership with Cray Research to further advance supercomputing capabilities for chemical engineering and process simulation. As part of the agreement, Dow has acquired a CRAY C92A supercomputer installed at Cray Research's computer facility in Eagan, Minnesota. Dow acquired the system primarily for computational fluid dynamics (CFD) and process simulation—two rapidly growing supercomputer applications in the chemical industry—but also plans to use it for computational chemistry and environmental modeling applications. Installation of the CRAY C92A supercomputer at Cray Research's facility allows Dow to benefit from Cray Research's expertise in managing multi-user supercomputers. A portion of the system will be dedicated to advanced research in chemical engineering and process simulation, and the remainder of the system will be devoted to Dow's chemists and engineers throughout the world, who will have around-the-clock access to the system through high-speed networks.

**Bayer AG** is the first European chemical firm to order a Cray Research supercomputer system, a two-processor, air-cooled CRAY C92A system featuring very large DRAM memory capacity installed at Bayer's Central Research Facility in Leverkusen, Germany. Bayer plans to use the new system to solve large, computationally intensive problems in process simulation, such as planning and laying out production facilities, and to optimize plant operations for safety, environmental factors, and cost-effectiveness. Bayer and Cray Research also have agreed to collaborate extensively on developing and optimizing steady-state and dynamic process simulation software. The focal points of the collaboration are:

- Analysis and performance optimization of plant simulation software
- Optimization of application software through the introduction and testing of specialized software tools
- Development and testing of new computer-aided methods for simulating complex chemical plants on Cray Research's CRAY T3D system
- Porting and optimization of applications software on multiprocessor systems
- Testing of parallel computers for the use of this application software on real production problems

**Taisho Pharmaceutical** became Cray Research's first pharmaceutical customer in Japan when it ordered a two-processor CRAY EL92 system to be installed at the company's research center. Taisho also purchased UniChem, Cray Research's popular quantum chemistry modeling package; Taisho will use the UniChem software in conjunction with Gaussian, Amber, CHARMm, and Mopac packages for computational chemistry and drug design.

The **Minnesota Supercomputer Center, Inc. (MSCI)** has installed a 128-processor CRAY T3D system. The new MPP system will be closely coupled with MSCI's existing eight-processor CRAY C916 parallel vector supercomputer system. MSCI and Cray Research will target the petroleum and automotive industries as they work together to develop new commercial applications and to help port leading third-party applications onto the CRAY T3D system.

**Stichting Academisch Rekencentrum Amsterdam (SARA),** the Dutch national supercomputer center in Amsterdam, has installed a new CRAY C98 supercomputer system with four CPUs and 256 million words of central memory. The CRAY C98 system will be used by research institutes and universities in the Netherlands; purchase of the system was funded by the Nederlandse Organisatie voor Wetenschappelijk Onderzoek (NWO), the Dutch Organization for Scientific Research. The system will be used for research in chemistry, fluid dynamics, structural analysis, and other scientific fields. The CRAY C98 system replaces a four-year-old, four-processor CRAY Y-MP system.

**The U.S. Environmental Protection Agency (EPA)** has ordered a CRAY C94 supercomputer to be installed at the National Environmental Supercomputer Center in Bay City, Michigan. The CRAY C94 system replaces the EPA's existing CRAY Y-MP supercomputer and will be used by researchers nationwide to model air quality to enable the EPA to monitor compliance with the Clean Air Act and to measure the effects of pollutants on groundwater, vegetation, and animals. Scientists are currently using the EPA's CRAY Y-MP system to study the Grand Canyon, the Great Lakes, and the Chesapeake Bay.

**The Ohio Supercomputer Center (OSC)** has acquired an air-cooled 32-processor CRAY T3D system, which will be housed at the OSC facility in Columbus, which already includes CRAY Y-MP8 and CRAY EL systems. OSC and Cray Research will use the new system to collaborate on advanced research in medical imaging to develop faster, more accurate methods for transferring and analyzing images gained from MRI (magnetic resonance imaging) and other digital medical imaging technologies. "We want to achieve real-time medical imaging, which could have very significant impact on diagnosis, surgery planning, and medical education," said OSC director Charles F. Bender.

## Cray Research announces graduate fellowships in computational chemistry

Benny G. Johnson, Carnegie Mellon University, Jonathan P. Knight, Massachusetts Institute of Technology, and John Lobaugh, University of Pennsyl-

vania, are recipients of the Cray Research Fellowships in Computational Chemistry for the 1993-94 academic year. The awards, presented by Cray Research in collaboration with the American Chemical Society's (ACS) Division of Physical Chemistry, focus on innovative developments and applications of methods in theoretical chemistry or related disciplines. Emphasis is on large-scale numerical simulations on supercomputer systems.

The Cray Research Fellowship in Computational Chemistry was established to encourage doctoral degree studies in computational chemistry; fellowships are awarded on a competitive basis to graduate students in the research and dissertation stage of their doctoral programs. Funded by the Cray Research Foundation, the fellowships provide a cash stipend of $5000 for each student per school year as supplementary financial support.

## Newest Cray PVM products support broader uses of distributed computing

Cray Research has announced two PVM-based products, Cray Network PVM-3 and Cray MPP PVM-3, which incorporate Version 3 of the PVM de facto standard. These products allow Cray Research supercomputer users to build distributed programs using heterogeneous systems on a network; develop interdisciplinary applications—two or more applications that simultaneously share information and communicate with each other while in operation; and develop MPP applications based on the message passing paradigm for the CRAY T3D system.

A key component in Cray Research's Open Supercomputing strategy, the flexible Cray Network PVM-3 product allows users to develop distributed applications among Cray Research and other computing systems on a heterogeneous network, among networked clusters of Cray Research systems, between a CRAY T3D system and its host (CRAY Y-MP or CRAY C90 systems), or within one Cray Research supercomputing system.

## Visual Numerics to market CF90 Programming Environment

Cray Research and Visual Numerics, Inc., have agreed to cooperate in the development and marketing of leading Fortran 90 technologies. Visual Numerics will market and distribute Cray Research's CF90 Programming Environment for RISC workstations on a nonexclusive, worldwide basis. Visual Numerics will also develop the industry-leading IMSL Fortran 90 libraries to interoperate with the CF90 Programming Environment. Cray Research has a worldwide, nonexclusive option to distribute the IMSL Fortran 90 libraries. Each company will support and service its own products under the arrangement. The agreement targets binary-compatible versions of both companies' products for SPARC platforms, including Sun products and the CS6400 system from Cray Research subsidiary Cray Research Superservers.

## Cray Research offers high-performance RAID network devices

Cray Research is expanding its redundant array of independent disks (RAID) product offering by introducing the Cray Research Network Disk Array, a bulk storage device designed to reside on high-performance computer networks. The new RAID network device enables users to store data on the network rather than on a storage device directly connected to and accessible only from a single system on the network.

The new network array from Cray Research can more than double the amount of data accessible to users via one channel. Connected via a HIPPI channel, the Network Disk Array provides up to 232 gigabytes of data storage for Cray Research systems with the Model E input/output (I/O) subsystem.

With the Cray Research Model E HIPPI disk driver software and RAID configurations, the disk array is capable of data transfer rates exceeding 60 megabytes per second. The disk driver communicates with the network disk array using Intelligent Peripheral Interface-3 (IPI-3) protocol and supports reconstruction of data concurrent with array operations.

## C++ libraries to augment Cray C++ Compiling System

Continuing its commitment to C++ as an important programming language in high-performance scientific computing, Cray Research announced the availability of the Cray Research C++ Libraries, to augment its Cray C++ Compiling System.

The industry standard C++ libraries, based on library products by Rogue Wave Software, Inc., a major supplier of scientific class libraries for workstations and PCs, enable scientists and engineers to write code using familiar objects such as molecules, matrices, or meshes. This allows users to focus on the high-level concepts of their disciplines and reduce time spent implementing those concepts in the software code.

## FCA-1 Channel Adapter provides threefold improvement on FDDI transfers

Cray Research has announced the availability of the FCA-1 Channel Adapter, a built-in, direct Fiber Distributed Data Interface (FDDI) connection for its supercomputing systems that provides up to three times faster FDDI transfer speeds at a lower cost than previous FDDI interface options. The FCA-1 adapter, built into the supercomputer's input/output (I/O) subsystem, can transfer data at up to 70 megabits per second using industry standard protocols.

## Keeping departmental supercomputing on the upgrade path

Cray Research has created a program designed to address market demand for increasingly powerful, production supercomputing systems beginning at well under $1 million. Customers who order CRAY EL98 systems, Cray Research's current departmental supercomputer system, and a next-generation system, currently in final development, are eligible for lower combined pricing. Volume shipments for the next-generation departmental supercomputer from Cray Research are slated to begin in first-quarter 1995 and customers in the new program will receive priority shipments at that time.

Pricing for the CRAY EL98 systems begins at approximately $300,000 (U.S.). The next-generation departmental supercomputer systems are expected to be 6 to 12 times more powerful than the company's current departmental systems at the same price points.

The 1995 systems will be binary compatible with the company's current departmental products. The next-generation departmental systems are also compatible with larger Cray Research parallel vector supercomputers, including the top-of-the-line CRAY C916 system, and can be connected to the company's CRAY T3D massively parallel processing system.

# APPLICATIONS UPDATE

## Cray Research's PATP program to advance MPP application development

Massively parallel processing (MPP) technology will make it possible to solve a range of important, currently intractable problems. Solving these problems will advance scientific knowledge, boost industrial competitiveness, and improve the quality of our lives. However, few of the software applications needed to address these barrier-breaking problems exist today on MPP systems.

Cray Research's Parallel Application Technology Partners (PATP) program is designed to rapidly expand the number of applications available in the new MPP arena. The PATP program uses the company's first MPP system, the CRAY T3D system, as a development platform for running these applications—at unprecedented speeds. The applications are developed through partnerships between Cray Research and leading research institutions, industrial firms, and independent software vendors around the world. The PATP program has targeted computational methods and algorithms, as well as entire applications.

The PATP program makes larger numbers of applications available more quickly, making the CRAY T3D system more useful for a greater number of organizations. PATP members benefit by the early acquisition of a cost-shared CRAY T3D system, gaining access to a larger CRAY T3D system, having Cray Research computational experts on site, and through their affiliations with other PATP members.

There are four PATP members: the Pittsburgh Supercomputing Center (PSC); NASA's Jet Propulsion Laboratory (JPL), Pasadena, California; the Swiss Federal Institute of Technology Lausanne (Ecole Polytechnique Fédérale de Lausanne, or EPFL); and a joint PATP program with Los Alamos National Laboratory (LANL) and Lawrence Livermore National Laboratory (LLNL).

As part of its PATP agreement, PSC received the first CRAY T3D system. PSC will focus on software programs in computational chemistry, materials science, computational fluid dynamics, and biomedical applications. Some of these programs will be ported wholly to the CRAY T3D system and some will run heterogeneously between the CRAY T3D and CRAY C90 systems.

One such code is AMBER, a popular code used by chemists for modeling large systems of biological interest, especially solvated proteins. According to PSC scientific programmer Nick Nystrom, AMBER is important in biomedical computing for the grand challenge protein folding problem, which is integral to future drug design and understanding processes within living organisms.

"AMBER is running on the CRAY T3D and producing accurate results," said Nystrom. Nystrom hopes to see significant speedups on the CRAY T3D system over the CRAY C90 system and up to two orders of magnitude over typical workstation implementations of AMBER. He noted that AMBER is popular among chemists using workstations, as well as those using Cray Research parallel vector supercomputers like the CRAY C90 system.

In addition to AMBER, PSC is also helping develop CRAY T3D versions of the following codes:

- ☐ Car-Parrinello
- ☐ CHARMm
- ☐ FLAPW
- ☐ GAMESS USA
- ☐ Gaussian
- ☐ QCHEM
- ☐ Shake-and-Bake
- ☐ X-PLOR
- ☐ MAXSEGS

At JPL, the supercomputer is critical to the organization's mission to conduct robotic space missions for NASA. JPL intends to use the CRAY T3D system to develop real-time movies using a new parallel algorithm and port applications in atmospheric and oceanic modeling, spacecraft design, and electromagnetics/antenna design. In addition, JPL's CRAY T3D system also services the research community at the California Institute of Technology (Caltech). Projects there include some of the most advanced research in areas of molecular modeling, materials science, and parallel computing. One example is the "PAMP-CAD" project led by Vincent McKoy of Caltech. McKoy and his research team are creating a whole new set of tools to aid in the production of semiconductor components—an area of critical importance to U.S. technology leadership.

EPFL, a federal academic education and research institute, plans to focus its PATP program efforts on developing parallel applications in these areas:

- ☐ Materials science, to substantially increase the number of atoms or molecules in a simulation to look for new drugs for medicine, to develop new materials or new processes (for example, in relation with nanotechnology), and to better understand biological mechanisms.
- ☐ Fluid dynamics, with the capacity to model and simulate industrial flows in complex systems such as turbines and turbomachinery, energy production and distribution, combustion in heat exchangers and engines, chemical processes, ships, automobiles, aeronautics, high-speed terrestial transports in tunnels, meteorology and climate, and cardiovascular systems.
- ☐ Plasma physics, where the simulation in three dimensions of magnetically confined plasma is required to design the fusion reactors of the next century.
- ☐ Image processing for image compression and decompression methods, high definition television, or artificial vision with applications in robotics and quality control.

LANL and LLNL are using their PATP efforts to forge links between their research base and industry, which helps ensure that real-world problems are being tackled. Each of the 16 PATP projects to date has industrial partners associated with it. The PATP projects at LANL and LLNL are in these categories:

- ☐ Environmental modeling
- ☐ Petroleum
- ☐ Materials design
- ☐ Advanced manufacturing
- ☐ Parallel computing

One project example includes the development of a general reservoir simulator for MPP systems so that performance forecasting of oil and gas reservoirs, using geostatistics, can be better quantified. The methods used in the

simulator would need to run several million cells per trial, which requires the use of MPP systems, especially as demand increases for more accurate simulations over larger volumes. Another example is the development of a massively parallel implicit hydrodynamics methodology that could be used to solve complex hydrodynamic problems; the methodology could also be extended to solving combustion, pollution, and non-isothermal flow through porous media problems. Environmental assessment and restoration efforts would benefit from solutions to these problems, since the methodology is scalable to large-scale environmental problems through highly accurate representations of heterogeneous media.

## UniChem III Consortium technology delivered to consortium members

The final version of the new UniChem features developed in Phase III of the UniChem consortium has been delivered to members of the UniChem III consortium.

In the density functional and materials area, analytic second derivatives for closed shell systems and local potentials have been incorporated in the DGauss density functional code, resulting in a roughly five-fold speedup over the finite difference method. Other enhancements to DGauss include density of states (DOS) calculations, photoelectron spectra (PES) calculations, and calculations of the NMR spectrum. DBind, a new code based on tight binding technology, supports calculations of properties of periodic systems.

The quantum molecular dynamics capability has been extended in a number of directions. Bond distances can now be constrained during a quantum dynamics calculation, and a new solvent model designed primarily to simulate solvent effects based on local orbitals has been introduced.

A new code computes the chemical similarity between molecules, based on either the electron density or electrostatic potential as computed by DGauss. It can compare entire molecules (global similarity) or parts of molecules (local similarity).

In addition, a program to compute atom-centered point charges has been developed. The program uses the electrostatic potential computed by DGauss. The user can constrain the charges to equal one another, select the size of the grid, and fix the value of some of the charges and compute the remaining charges.

The UniChem graphical user interface has been enhanced to support the new functionality. The interface now provides point-and-click setup options for DBind and the similarity code, as well as options to set up dynamics calculations with MNDO91, a version of the UniChem semi-empirical code. A solids builder has been added to construct 3-D periodic systems as input to the tight binding code. New analysis capabilities for solids include 2-D and 3-D displays of Fermi surfaces and plots of energy surfaces and densities of states. Molecular dynamics analysis tools have been added, allowing the computation and display of radial distribution functions, time correlation functions, and dynamical trajectories.

These features are for exclusive use of consortium members at this time; they are scheduled to become available in product versions in the near future. Members of the UniChem III consortium include Asahi Chemical, DuPont, Eli Lilly, Exxon R&E, and Sumitomo Chemical.

## SUPERMOLECULE performs well on heterogeneous CRAY T3D system

SUPERMOLECULE, an academic ab initio program package developed at the University of Minnesota, performs Hartree-Fock energy calculations and geometry minimizations that can be carried out in an I/O-based, incore, or "direct" fashion for a wide range of Gaussian basis sets. These direct calculations can be performed to obtain frequency-dependant dipole polarizabilities, excited state energies, and correlation energies of large molecules. These properties can also be computed with the new RI approximation, which substantially increases throughput. SUPERMOLECULE has been extensively parallelized for CRAY Y-MP and CRAY C90 systems using Cray Research's Autotasking directives and libraries.

In addition, the program has been parallelized for the CRAY T3D system using PVM 3.0. While computations can be carried out completely on the CRAY T3D system, performance is often enhanced by using the front-end host for specific tasks that are not well-suited for the CRAY T3D processors. This heterogeneous mode is well-suited for ab initio calculations and allows better performance scaling for large numbers of processors than on the MPP portion of the CRAY T3D system alone. As an example, the Hartree-Fock energy of 18-crown-6 can be obtained in only 193 seconds on a 256-processor CRAY T3D system in heterogeneous mode. This calculation requires 486 seconds when run only on the MPP portion of the CRAY T3D system.

## First European Gaussian workshop

The first European Gaussian workshop was held at the Stichting Academisch Rekencentrum Amsterdam (SARA) in the Netherlands December 7-10, 1993. This workshop was jointly organized by Gaussian Inc., SARA, and Cray Research. Topics covered included an overview of the theory and features of the *Gaussian 92* program in a series of lectures and hands-on working sessions with SARA's CRAY Y-MP system. *Gaussian 92* is a user-friendly program for performing ab initio and semi-empirical molecular orbital calculations. All of the ab initio methods available in *Gaussian 92* were covered, along with discussion on choosing methods appropriate to the chemistry being studied. Michael Frisch, Douglas Fox, Berny Schlegel, Michael Robb, and Carlos Sosa assisted the participants in the working sessions and presented lectures on

- ☐ Building Gaussian input decks
- ☐ Using the UniChem user interface for Gaussian calculations
- ☐ Model chemistries (basis sets, level of theory)
- ☐ SCF methods (RHF/UHF/ROHF, GVB, MCSCF)
- ☐ Stability and convergence of SCF wavefunctions
- ☐ Geometry optimization: techniques for finding energy minima
- ☐ Studying transition states: optimization and reaction paths
- ☐ Electron correlation methods
- ☐ Excited states via CI singles
- ☐ Interpretation of results and molecular properties
- ☐ Solvent effects on molecular electronic structure
- ☐ Gaussian utilities
- ☐ Guidelines for choosing algorithms and estimating resources
- ☐ Performance of model chemistries

Gaussian users from The Netherlands, Germany, Spain, Sweden, Italy, Israel, Belgium, France, Norway, Finland, and Denmark attended the workshop. For further information on future Gaussian workshops contact help@gaussian.com.

# USER NEWS

## Visualization enhances ultrasonic inspection of stainless steels at AEA Technology

Stainless steels are often used in industrial application because they are tough, ductile over a wide range of temperatures, and usually chemically inert. Much of the pipework in light-water and fast-breeder nuclear reactors is made of stainless steel. The pump-bowl of the first pressurized water reactor (PWR) in Britain is made of cast stainless steel; this reactor is being constructed for Nuclear Electric at Sizewell on the east coast of England.

Techniques such as radiography and dye-penetrant inspections help ensure that stainless steel components contain no significant defects. When the reactor begins to generate power, the in-service inspection, however, presents access problems for radiographic equipment. Ultrasonic inspection is being investigated as a possible solution. The difference between stainless steels and other, regularly inspected materials is their grain size. Cast austenitic materials (nonmagnetic solid solutions of ferric carbide or carbon in iron) often have grains of a few millimeters, compared with a few tens of microns in ferritic steels. To achieve adequate resolution, so that the position and size of any defect can be adequately determined, ultrasonic frequencies of a few megahertz usually are used in inspections.

Andrew Temple, a senior scientist at the United Kingdom's Atomic Energy Authority (AEA Technology) Harwell Laboratory has been studying this problem at the request of the United Kingdom's Health and Safety Executive (HSE).

Temple developed a unique computer code to simulate the time-dependent propagation, scattering, and mode conversion of short duration pulses of elastic waves in inhomogeneous anisotropic materials. The code, Swam3D, is fully three-dimensional and requires the power of a high-end Cray Research system. Originally written for the CRAY-2 system at the Harwell Laboratory, the code recently was moved to a CRAY Y-MP system there.

Swam3D is unusual in its ability to handle elastic constants which vary from position to position, even on a scale of one-tenth of a wavelength. The cast austenitic material is known to take one of

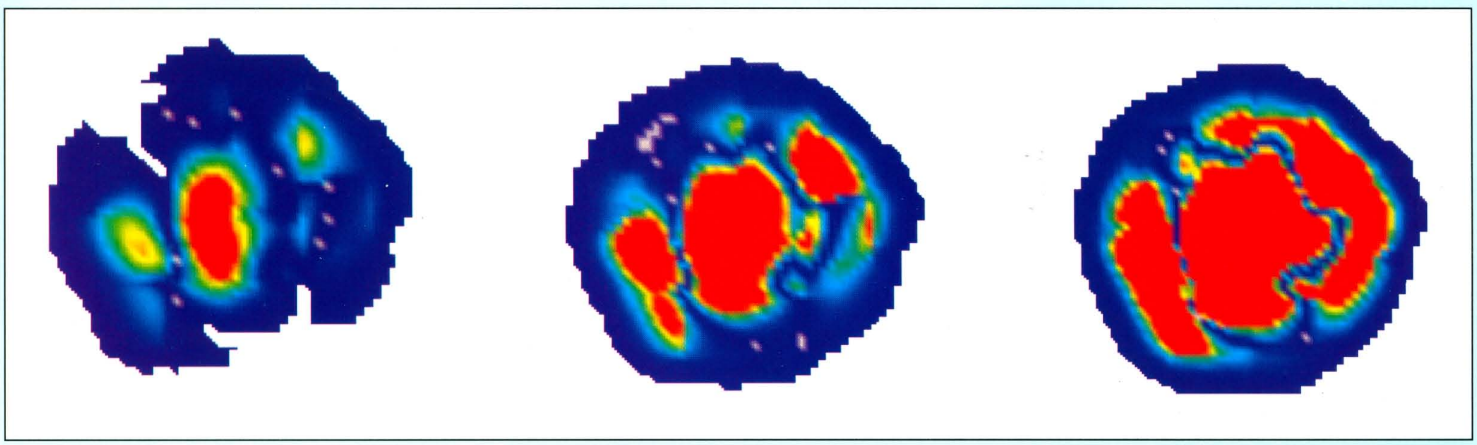

Clip planes at 1.5 µs separated by 0.2 mm, perpendicular to the principal direction of wave propagation, with color used to show energy density (red high, blue low). The grains have caused the beam to split into several distinct parts.

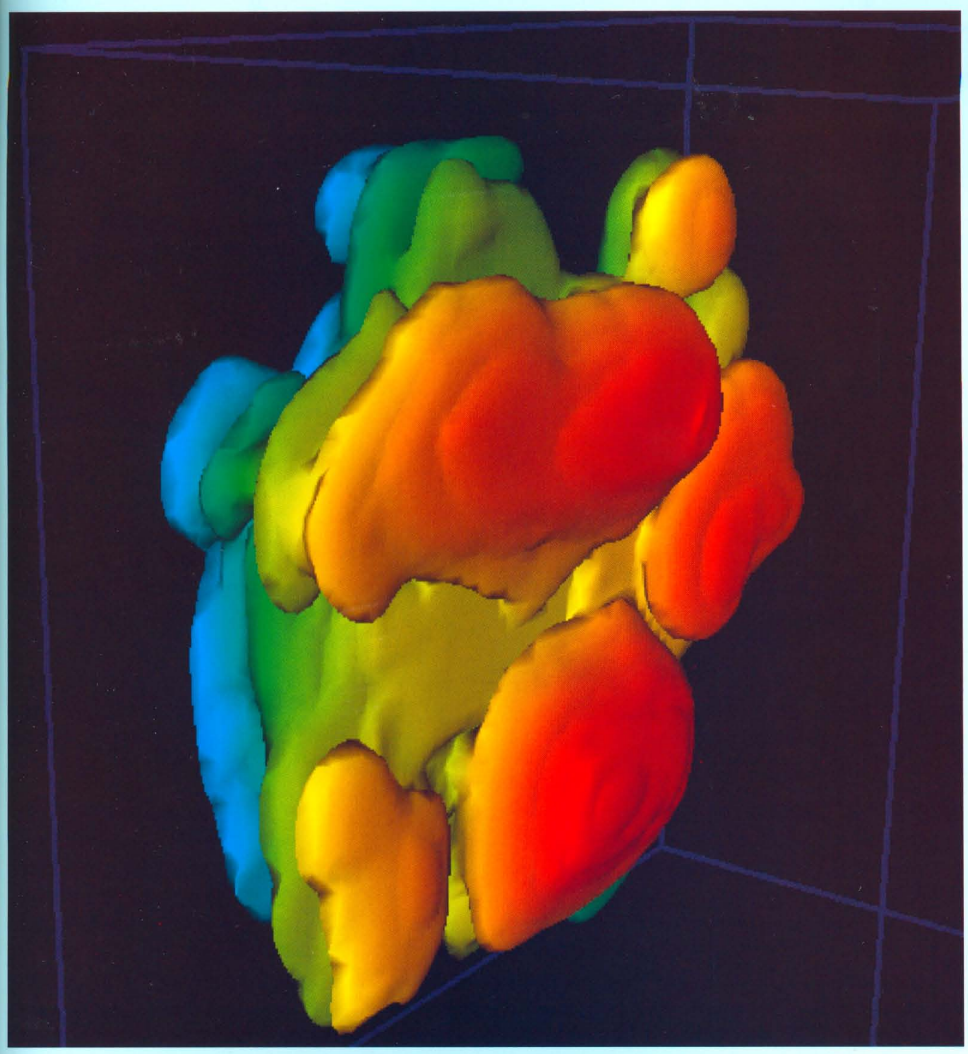

Isosurface of the quasi-compression wave energy 1.5 µs after the source starts to generate a single cycle of sine wave on the rear face of the cube. If the material were isotropic and homogeneous, this surface would be smooth and continuous. The wavefront is almost filling the cube and has passed through about five grains with random orientations.

two distinct morphologies: an equiaxed or columnar structure, depending on the manufacturing process. In the equiaxed structure, the crystal axes within the grain are taken to be randomly oriented; no matter which direction a wave travels through the material, there will be an elastic mismatch at each grain boundary with reflection and refraction as a consequence.

Elastic waves have a polarization associated with them. This distinguishes compression waves, with a polarization along the direction the wave is traveling, from shear waves, in which the polarization is perpendicular to the direction of travel. In anisotropic materials, the situation is more complex since energy transport (via the group velocity) is not necessarily parallel to the wavevector (phase velocity). At each grain boundary there will be conversion between polarizations. This is known as mode conversion.

There are two major problems in the ultrasonic inspection of austenitic steels. First, because of the complicated refractions at the grain boundaries, it is hard to tell where the ultrasonic waves will travel. Second, it may be hard to distinguish a reflection from a defect amid the "noise" of reflections from grain boundaries.

To visualize the propagation of elastic waves through these materials, Temple devised a method for creating nonuniform grains and predicting propagation and scattering with Swam3D. By writing out the compression and shear wave components in Cray Research's MPGS format, the propagation of compression and shear wave components can be visualized.

For these calculations, only a small physical region has been modeled to develop the visualization. The material is divided into an assembly of 6 x 6 x 6 hexagonal prisms; each represents a single grain approximately equal in length to the shear wavelength. The compression wavelength is roughly twice the shear wavelength.

The finite difference mesh contains 132,651 nodes; some 400 timesteps are included in the whole visualization. While this is a small calculation, the complexity of the interaction of the wave with the structure is apparent. To create a real-world simulation, it is necessary to consider propagation over distances of a few tens of millimeters, or about 30 grains. The resulting calculation on a mesh of 15,813,251 nodes for 2000 timesteps took under 10 hours of CPU time on a CRAY C90 system. Cray Research's Kevin Fox and Chris Baker dumped the image of the wave fronts at every timestep and were thus able to monitor the calculation as it progressed and produce a video of the propagation of the wave through the grainy material.

## Pseudospectral approach to computational chemistry greatly reduces solution times

Rich Friesner of Columbia University has developed a pseudospectral approach to speeding up Hartree-Fock calculations, which compute electron distributions as a result of interaction with an averaged field representing all the other electrons in the field. Friesner's approach reduces the escalation in computing time that usually accompanies an increase in basis functions involved in a Hartree-Fock calculation. The average number of basis functions is typically between 100 and 1000. Doubling the number of basis functions usually means a 16-fold growth in the amount of computational power. The pseudospectral approach halves the exponential escalating effect, making it possible to tackle much larger molecules.

Using the Pittsburgh Supercomputing Center's CRAY C90 system for a three-month period, Friesner ran his code on a large number of test cases involving hundreds of runs and nearly 300 hours of CRAY C90 computing time. Friesner attributes his success to the CRAY C90 system, saying that it eliminated concerns about memory and disk restrictions. He also said that the CRAY C90 system reduced his development process by a factor of two or three.

Friesner has compared his pseudospectral calculations to *Gaussian 92*, one of the most frequently used programs for electronic structures, and depending upon the desired accuracy, has achieved speeds four to ten times faster.

# GALLERY

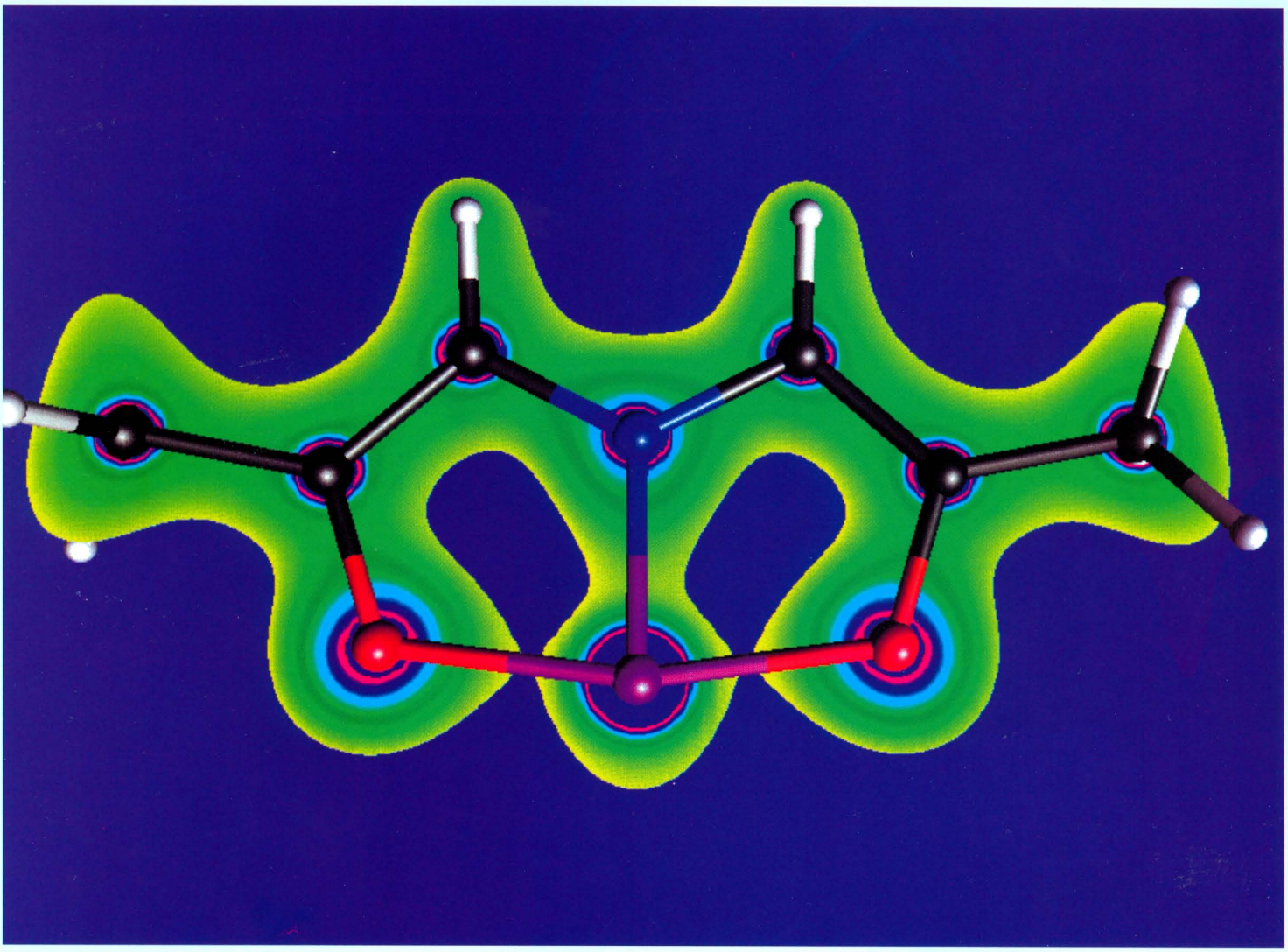

False-color electron density in the dominant molecular plane for the ADPO molecule 3,7-dimethyl-5-aza-2,8-dioxa-1-phosphabicyclo-[3.3.0]octa-2,4,6-triene. The electron density was calculated from the DFT optimized structure with the DGauss program from the UniChem package. The contours (outer = 0.75 e/Å$^3$ and inner = 10 e/Å$^{3)}$ were displayed by using the UniChem interface on a Silicon Graphics workstation. The plot shows the presence of the 3-center, 4-electron hypervalent bond between the phosphorous and the oxygen atoms which are in the "apical" positions. The loss of electron density between the oxygen atoms and the phosphorus is indicative of the hypervalent bond. Image courtesy of A. J. Arduengo, D. A. Dixon, and S. C. Walker, DuPont Experimental Station, Wilmington, Delaware.